DISSERTATION

AEDES DENSONUCLEOSIS VIRUS ANALYSIS AND EXAMINATIONS IN BIOPROCESSING

Submitted by

Rachel Specht
Chemical and Biological Engineering

In partial fulfillment of the requirements
For the Degree of Doctor of Philosophy
Colorado State University
Fort Collins, Colorado
Summer 2007

ABSTRACT OF DISSERTATION

AEDES DENSONUCLEOSIS VIRUS ANALYSIS AND EXAMINATIONS IN BIOPROCESSING

Aedes densonucleosis virus (AeDNV) is a mosquito specific parvovirus that infects the *Aedes aegypti* mosquito. There is potential to develop AeDNV as a vector control agent. This work presents several different topics centered on AeDNV. In particular, the ultrafiltration of AeDNV, expression of AeDNV structural protein in *Pichia pastoris* and identification of virus binding proteins were explored. The final portion of this work presents the investigation of performance differences between an anion exchange resin and membrane adsorbers.

Purification of AeDNV using tangential flow ultrafiltration was examined. The performance of ultrafiltration membranes, with molecular weight cut-offs (MWCO) of 300, 100, 50, and 30 kDa, was investigated. The virus was grown using two cell culture medias, with and without serum. The ideal ultrafiltration membrane will reject the AeDNV while allowing the host cell proteins (HCP) from the mosquito tissue culture to pass through its pores. The 300 kDa membrane does not reject all AeDNV, leading to a decrease in membrane flux and loss of virus particles. The 50 and 30 kDa MWCO membranes reject virus but also reject HCP. The 100 kDa MWCO membrane rejects virus and allows the HCP from the serum free cell culture to pass through the pores. The ultrafiltration concentrates the virus 10-fold.

To examine the role of structural proteins in virus assembly, the AeDNV major capsid protein was expressed in the methylotrophic yeast *Pichia pastoris*. High cell density fermentation was carried out in a three-liter bioreactor. The protein spontaneously assembles into virus-like particles (VLPs) as determined by electron microscopy. The VLPs are antigenically similar to AeDNV native capsids as determined by enzyme-linked immunosorbant assay. AeDNV establishes a persistent infection in C6/36 *Aedes albopictus* mosquito cells, with only a small percentage (1-2%) of cells producing viral antigen. When VLPs are incubated with C6/36 cells, only a similar small percentage of cells bind antigen. Thus, it seems that only a small percentage of C6/36 cells have exposed cellular receptors located on their surface. To identify the molecules responsible for binding AeDNV, a virus overlay protein blot assay and a pull-down assay were performed with biotinylated densovirus-like particles. Three cellular proteins, with approximate molecular weights of 220, 110 and 67 kDa, that specifically bind AeDNV were identified in both assays as putative virus receptors. Binding of the AeDNVLPs was blocked when blots were first incubated with AeDNV with a virus to cell ratio of 10,000.

The performance differences between anion exchange resin and membrane adsorbers for trace impurity removal in biomanufacturing processes were investigated. The ability of anion exchange membranes and resins to remove HCP from monoclonal antibody feedstocks was evaluated and compared based on several factors: load

density, HCP level in the feedstock, and residence time. Strength of binding was determined to be an indicator of HCP removal performance.

Rachel Specht
Department of Chemical and
Biological Engineering
Colorado State University
Fort Collins, Colorado
Summer, 2007

ACKNOWLEDGEMENTS

There is a multitude of people that I would like to thank and who contributed greatly during my PhD studies. The first is my wonderful husband Brian; thank you for your love, patience and constant support. My advisors Dr. Ranil Wickramasinghe and Dr. Jon Carlson thank you for working together and being there when I needed you. Many people at Colorado State that assisted in the research presented in my thesis. I would like to thank David Grzenia and Dr. Binbing Han for all of their work in virus ultrafiltration and Petra Gest for her hard work IFA staining yeast. I would like to thank all members past and present in the Carlson lab for helping me to learn how to do everything! Especially Dr. Dan Konet for teaching me so much. I would like to thank my committee members Dr. Larry Belfiore and Dr. Jim Linden. Last, I would like to thank my co-op manager at Genentech Inc., Dr. Chris Teske, who has been so supportive and a great mentor.

TABLE OF CONTENTS

LIST OF FIGURES

LIST OF TABLES

LIST OF ABBREVIATIONS

ABC: Avidin-biotin complex

AeDNV: *Aedes* Densonucleosis virus

AOX: Alcohol oxidase enzyme

BSA: Bovine serum albumin

Da_I: Damkohler number of the first kind

DAPI: 4',6-diamidino-2-phenylindole

ELISA: Enzyme-linked immunosorbant assay

FITC: Fluorescein isothiocyanate

HCP: Host cell proteins

IFA: Immunofluorescence assay

MAb: Monoclonal antibody

MPB: Model Protein B

MWCO: Molecular weight cut-off

NS1: Non-structural protein 1

NS2: Non-structural protein 2

OD600: Optical density at 600 nm

p*I*: Isoelectric point

QPCR: Quantitative polymerase chain reaction

QSFF: Q-Sepharose Fast Flow

SDS-PAGE: Sodium dodecyl sulfate- polyacrylamide gel electrophoresis

VLP: Virus-like particle

VOPBA: Virus-overlay protein binding assay

VP1: Viral major structural protein

VP2: Viral minor structural protein

Chapter 1

Purification of *Aedes* Densonucleosis Virus by Tangential Flow Ultrafiltration

1.1 Introduction

There is a growing need and interest in improved methods for virus purification. Improved virus purification techniques are needed in the biotechnology area including gene therapy, and vaccine manufacturing (Braas et al., 1996, Kamen and Henry, 2004). Current purification techniques in the laboratory are inappropriate for scale up production of viral vectors. Ultrafiltration is a good purification technique because it is operated at low temperatures and pressure and does not require chemical additives. Laboratory purification is typically carried out using ultracentrifugation. This method is very time consuming as one equilibrium centrifugation step can take over 20 hours (Bisht et al., 2002, Brumfield et al., 2004). Ultracentrifugation requires multiple cycles and can be very time consuming.

There is potential to develop *Aedes* densonucleosis virus (AeDNV) as a vector control agent (Afanasiev and Carlson, 2000, Carlson et al., 2006). The development of AeDNV for use as a marketable biocontrol agent requires a purification process that

is simple and inexpensive. Previous work has shown *A. albopictus* C6/36 cells can be adapted to grow in serum free medium and be used for the production of mosquito densovirus. The scale up of C6/36 cells from adherent cells to cell suspension in a spinner flask shows that the cells can be grown continuously in a bioreactor. This characteristic makes the production of mosquito densovirus more economically feasible (Suchman and Carlson, 2004).

1.1.1 Ultrafiltration

Tangential flow ultrafiltration is frequently used in the biopharmaceutical industry for bioreactor harvesting, purification, concentration and buffer exchange of protein products. However, few published studies are available in the literature on the use of tangential flow filtration for the recovery and purification of virus particles. Ultrafiltration has largely replaced size exclusion chromatography in biological manufacturing processes (van Reis and Zydney, 2001). Ultrafiltration membranes are design to reject proteins greater than a specified molecular weight based on the pore size of the membrane. Ultrafiltration membranes are rated by molecular weight cut off (MWCO). Proteins above the MWCO given in kDa are rejected by the membrane and remain in the retentate while proteins below the MWCO pass through the membrane into the permeate stream in tangential flow filtration.

Normal flow ultrafiltration has been implemented for virus filtration in the biotechnology industry (van Reis and Zydney, 2001; Christy and Vermant, 2002). The goal of the virus filtration is to remove potential viral contaminants from the

product of interest. Viruses are rejected by the membrane and the biological product of interest passes into the product stream.

In our case AeDNV is the product of interest and the aim is to keep the virus in the retentate stream while allowing host cell proteins and other contaminants to pass through the membrane into the permeate stream. The recovery and purification of viruses has relevant applications in gene therapy and viral vaccines. Several tangential flow ultrafiltration membranes with molecular weight cut offs of 30, 50, 100, 300 kDa have been evaluated for their virus purification characteristics.

1.1.2 *Aedes* Densonucleosis Virus

Aedes Densonucleosis Virus (AeDNV) is a parvovirus that infects *Aedes aegypti* mosquito. The *Aedes aegypti* mosquito is a carrier of both the virus that causes yellow fever and dengue virus. Densonucleosis virus, also called densovirus, has been found in many species of insects of different orders. Densovirus was first observed by French scientists in *Galleria mellonella* caterpillars in 1964 (Fédière, 2000). Densovirus was first detected in *Aedes aegypti* laboratory mosquitoes at Kiev State University (Buchatsky, 1989).

Aedes densonucleosis virus is a member of the family Parvoviridae. Parvoviridae are small icosahedral non-enveloped viruses that contain negative sense single stranded linear genome (Afanasiev and Carlson, 2000). The AeDNV virion is 18-20 nm in diameter. There are four proteins encoded in the genome: non-structural protein 1 (NS1), non-structural protein 2 (NS2), virion (capsid) major structural protein (VP1),

and virion (capsid) minor structural protein 2 (VP2). The genome and virus expression is diagramed in Figure 1.1. The major protein VP1 has a molecular weight of 40 kDa. VP1 cleaves to form VP2. There are 60 VP proteins per virion made up of a combination of major and minor VP proteins. The isoelectric point of VP1 is 8.02, the isoelectric point of the virion is 5.6 (Buchatsky, 2003). The non-enveloped virus is stable under harsh conditions. AeDNV is able to withstand temperatures of 60°C and pH from 1 to 12 and is resistant to organic solvents such as ester and chloroform. Field tests have shown infectivity of the virus remains after 1 year in water (Buchatsky, 1989).

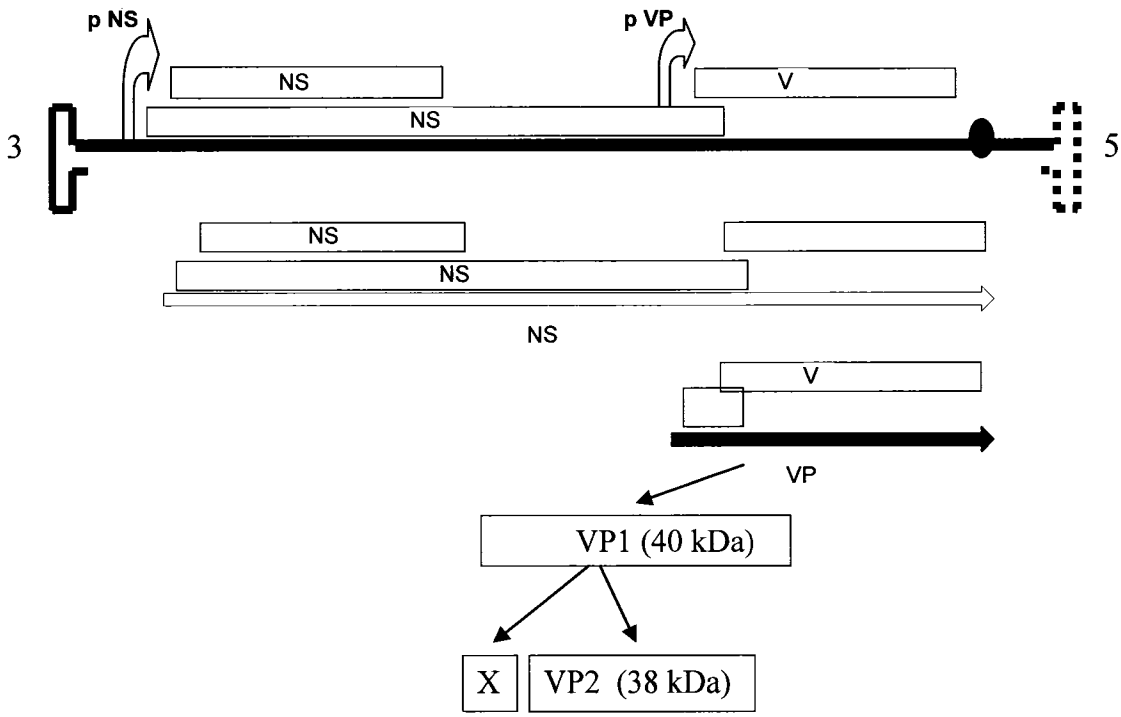

Figure 1.1: AeDNV genome and expression

The complete DNA sequence for AeDNV was determined in 1991; in 1994 an infectious clone of the AeDNV genome, pUCA, was made (Afanasiev et al., 1991, 1994). pUCA is used as a vector for delivery of foreign genes in cell culture and mosquitoes. A double subgeonomic Sindbis virus (TE/3'2J/VP) has been engineered to express the structural proteins of AeDNV. Using TE/3'2J/VP to express the structural proteins and an infectious clone of AeDNV to express the non structural protein eliminates the possibility of recombination resulting in wild-type infectious virus (Allen-Miura et al., 1999). Transfection of C6/36 cells with TE/3'2J/VP plasmid leads to the expression VP1 resulting in empty virus formation. AeDNV that expresses green fluorescent protein (GFP) from the pNS promoter has been made, the construct that expresses the GFP protein as a fusion protein to the NS1 C terminus showed the highest level of GFP expression. Transducing virions with the NS1-GFP gene are used to infect mosquito larvae. Expression of GFP allowed for the study of organs that are infected with the virus. The anal papillae were the most commonly infected organ system early in the infection (Afanasiev et al., 1999)

AeDNV is a good model parvovirus because of the simple well defined cell culture protocols in mosquito cells and absence of cytopathic effects. Mosquito cell culture is less expensive than mammalian cell culture that is needed to produce parvoviruses of interest such as adeno-associate virus and minute mice virus. Currently AeDNV particles are purified from cell culture and mosquitoes by ultracentrifugation using density gradients. This process is time consuming, the use of tangential flow

ultrafiltration may allow for short processing time and more efficient purification process.

1.2 Materials and Methods

1.2.1 Production of AeDNV Particles in Serum and Serum-Free Media

C6/36 *Aedes albopictus* cells (Igarashi, 1978) were grown in a 28°C incubator to an approximate 80% monolayer in 75-cm^2 flasks maintained by Leibovitz's L-15 media (Gibco, Invitrogen, Carlsbad,CA) supplemented with 10% fetal bovine serum and 1% penicillin-streptomycin (Invitrogen). Effectene Transfection Reagent (Qiagen, Valencia, CA) was used to transfect C6/36 cells according to the manufacturer's protocol for adhered cells. The cells were transfected with pUCA plasmid (Afanasiev, et al., 1994). The cells were incubated at 28°C for 8 to 16 hours, then the complex was removed, the cells were washed twice with phosphate buffered saline and fresh supplemented media was added. The transfected cells were lysed by freezing and thawing three times 60 hours post transfection. The cell lysate was transferred to conical tubes and centrifuged in a Beckman GS-6R centrifuge (Beckman, Fullerton, CA) at 3750 rpm for 15 minutes at 4°C to remove cellular debris. The supernatant containing AeDNV particles were filtered using a 0.45 μm sterilized filter (Nalge Nunc International, Rochester, NY) and then stored at -80 °C for future use. The AeDNV particles produced by this cell culture technique are referred to as virus in serum medium.

AeDNV particles were also produced using the *A. albopictus* cell line C6/36 in a serum-free medium (Suchman and Carlson, 2004). The cells replicate faster when grown in serum-free medium compared to serum medium grown cells. Cells were grown in T-75 flasks containing 14 ml of serum- and protein-free medium (SFPFM) (SF-900 II SFM, Invitrogen Corporation, Grand Island, NY) at 28°C. When the cells reached 40% confluent, they were transfected with pUCA using a Qiagen Effectene kit. The media was changed 8-18 h post-transfection to remove the pUCA plasmid. Transfected C6/36 cells were then transferred from the T-75 flask to a 100 ml spin flask (stirred bioreactor) (Wheaton Science Products, Millville, NJ) at a cell concentration of 5.5×10^5 cell/ml. The total medium volume was 100 ml. The bioreactor was stirred at 300 rpm at 28°C. After 5-6 days, when the cell concentration reached approximately $5\text{-}6 \times 10^6$ cells/ml, cells were transferred to a second 500 ml bioreactor at a cell concentration of 5.5×10^5 cells/ml and a medium volume of 300 ml. About a week later, the cells were collected, frozen, and thawed three times then centrifuged at 3,750 rpm for 15 min at 4°C to remove cellular debris. The supernatant containing AeDNV particles was filtered using a 0.45 μm filter and stored at -80 C for future use. AeDNV particles produced by this cell culture technique are referred to as virus in serum-free medium.

The scale up from a 500 ml spinner flask to a 3 L Applikon bioreactor was briefly investigated. C6/36 cells were grown in suspension as previously described. Uninfected cells were diluted to a cell density of 5×10^5 cells/ml in SF-900 serum free medium (Invitrogen) and transferred aseptically to Applikon bioreactor system

with a 3 L stirred tank reactor with an ADI 1030 Bio Controller, ADI 1032 Stirrer Controller P100, and flow console (Applikon Dependable Instruments, The Netherlands). Stirrer speed was controlled at 250 rpm. Air was sparged into the reactor to maintain 20% dissolved oxygen. Temperature was controlled using an electric heating jacket at 28°C. Samples were collected and cell density was measured using a hemocytometer and 2% trypan blue to count live cells.

1.2.2 Tangential Flow Filtration

Tangential flow filtration was conducted using flat sheet Sartocon Slice 200 cassettes (Sartorius AG, Germany). Figure 1.2 shows the experimental setup. The Sartocon Slice 200 cassettes consist of four membranes 15 cm in length. The height of the feed channel is 200 μm. Four ultrafiltration membranes, Sartorius polyethersulfone 308 1465902E SG, 308 1465002E SG, 308 1466802E SG and 308 1467902E SG, with respective molecular weight cut offs (MWCO) of 30, 50, 100, and 300 kDa were tested in this study. All membranes had a nominal filtration surface area of 200 cm^2 (0.02 m^2).

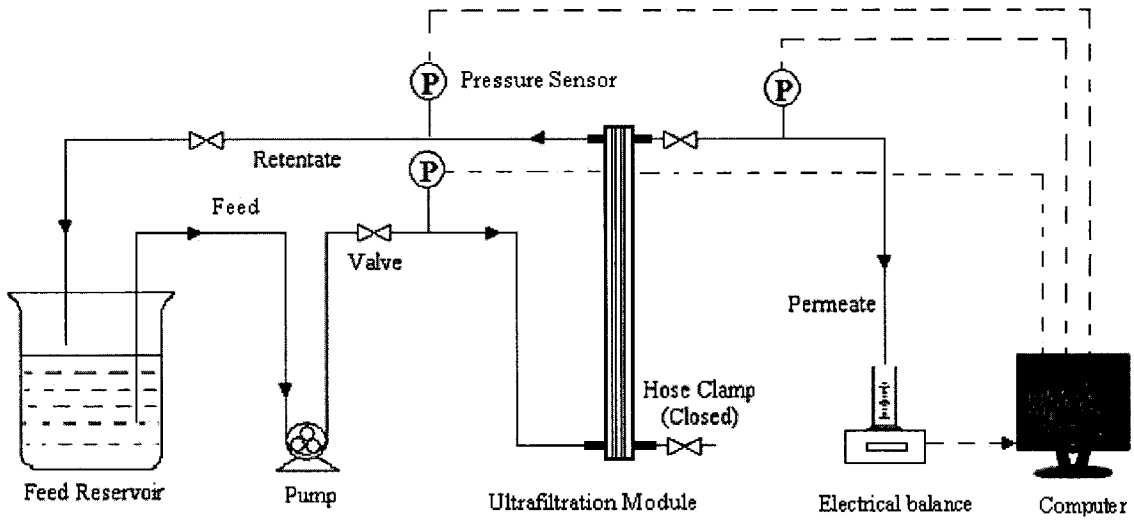

Figure 1.2: Experimental Setup

All experiments were run at a feed flow rate of 150 ml/min controlled by a peristaltic pump. The permeate flow was not controlled. All experiments were run in concentration mode (retentate was returned to the feed reservoir but not the permeate). The mass of permeate collected was measured by a balance (Mettler Toledo, Columbus, OH) and recorded by an online personal computer. The feed retentate and permeate pressures were measured by three micro switch sensing and control sensors (Honeywell International Inc., Morristown, NJ). The data were also automatically recorded on the same online personal computer.

The calculated average transmembrane pressure was around 0.4 bar with a variation from 0.35-0.45. Fluctuations in the instantaneous transmembrane pressure due to the action of the peristaltic pump were observed. The permeate side pressure was always close to zero. A very slight increase in the transmembrane pressure, about 0.02 bar,

was observed as the feed was concentrated due to an increase in the feed viscosity. Pressure readings were accurate to ±5% of the average value.

Prior to commencement of the virus filtration experiments, DI water fluxes were measured at the operating conditions used for the virus filtration experiments. After empting the reservoir of water, 500 ml of virus-containing medium was added to feed reservoir. The feed was pumped through the module at 150 ml/min while the permeate outlet was closed. After a few minutes, the permeate outlet was slowly opened. At regular intervals, 1 ml samples were taken from the feed, retentate and permeate for analysis of virus titer and protein concentration. This process was continued until 400-450 ml permeate had been collected, i.e., the contents of the feed reservoir were concentrated about 10 fold.

At the end of the virus filtration experiment, the membrane was flushed using DI water followed by 1 M NaOH solution at 50°C for 1 h. Then the DI water flux was measured. After cleaning it was ensured that the water flux was at least 95% of the initial water flux. The membrane was then stored in a 0.1 M NaOH solution supplemented with 20% ethanol by volume.

Samples of the feed, retentate and permeate were analyzed by QPCR assay for virus titer and protein concentration. All samples were analyzed in triplicate and average results reported.

1.2.3 PCR Assay

A quantitative real time PCR (QPCR) based assay was used to determine the virus titer in the infective solutions as AeDNV does not show cytopathic effects. The primers and probe were designed within a conserved region of the viral NS1 gene. Primer Express oligo design software (Applied Biosystems, Foster City, CA) was used to design forward primer CAT ACT ACA CAT TCG TCC TCC ACA A; reverse primer: CTT GCT GAT TCT GGT TCT GAC TCT T; TaqMan® Probe FAM CCA GGG CCA AGC AAG CGC CTA MRA. The reaction was performed in 96-well format skirted v-bottomed polypropylene micro plates (MJ Research, Inc., Waltham, MA) with optical caps (Applied Biosystems, Foster City, CA).

Real time PCR master mix is prepared using the Brilliant Quantitative PCR master mix (Stratagene, La Jolla, CA). Each well (20 µl/reaction) consisted of 4 µl unknown sample or standard DNA pUCA plasmid, and 16 µl master mix. The thermal cycling conditions were: stage 1 - 50°C for 2 min; stage 2 - 95°C for 10 min; stage 3 - 95°C for 15 sec; stage 4 60°C for 1 min, cycles of stage 3 and 4 were repeated 40 times. All reactions were performed in the Opticon 2 DNA Engine (MJ Research). Standards for PCR were prepared by serial dilution of pUCA from 10^9 to 10^3 genome equivalents/µl. The genome equivalents were calculated based on the assumption that 1 µg of pUCA is equivalent to 1.34×10^{11} genomes of AeDNV (Paterson et al., 2005).

All samples were analyzed three times, and average results are reported. The accuracy of the PCR assay was determined by analyzing 12 samples of the same infective solution and found to be within ±0.5 log units.

1.2.4 Total Protein Assay

Protein concentration was measured using a BCA protein assay kit (Pierce, Rockford, IL) following the manufacturer's instruction. Using a 96-well micro plate (Nalge Nunc International), 25 µl of unknown sample or standard albumin was added to the wells. Next 200 µl of working reagent was added to each well. The plate was covered and incubated at 37 °C for 30 min. After cooling to room temperature, the absorbance of each sample at 562 nm was measured using a micro plate spectrophometer (Benchmark Plus microplate spectrophometer, Bio-Rad Laboratories, Hercules, CA). As described by the manufacturer, the protein concentration is determined and reported with reference to a standard albumin solution provided by the manufacturer. All samples were analyzed in triplicate, and average values are reported. The accuracy of the protein assay is greater than 6% of the mean. Since the working range of the assay is 20-2,000 g/ml, samples were diluted 10-fold.

1.3 Results

The water fluxes for the four membranes are shown in Table 1.1. The variation of permeate flux as a function of time is given in Figures1.3 and 1.4. Results for the

four ultrafiltration membranes with medium from the C6/36 tissue cell culture with serum are shown in Figure 1.3. Flux through the four membranes with the medium from the experiments with C6/36 tissue cell culture grown in suspension in serum free medium. In both cell culture systems the 300 kDa membrane has the highest flux. The 100 kDa and 50 kDa have approximately equal fluxes due to differences in Sartorius membrane manufacturing processes. The 30 kDa membrane yields the lowest flux. There is a significant difference in flux between the two cell culture medias, the differences range from 37% to 54% for the membranes. The difference in flux is assumed to be caused by differences in media formulation. The formulation of L-15 is known, but the formulation of the SF-900 medium is unknown. The L-15 medium is formulated for adherent cells and does not contain antifoaming agents or surfactants, the SF-900 medium is formulated for cells grown in suspension and contains antifoaming agents or surfactants that may cause a difference in observed permeate flux. All membranes process equal volumes, therefore a higher permeate flux results in a short processing time. In all cases the water fluxes are higher than the media fluxes. This is not an unexpected result as the viscosities of the media are greater than water.

Molecular weight cut-off (MWCO)	DI water flux (L/m2/h)
30	28.7
50	68.1
100	55.3
300	104.1

Table 1.1: Deionized water flux

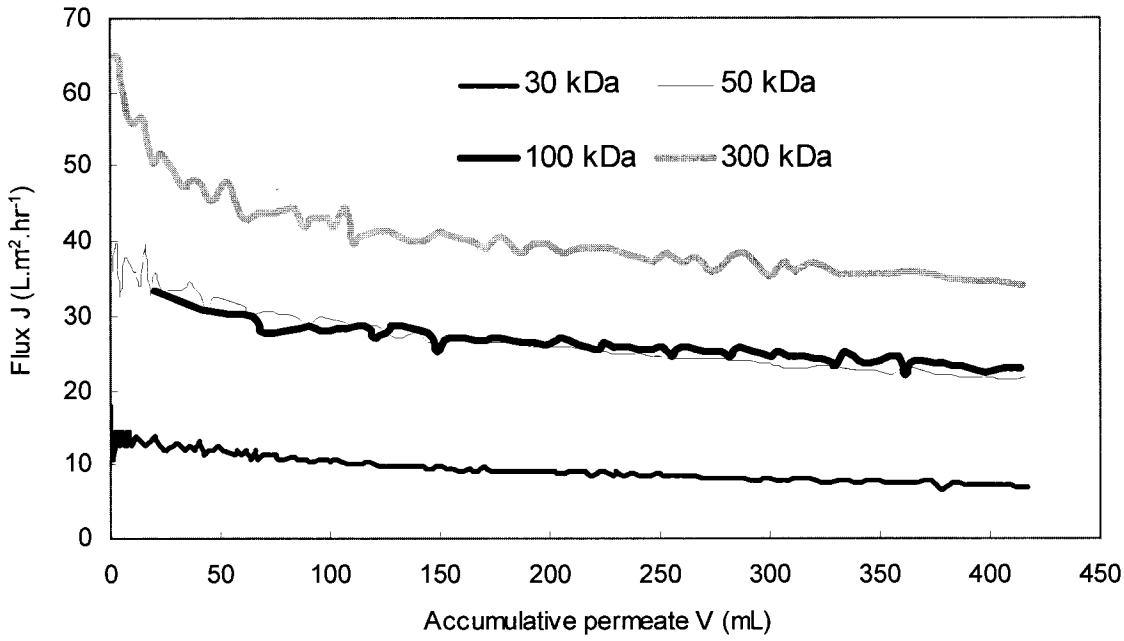

Figure 1.3: Variation of permeate flux with serum medium for the four ultrafiltration membranes. The 300 kDa has the largest flux, the 100 kDa and 50 kDa membranes have similar fluxes and the 30 kDa membrane has the lowest flux.

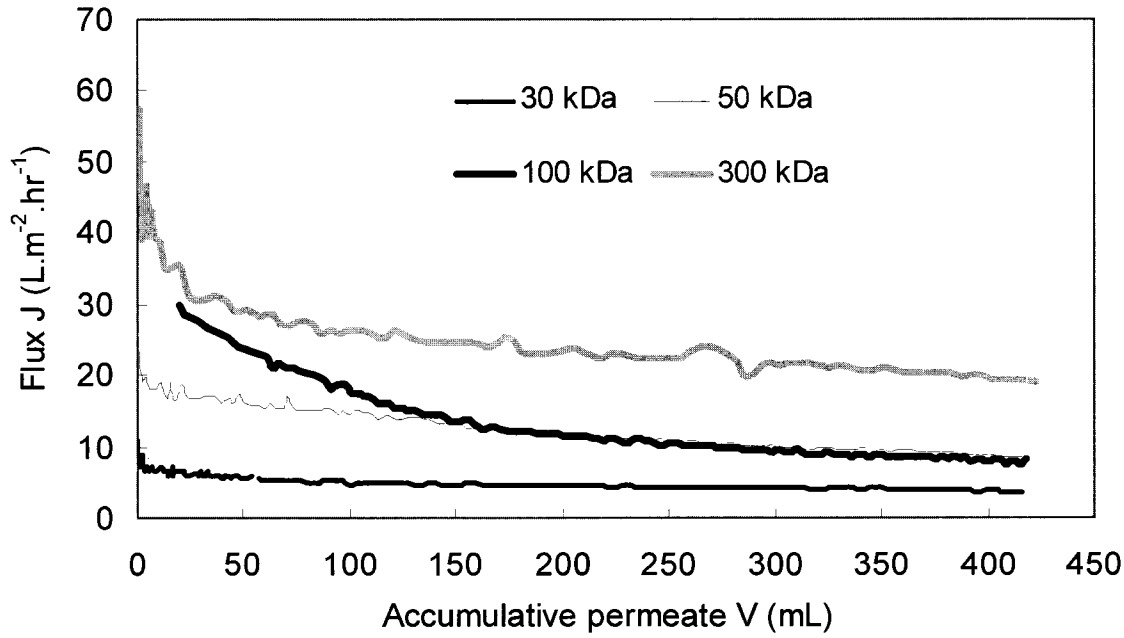

Figure 1.4: Variation of permeate flux with serum free medium for the four ultrafiltration membranes. The 300 kDa has the largest flux, the 100 kDa and 50 kDa membranes have similar fluxes and the 30 kDa membrane has the lowest flux.

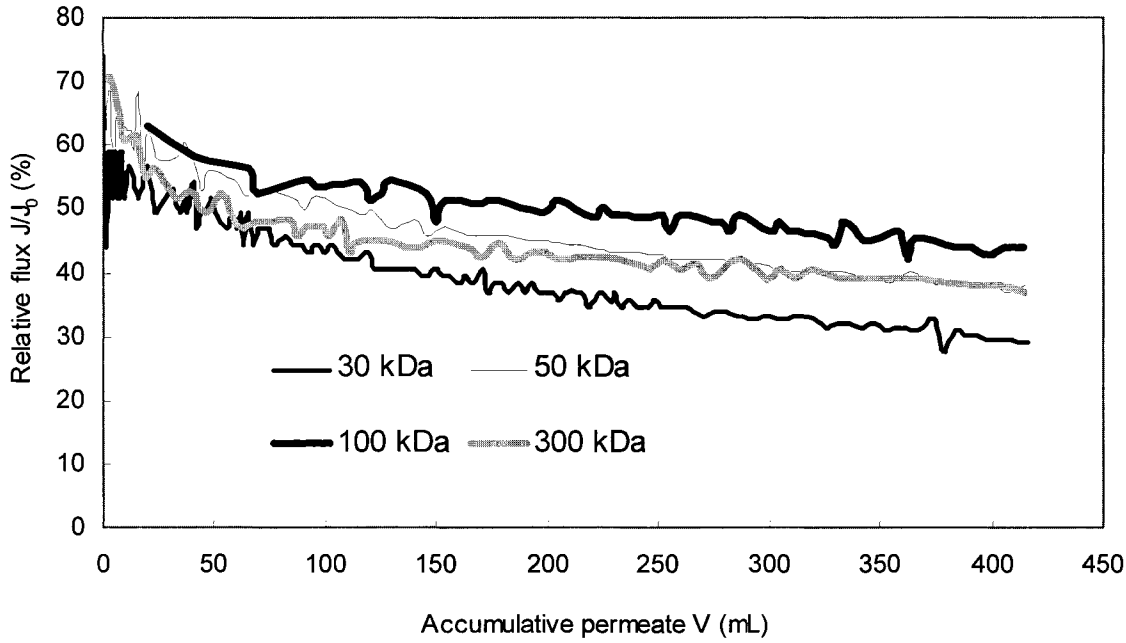

Figure 1.5 Variation of relative permeate flux with permeate volume for serum containing medium. The relative flux is defined as the measured flux divided by the water flux.

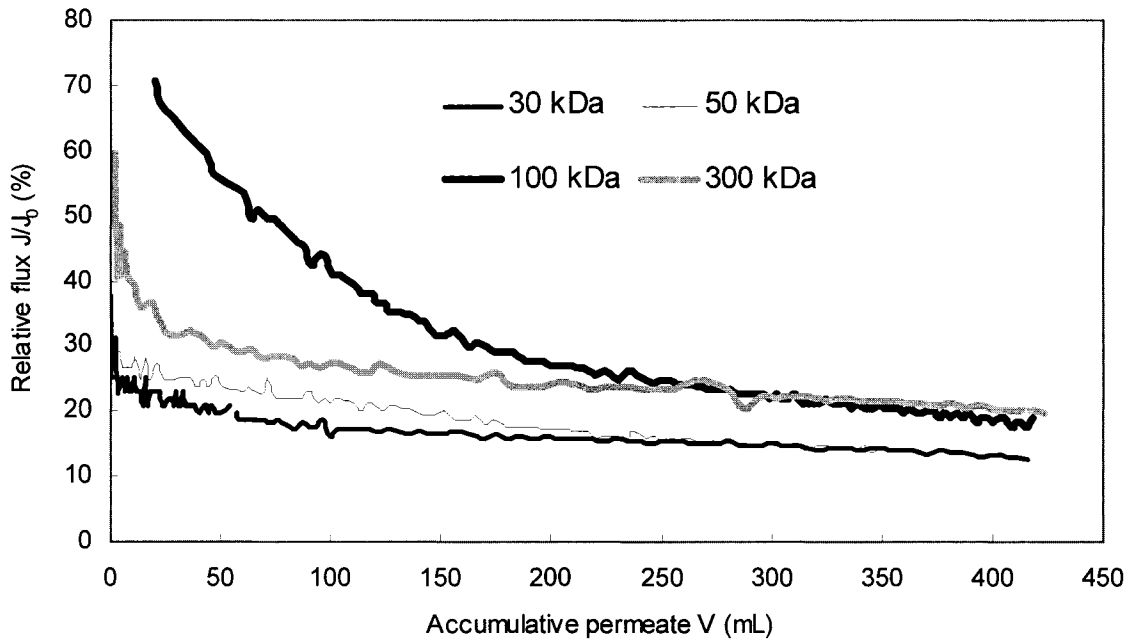

Figure 1.6 Variation of relative permeate flux with permeate volume for serum free medium. The relative flux is defined as the measured flux divided by the water flux.

Figures 1.7 to 1.10 show the variation of virus titer and protein as a function of accumulative permeate volume. Figure 1.7 shows the AeDNV virus titer in the retentate as a function of accumulated permeate volume for the serum cell culture. Samples were collected from the feed vessel, retentate and permeate vessel as every 25 ml of permeate collected. No AeDNV was detected in the permeate for the 30, 50, 100 kDa membranes. The total volume of retentate is reduced 10-fold, leading to a 10-fold increase in virus titer. The AeDNV titer increases over time for all membranes except for the 300 kDa. Virus is detected in the permeate of the 300 kDa membrane. In the case of the 300 kDa membrane the virus titer in the retentate decreases as the viral titer in the permeate increases, which indicates viruses pass through the membrane during the experiment. The first fraction collected from the permeate of the 300 kDa membrane shows a greater concentration of virus than the retentate. The membranes were evaluated with AeDNV produced in serum free cell culture; the results are shown in Figure 1.8. The AeDNV titer is lower in the serum free medium compared to the medium containing serum. As observed in the serum medium experiments, all virus is rejected by the 30, 50, and 100 kDa membranes, while AeDNV passes through the 300 kDa membrane and is detected in the permeate.

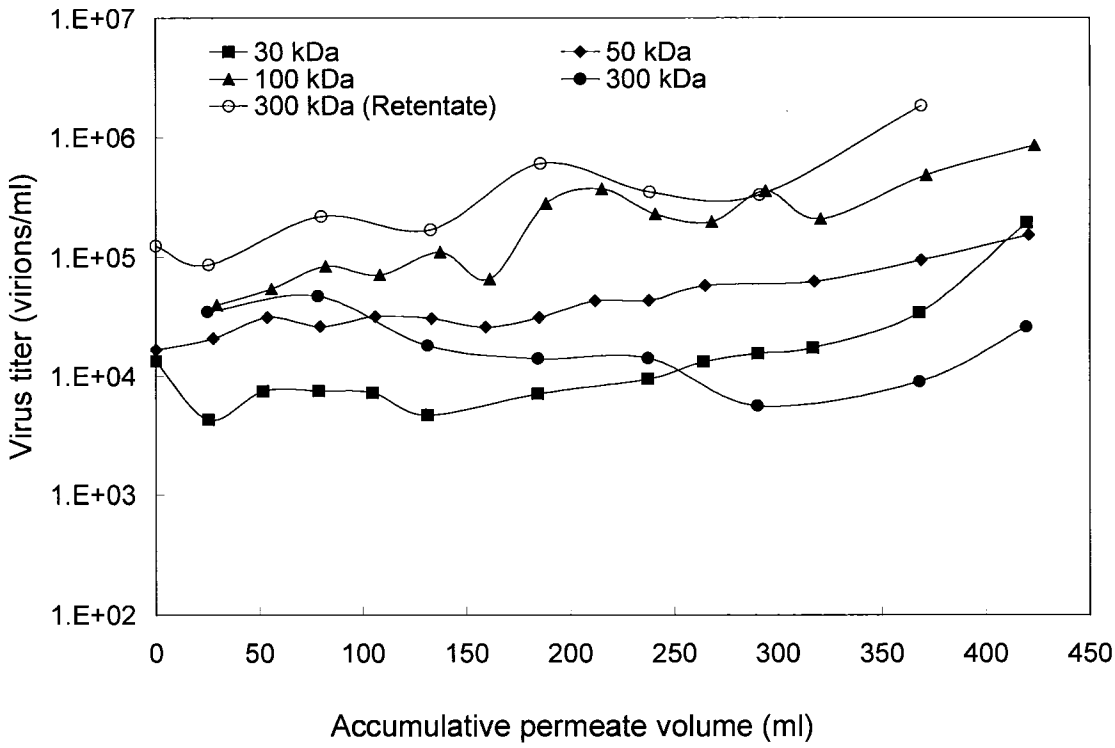

Figure 1.7: Virus titer (virions/ml) in the serum medium feed reservoir as a function of permeate volume collected.

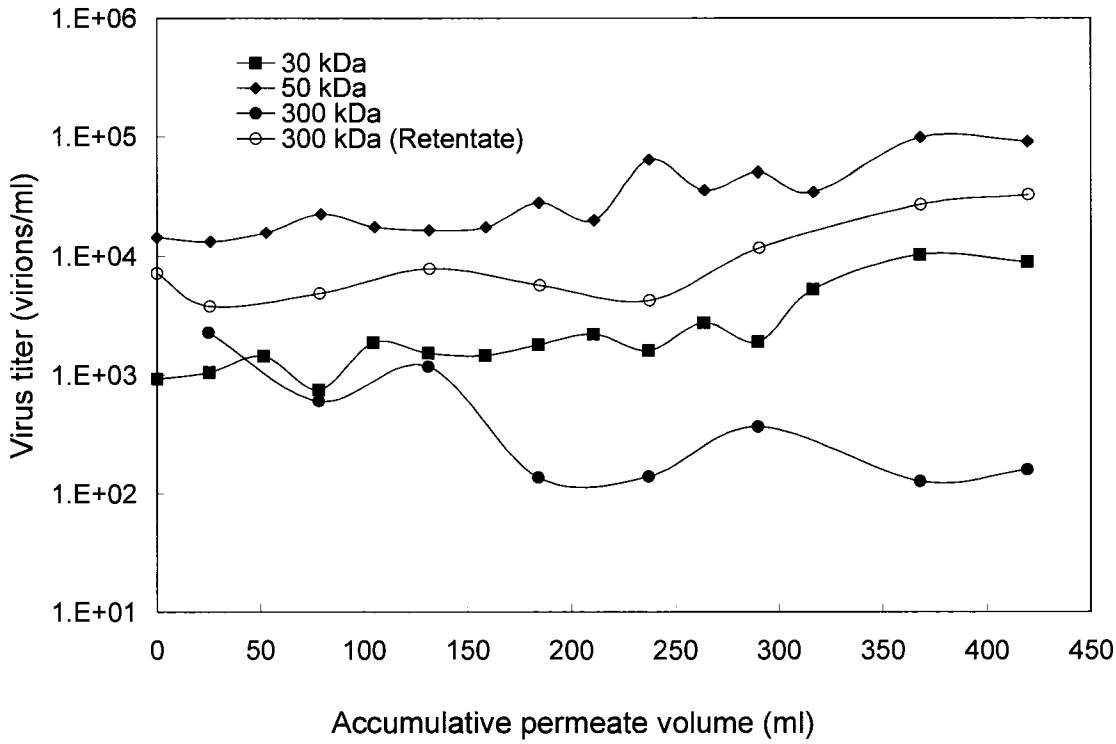

Figure 1.8: AeDNV viral titer (virions/ml) in the serum free medium feed reservoir as a function of permeate volume collected.

Figure 1.9 shows the protein concentration in the permeate and retentate as a function of the accumulated permeate volume for the serum medium. The host cell protein and protein contained in the serum are small in size and are expected to pass through all of the membranes. The protein concentration increases in the retentate for all membranes evaluated. The 30 and 50 kDa membranes have smaller pore sizes and therefore reject more protein then the 100 and 300 kDa membranes.

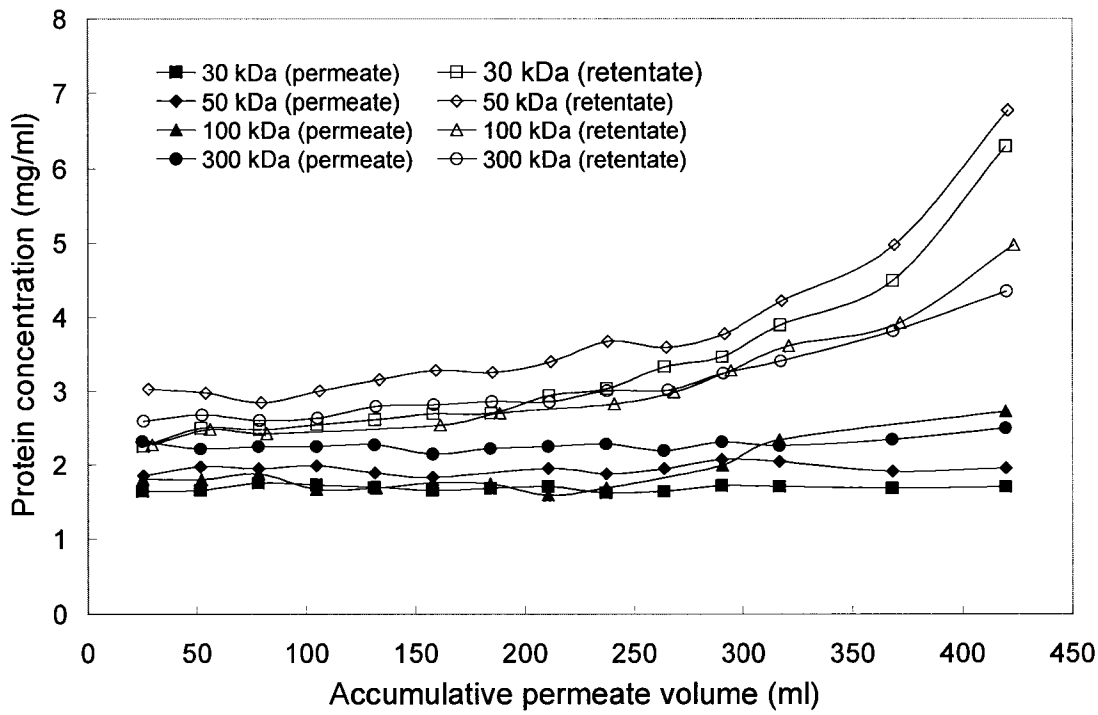

Figure 1.9: Total protein concentration as a function of collected permeate volume for serum cell culture.

Figure 1.10 shows the protein concentration in the permeate and retentate as a function of accumulated permeate volume for the serum free medium. The host cell proteins from the cell culture are expected to pass through all of the membranes as

previously observed in the serum experiments. The 50 kDa membrane rejects the most protein shown by the largest increase in total protein concentration. The 100 kDa membrane allows the greatest amount of protein to pass into the permeate. At the end of the filtration the 100 kDa retentate fraction has the lowest total protein concentration compared to the 30, 50, and 300 kDa membranes. This result differs from the serum medium experiments shown in Figure 1.9.

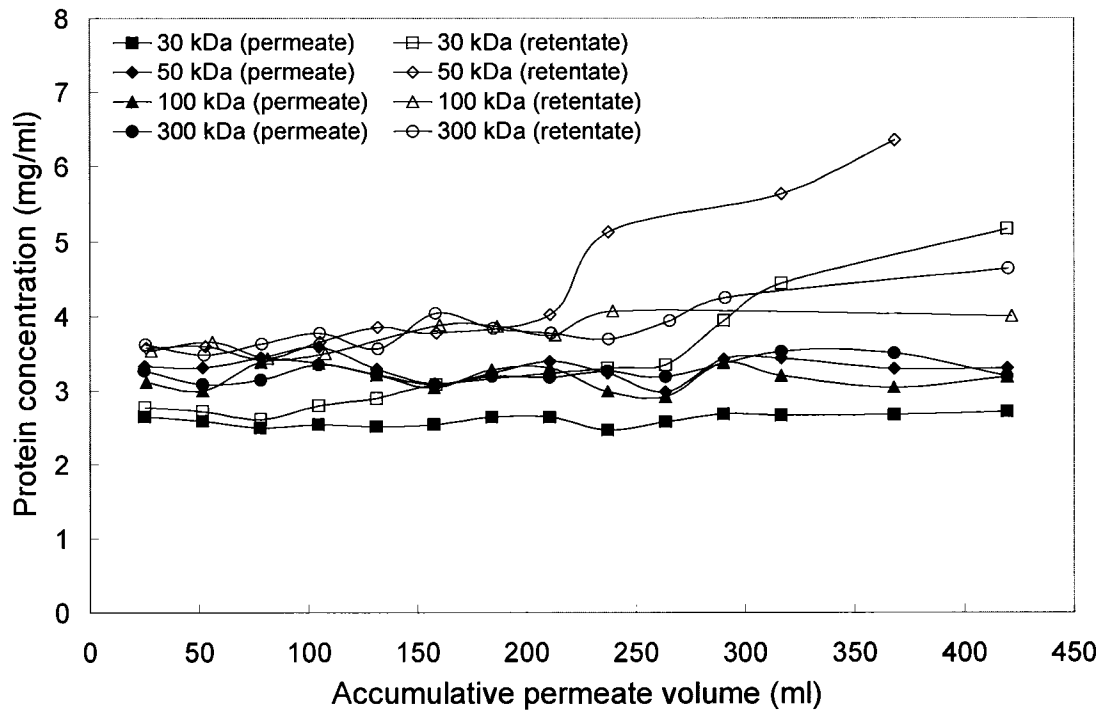

Figure 1.10: Total protein concentration as a function of collected permeate volume for serum free cell culture.

The scale up of uninfected C6/36 cells grown in serum free medium was investigated. The cell density (cells/ml) as a function of time (hr) is shown in Figure 1.11. Run 1 ended after 176 hours of in the bioreactor due to contamination. Run 2 ended after 96

hours due to contamination. The results show that C6/36 cells can be grown in a bioreactor and high cell densities are attainable. The scale up of C6/36 cells requires future experiments to determine the appropriate growth conditions.

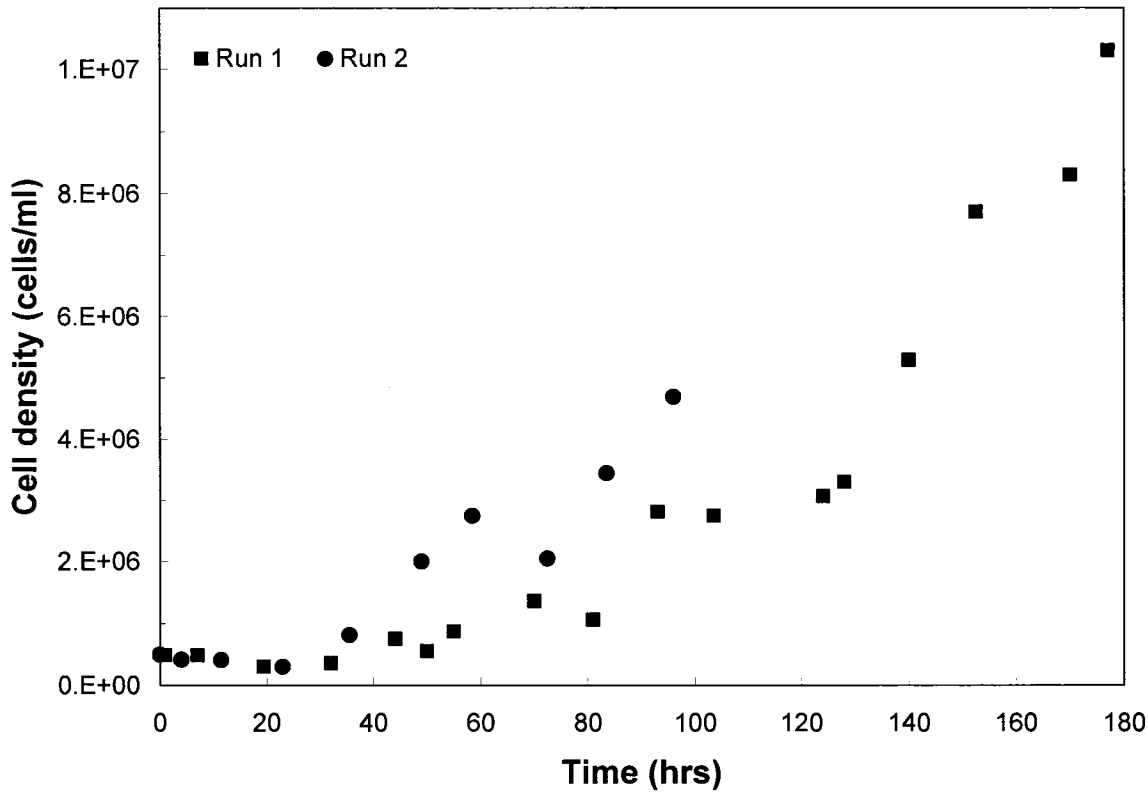

Figure 1.11: C6/36 cell density as a function of time.

1.4 Discussion

An ideal ultrafiltration membrane must reject virus and allow maximum host cell protein and protein present in the medium to pass through the membrane into the permeate. The flux of the membrane should be higher allowing short processing time. Based on these criteria the 100 kDa membrane shows the best separation characteristics. The 100 kDa membrane rejects virus, compared to the 300 kDa

membrane. The 100 kDa rejects less protein compared to the 30, and 50 kDa membranes in both serum and serum free media cases. The flux of the 100 kDa is in the middle range for the membranes evaluated.

For serum containing medium, Figure 1.5 indicates that the relative flux for the 300 kDa membrane is lower than the relative flux for the 100 kDa membrane. Figure 1.6 indicates that for the serum-free medium, again the flux for the 300 kDa membrane is similar to or lower than the relative flux for the 100 kDa membrane. Figure 1.7 and 1.8 indicate that virus particles pass through the pores of the 300 kDa membrane. Ultrafiltration membranes do not consist of parallel cylindrical pores, the pores are tortuous. A pore size distribution also exists. It is likely that some virus particles are trapped in the pores of the 300 kDa membrane leading to a greater drop in permeate flux compared to the 100 kDa membrane. Wickramasinghe et al., 2005 observed a similar result during tangential flow filtration of human influenza viruses. These virions are much larger than parvovirus at approximately 100 nm verses 20 nm in size. Using a 0.1 μm pore size microfiltration membrane, permeate fluxes were much lower that predicted on the basis of the fluxes for membranes with smaller pore sizes. Since human influenza virus particles have an average size of 100 nm, these particles can become entrapped within the pores of the microfiltration membrane.

1.5 Conclusions

Tangential flow ultrafiltration of AeDNV particles was conducted. Membranes with MWCOs of 30, 50 and 100 kDa reject the virus particles, whereas 300 kDa membranes do not completely reject the virus particles. The decrease in permeate flux during ultrafiltration is greatest for the 300 kDa membranes, suggesting entrapment of virus particles in the membrane pores. Further, the cell culture growth media has a strong influence on the permeate flux. All four membranes show some protein rejection. Since AeDNV particles are similar in size to large proteins, removal of large proteins in the permeate while concentrating virus particles in the retentate will require careful optimization of the membrane morphology and operating conditions.

References

Afanasiev, B.N., Galyov, E.E., Buchatsky, L.P., Kozlov, Y.V. (1991). Nucleotide-sequence and genomic organization of *Aedes*-densonucleosis virus. *Virology.* 185, 323-336.

Afanasiev, B.N., Kozlov, Y.V., Carlson, J.O., Beaty, B.J. (1994). Densovirus of *Aedes aegypti* as an expression vector in mosquito cells. *Experimental Parasitology.* 79, 332-339.

Afanasiev, B.N. and Carlson, J.O. (2000). Brevidensovirus Parvoviridae, Densovirinae. In Christian A. Tidona, Gholamreza Danai (Eds). The Springer Index of Viruses. Springer: New York.

Afanasiev B.N., Ward T.W., Beaty B.J., Carlson J.O. (1999). Transduction of *Aedes aegypti* mosquitoes with vectors derived from *Aedes* densovirus. *Virology.* 257, 62-72.

Allen-Miura, T., Afanasiev, B.N., Olson, K.E., Beaty, B.J., Carlson, J.O. (1999). Packaging of AeDNV-GFP transducing virus by expression of densovirus structural proteins from a sindbis virus expression system. *Virology.* 257, 54-61.

Bisht, H., Chugh, D.A., Raje, M., Swaminathan, S.S., Khanna, N. (2002). Recombinant dengue virus type 2 envelope/hepatitis B surface antigen hybrid protein expressed in *Pichia pastoris* can function as a bivalent immunogen. *J Biotechnol.* 99, 97-110.

Braas, G., Seale, P.F., Slater, N.K., Lyddiatt, A. (1996). Stategies for the isolation and purification of retroviral vectors for gene therapy. *Bioseparation.* 6, 211-228.

Brumfield, S., Willits, D., Tang, L., Johnson, J.E., Douglas, T., Young, M. (2004). Heterologous expression of the modified coat protein of Cowpea chlorotic mottle bromovirus results in the assembly of protein cages with altered architectures and function. *Journal of General Virology.* 85, 1049-1053.

Buchatsky, L.P. (1989). Densonucleosis of bloodsucking mosquitoes. *Diseases of Aquatic Organisms.* 6, 145-150.

Buchatsky, L.P. (2003). Personal communication. October 2003.

Carlson, J., Suchman, E., Buchatsky, L. (2006). Densoviruses for Control and Genetic Manipulation of Mosquitoes. *Advances in Virus Research.* 68, 361-392.

Christy, C. and Vermant, S. (2002). The state of the art filtration in recovery processes for biopharmaceutical production. *Desalination.* 147, 1-4.

Fédière, G. (2000). Epidemiology and pathology of densovirinae. In Faisst, S and J Rommelaere (Eds). Parvoviruses: from molecular biology to pathology and therapeutic uses. Karger: New York. p.p. 1-11.

Igarashi, A. (1978). Isolation of a Singh's Aedes *albopictus* cell clone sensitive to Denge and Chikungunya viruses. *Journal of General Virology.* 40, 531-544.

Kamen, A. and Henry, O. (2004). Development and optimization of an adenovirus production process. *J Gene Med.* 6, S184-S192.

Paterson, A., Robinson, E., Suchman, E., Afanasiev, B, Carslon J. (2005). Mosquito densonucleosis viruses causes dramatically different infection phenotypes in C6/36 *Aedes albopictus* cell line. *Virology.* 337, 253-261.

Suchman, E. and Carlson, J.O. (2004). Produciton of mosquito densonucleosis viruses by *Aedes albopictus* C6/36 cells adapted to suspension culture in serum-free protein-free media. *In Vitro Cellular and Developmental Biology- Animal.* 40, 74-75.

van Reis, R. and Zydney, A.O. (2001). Membrane Separations in Biotechnology. *Current Opn. in Biotech.* 12, 208-211.

Wickramasinghe, S.R., Kalbuß, B., Zimmermann, A., Thom, U. (2005). Tangential flow microfiltration and ultrafiltration for human influenza virus concentration and purification. *Biotech and Bioeng.* 92, 199-208.

Chapter 2

Expression of AeDNV major capsid protein VP1 in *Pichia pastoris* and scale up

2.1 Introduction

The methyltropic yeast *P. pastoris* is capable of metabolizing either glucose or methanol as its sole carbon source (Cregg et al., 1985). The first step in the metabolism of methanol is the oxidation of methanol to formaldehyde by the enzyme alcohol oxidase (AOX). When *P. pastoris* is metabolizing glucose, the AOX1 message is undetectable. AOX1 is only up-regulated in the presence of methanol. AOX has a poor affinity for oxygen, and *P. pastoris* compensates for this by producing large amounts of the enzyme. Under appropriate induction conditions, alcohol oxidase may account for as much as 30% of total cellular protein (Couderc and Baratti, 1980). The promoter region for the expression of the gene that encodes the enzyme alcohol oxidase 1 (AOX1) has been characterized and isolated and high levels of expression of recombinant proteins that are linked to the AOX1 promoter has been achieved (Cregg et al., 1989, Higgins and Clark, 1998). *P. pastoris* is able to grow in defined medium and high cell density fermentation protocols have been established (Stratton et al., 1998).

The *P. pastoris* expression system has been used to express well over 500 different proteins, many at concentrations, which make them of commercial interest (Cregg at al., 1993). Previous studies have shown the ability of VLPs to assemble in *P. pastoris*, the first being hepatitis B surface antigen (HBsAg). High-density fermentation resulted in expression levels of 0.4 g HbsAg /L of culture for use as a vaccine (Cregg et al., 1987). *Pichia pastoris* has been used as an expression system to produce many empty virus capsids as summarized in Table 2.1. Here we report the production of AeDNVLPs in *Pichia pastoris*.

Virus	Gene expressed	Reference
Hepatitis C virus	Core-E1	Falcon et al., 1999
Cowpea chlorotic mottle bromovirus	CCMV coat protein	Brumfield et al., 2004
Hepatitis C virus	HCcAg	Acosta-Rivero et al., 2001
Dengue virus	CprME	Sugrue et al., 1997
Dengue virus type 2 envelope protein fused with hepatitis B surface antigen	Den2E as a chimera with HBsAg	Bisht et al., 2001
Hepatitis B virus	HBsAg	Cregg et al., 1987
Bovine herpes virus	Glycoprotein D	Zhu et al., 1997

Table 2.1: Empty virus capsids expressed in *Pichia pastoris*

P. pastoris is an ideal candidate for growth in a bioreactor. Much of the work to determine the optimal growth conditions were characterized in the 1970s when *P. pastoris* was being developed as a single cell protein for animal feed. Over the past decade, the interest in *P. pastoris* for heterologous protein expression has increased tremendously. The number of proteins expressed in *P. pastoris* is well over 500. The production of virus-like particles for the development and manufacturing of vaccines in *P. pastoris* has been demonstrated by the development hepatitis B surface antigen,

dengue VLPs, and cowpea chlorotic mottle bromovirus VLPs (Cregg et al., 1989, Surgue et al., 1997, Brumfield et al., 2004). The process features and benefits that make P. pastoris of commercial interest are summarized in Table 2.2.

Feature	Process Benefits
Simple, defined nutritional requirements	Low fermentation media costs
Unicellular growth morphology	Mass transfer of nutrients in fermentation
Short doubling time and growth to high cell densities	High productivity and throughput
No specialized bioreactor required	Use of existing fermentation vessels
Potential for expression of soluble product	Process efficiency
Potentially few native proteins secreted, low protein background in media	Facilitates integrity and purification of the expressed protein
Posttranslational modifications	Product functionality
Absence of potential human adverse agents	Product quality

Table 2.2: Process features and benefits of producing recombinant protein in *P. pastoris* (Dale, 1999).

2.2 Methods and Materials

2.2.1 Cells and viruses

Production of AeDNV has been previously described (Paterson et al., 2005). Briefly, *Aedes albopictus* C6/36 cells were grown in Leibovitz's L-15 medium supplemented with 10% FBS and 1% penicillin-streptomycin. For preparation of virus the cells were grown to 60% confluency in 75 cm^2 tissue culture flasks and transfected with pUCA, an infectious clone of AeDNV (Afanasiev et al., 1994), using the protocol for stabled transfection of adherent cells with Effectene (Qiagen). On the forth day post transfection, the cells were lysed by freezing and thawing for three cycles. Cellular debris was cleared by centrifugation at 3000 x g.

2.2.2 Strains and vectors

E. coli DH5α and Mach1 strains were used as a host for DNA manipulations and cultured in low-salt LB medium supplemented with 250 μg/ml ampicilin or 100 μg/ml Zeocin for the selection of transformants. The wild type *P. pastoris* X-33 strain (Invitrogen) (Li et al., 2001; Schilling et al., 2001) was made chemically competent using the Pichia EasyComp™ Transformation Kit (Invitrogen). *P. pastoris* was cultured in YPD (Yeast extract, peptone, dextrose) and supplemented with 1M sorbitol and 100 μg/ml Zeocin for the selection of transformants. MGY or MMY (1.34% yeast nitrogen base, 100 mM potassium phosphate, 4 x 10-5% biotin, 1% glycerol or 1% methanol) media was used to grow the selected *P. pastoris* transformants and induce expression of the yeast optimized VP gene.

Codon optimization for expression of AeDNV VP in *P. pastoris* was performed by Genscript Corp (NJ). Genscript used a proprietary algorithm to optimize codon usage in the structural gene of AeDNV. The resulting optimized gene was placed in pUC57. All plasmids were constructed using standard techniques (Sambrook et al., 1989). The vector pPICZA (Invitrogen) is used as the expression vector for *P. pastoris*. pPICZA has pUC origin and has sequence homology for *P. pastoris*. pPICZA encodes the She ble gene for Zeocin resistance as a selectable marker. pPICZA was electroporated into DH5α. pPICZA has a multiple cloning site with single restriction sites EcoRI and ApaI after the 5' AOX1 promoter region.

Standard methods were used in the creation of AeDNV capsid expression vectors. The VP gene was cloned into the multiple cloning site of pUC57. pUC57 has ampicillin resistance. The VP gene was excised from pUC57 using the restriction enzymes EcoR1 and Apa1 and ligated in the same sites of pPICZA to create pPIC-VPO shown in Figure 2.1. The resulting plasmid were electroporated into DH5-α electrocompetent cells. Colonies that showed Zeocin resistance were screened using restriction digests and PCR. Several transformants containing the VP gene were isolated and sequenced. The native AeDNV VP gene was also inserted into pPICZA from the infectious AeDNV clone pUCA to form pPIC-VPN.

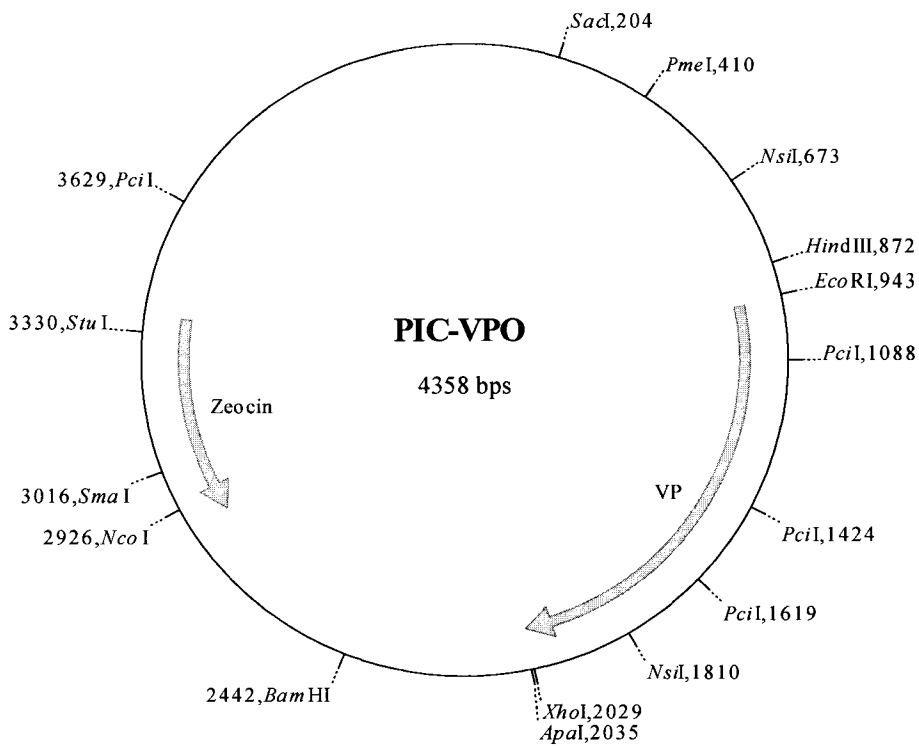

Figure 2.1: Plasmid PIC-VPO

2.2.3 Pichia transformation

VP expression plasmids were linearized with SacI and transformed following the manufactures protocol. The resulting transformation mixture was plated on YPDS plates supplemented with Zeocin. pPIC-VPN and pPIC-VPO were incorporated into the *P. pastoris* promoter region by homologous recombination.

2.2.4 PCR screening of Pichia transformants

P. pastoris transformants obtained using the Zeocin selection were analyzed for the presence of the VP gene insert by PCR. A single colony was picked from a plate that contained Zeocin and grown overnight in YPD medium. DNA was isolated using an Qiagen DNEasy tissue kit following the manufactures yeast protocol. The VP gene was amplified using the following AOX1 Pichia specific primers: 5'-GACTGGTTCCAATTGACAAGC-3' (forward primer) 5'-GCAAATGGCATTCTGACATCC-3' (reverse primer). Positive colonies were then grown in shaker flasks to assess expression levels.

2.2.5 Bioreactor

High cell density fermentation was carried out in an Applikon bioreactor system with a 3 L stirred tank reactor with marine type impeller, an ADI 1030 Bio Controller, ADI 1032 Stirrer Controller P100, and flow console (Applikon Dependable Instruments, The Netherlands). Fermentation was carried out similar to previously described methods (Stratton et al., 1998). The ADI 1030 controller has digital control outputs that are connected to a solenoid valve on the oxygen flowmeter, a masterflex

(Cole Palmer) variable speed pump for the cooling water in the cold fingers inside the vessel, a heating jacket, and fixed flow rate pumps for delivery of base to control pH. Cooling during high cell density fermentation is essential.

Fermentation basal salt medium (26.7 ml 85% H_3PO_4, 0.93 g $CaSO_4 \cdot 2H_2O$, 18.2 g K_2SO_4, 14.9 g MgSO4·$7H_2O$, 4.13 KOH, 40 g glycerol, per liter) was autoclaved in the vessel and allowed to cool to room temperature. The pH of the medium was kept constant at 5 using 28% ammonium hydroxide. The medium was supplemented with 2 ml trace salts solution PMT1 (6.0 g $CuSO_4 \cdot 5H_2O$, 0.8 g KI, 3.0 g $MnSO_4 \cdot H_2O$, 0.2 g $Na_2MoO_4 \cdot 2H_2O$, 0.2 g H_3BO_3, 0.5 g $CaSO_4 \cdot 2H_2O$, 20 g $ZnCl_2$, 65 g $FeSO_4 \cdot 7H_2O$, 0.2 g biotin, 5 ml conc. H_2SO_4, per liter). The medium was sparged with nitrogen and air to define 0% and 100% dissolved oxygen respectively. The dissolved oxygen level was set to 40% and maintained at this set point by the periodic addition of oxygen. Compressed air regulator was set at 10 psig and compressed oxygen regulator was set at 15 psig. The gases flowed into separate flow meters before being mixed and passing through two PolyVent 0.2 μm air filters.

The inoculum for the reactor was prepared by shaking 100 ml yeast cell culture in MGY overnight at 30°C until an OD600 between 2 and 6 is reached. The stirred tank reactor was inoculated and the stir speed is slowly ramped from 500 rpm to maximum of 1000 rpm. The DO control was set to 40%, temperature was controlled using the heating jacket and cold fingers at 30°C and pH of 5 is maintained by the addition of NH_4OH. The end of the first stage of fermentation is marked by an increase in

dissolved oxygen. The increase in DO indicates the glycerol is completely exhausted. The second stage is fed batch glycerol. A 50% w/v glycerol feed containing 12 ml PTM1 trace salts per liter of glycerol feed was fed at 9.2 ml/h/L initial fermentation volume. This stage last for 4 hr and further increases cell density. During the second stage DO spikes are perform to insure that glycerol was not accumulating in the vessel. A DO spike was preformed by shutting off the feed pump and timing how long it takes the dissolved oxygen to increase by 10%. At the end of stage two the glycerol feed pump was turned off and the DO increases rapidly to 100%. Stage three, methanol induction, began by feeding 100% MeOH into the stirred tank reactor at 3.5 ml/h. The feed rate was slowly increased over the next 7 hrs until a final feed rate of 9.5 ml/h was reached. DO spikes were preformed at hours 3, 5, and 7. The methanol induction stage was carried out between 30 to 70 hrs. Samples were taken every 24 hrs to analyze cell density and protein concentration.

2.2.6 Immunoblotting

For western blotting, denatured samples were resolved by 12-4% sodium dodecyl sulfate-polyacrylamide gel electrophoresis (SDS-PAGE) on a Bis tris NuPAGE gel (Invirotogen). The proteins were transferred electrophoretically to Hybond-ECL nitrocellulose membrane (Amersham, UK) using a NuPAGE blotting module (Invitrogen). Membrane was blocked for 1 h at room temperature or overnight at 4°C with phosphate buffered saline (PBS) (0.1 M NaCl, 2 mM KCl, 10 mM $NaHPO_4$, 1mM KH_2PO_4, pH 7.4) and Uniblock (Aspen Inc, Denver, CO). Blots were incubated with one of three polyclonal antibodies for 1 h at room temperature. AeDNV antisera made in rabbit, (generous gift of Dr. L. Buchatsky) which

recognizes only whole capsid, VP1 antisera made in goat that recognizes the first 20 amino acids of VP1 or VP2 antisera made in chicken that recognizes 21 amino acids in the VP protein post VP1-VP2 cleavage site (Cocalico Biologicals Inc). Blots were washed three times in PBS/0.1% tween 20. Membranes were incubated with species-specific secondary antibodies conjugated with horseradish peroxidase for 1 hr at room temperature. After three washes with PBS/0.1% tween 20 the HRP was developed using an Vector VIP staining kit.

2.2.7 Protein Quantification

Total protein concentration was determined using a BCA protein assay kit (Pierce). Samples were analyzed in triplicate. Bovine serum albumin was used as the standard protein. The A562 nm was measured using a microplate spectrophotomer Bio Rad Benchmark Plus.

2.2.8 Quantification of the AeDNV and VLPs

The concentration of AeDNV was determined by quantitative real time PCR using TaqMan probe as previously described by Paterson et al. 2005 and in Chapter 1 Section 1.2.3. Real-time PCR reactions were carried out in an Opticon 2 DNA Engine (MJ Research, Inc.). Standard curves were constructed using a series of 10-fold dilutions of pUCA. All samples were analyzed in triplicate.

The AeDNV empty capsid lacks a genome and therefore can not be quantified by real time PCR. An enzyme-linked immunosorbant assay was developed using known amount of AeDNV as standard. Graded amounts of semi-purified particles in PBS

were coated onto flat-bottom microtiter plates overnight at 37°C. Plates were blocked for 1 hr at 37°C with 2% BSA in PBS and washed five times with PBS/0.1% Tween 20. Bound particles were then reacted with AeDNV anti-serum raised in rabbits (generous gift from Dr. Leon Buchatsky) at a 1:1000 dilution in PBS with 0.1% Tween 20 for 1 hr at 37°C in a humid box and washed five times. Bound antibodies were detected using a 1:5000 dilution of peroxidase-conjugated goat anti rabbit IgG (Sigma) incubated for 1 hr at 37°C in a humid box. After washing five times with PBS, ABTS was reacted with HRP and color developed for 5-30 minutes. The A490 was measured using a microplate spectrophotomer Bio Rad Benchmark Plus.

2.2.9 Indirect Fluorescent Antibody Assay

An immunoflurescence assay (IFA) was preformed in solution according to methods described by Hasek et al., 2006. Briefly, cells are fixed using 7.4% formaldehyde centrifuged at 2000 rpm, washed with PEM buffer (0.1 M PIPES, 1mM EGTA, 1 mM $MgCl_2$). Cells are resuspended in permeablization buffer containing Zymolyase and Pepstatin A in KCP buffer (0.1 M K_2HPO_4, 0.033 M citric acid, pH 5.9). Cells are again centrifuged and resuspended in BSA/PEM buffer. Cells are then incubated with primary antibodies against AeDNV capsids raised in rabbit and VP protein raised in chicken, secondary antibodies are FITC anti-rabbit and ALEXA anti-chicken. Cells are mounted on polylysine-coated slides and visualized using an epifluorescence inverted microscope. Images were collected using a CoolSnap camera and software.

2.2.10 Electron Microscopy

Fractions from the sucrose gradient that were positive for capsid were further analyses by electron microscopy. AeDNV VLPs and native AeDNV capsid purified particles were adsorbed onto glow-discharge carbon coated grids for 2 min and negatively stained with 1% uranyl acetate.for 1 min. Samples were examined with a JOEL JEM 2000 EXII transmission electron microscope operating at 100 kV.

2.3 Results

Codon usage is critical to expression of high levels of recombinant proteins. Preferred codons are generally consistent across genes within a given genome and correlate with the most abundant aminoacyl-tRNAs present in a cell (Moriyama and Powell, 1997). Previous studies have shown that gene optimization often remarkably increases heterogeneous protein expression (Massaer et al., 2001; Sinclair and Choy, 2002; Woo et al., 2002; Yadava et al., 2003). The VP gene of AeDNV was optimized for codon usage that is more conducive to yeast. There is a large difference in the preferred codon usage between *P. pastoris* and AeDNV as shown in Table 2.3.

Amino acid	Preferred codon (AeDNV)	Frequency	Preferred codon (P. pastoris)	Frequency
Alanine	GCA/GCU/GCG/GCC	22/3/2/1	GCU/GCC	27/1
Arginine	AGA/CGA/CGC	13/4/1	AGA	18
Asparagine	AAC/AAU	16/10	AAC/AAU	25/1
Aspartic Acid	GAC/GAU	12/3	GAC/GAU	14/1
Cysteine	UGU	1	UGU	1
Glutamine	CAA/CAG	19/2	CAA	21
Glutamic Acid	GAA/GAG	20/1	GAG/GAA	13/8
Glycine	GGA/GGA/GGG/GGU	17/4/3/1	GGA/GGU	15/10
Histidine	CAU/CAC	4/2	CAU	6
Isoleucine	AUC/AUU/AUA	6/6/2	AUC/AUU	13/1
Leucine	CUA/UUG/UUA/CUU/CUC	7/5/3/2/2	UUG/CUC	18/1
Lysine	AAA/AAG	16/1	AAG/AAA	11/6
Methionine	AUG	17	AUG	17
Phenylalanine	UUC/UUU	10/3	UUC/UUU	12/1
Proline	CCA/CCU/CCG	12/2/1	CCA	15
Serine	UCA/AGC/AGU/UCG	10/4/3/1	UCU	18
Threonine	ACA/ACU/ACG/ACC	31/5/4/2	ACU	42
Tryptophan	UGG	5	UGG	5
Tyrosine	UAU/UAC	14/8	UAC	22
Valine	GUA/GUG/GUU	18/1/1	GUU	20
Stop	UAA	1	UAA	1

Percent Base	AeDNV	*Pichia pastoris*	Percent Difference
% A	42.43	31.94	24.73
% G	18.94	20.24	6.86
% T	18.48	26.56	43.72
% C	20.15	21.26	5.53

Table 2.3: Codon usage comparison between preferred codon usage for VP gene in AeDNV and *P. pastoris*.

P. pastoris was grown in a shaker flask and in a bioreactor. Figure 2.2 shows a plot of optical density measured at 600 nm (OD600) as a function of total growth time. One unit of OD600 is equivalent to 5×10^7 cells/ml. Methanol induction was started 24 hrs into the process. For the shaker flask shown in Figure 2.2 (A) the initial volume of MGY medium is 50 ml. After 24 h of growth, the cells are harvested by centrifugation and resuspended in MM medium to a final cell density of 1 OD600. This corresponds to a decrease in OD600 as the cells are diluted to a final volume is typically between 100 and 200 ml. The cell densities in the bioreactor and shaker flask reach a maximum and then decreases after 72 hrs of methanol induction, equivalent to 96 hrs total growth time. Cell density shown in Figure 2.2 (B) in the reactor reached a maximum OD600 of 490 corresponding to a wet cell weight 215 g/L. It was possible to obtain a high cell density and still maintain dissolved oxygen levels above 20% by increasing the stir speed and the periodic addition of pure oxygen into the air sparge stream. A marine type impeller and sintered steel gas sparger were used in the bioreactor configuration to ensure adequate oxygen delivery to the high cell density culture. Growth of *P. pastoris* in a bioreactor leads to an increase in final cell density and total protein expression as shown by an ELISA.

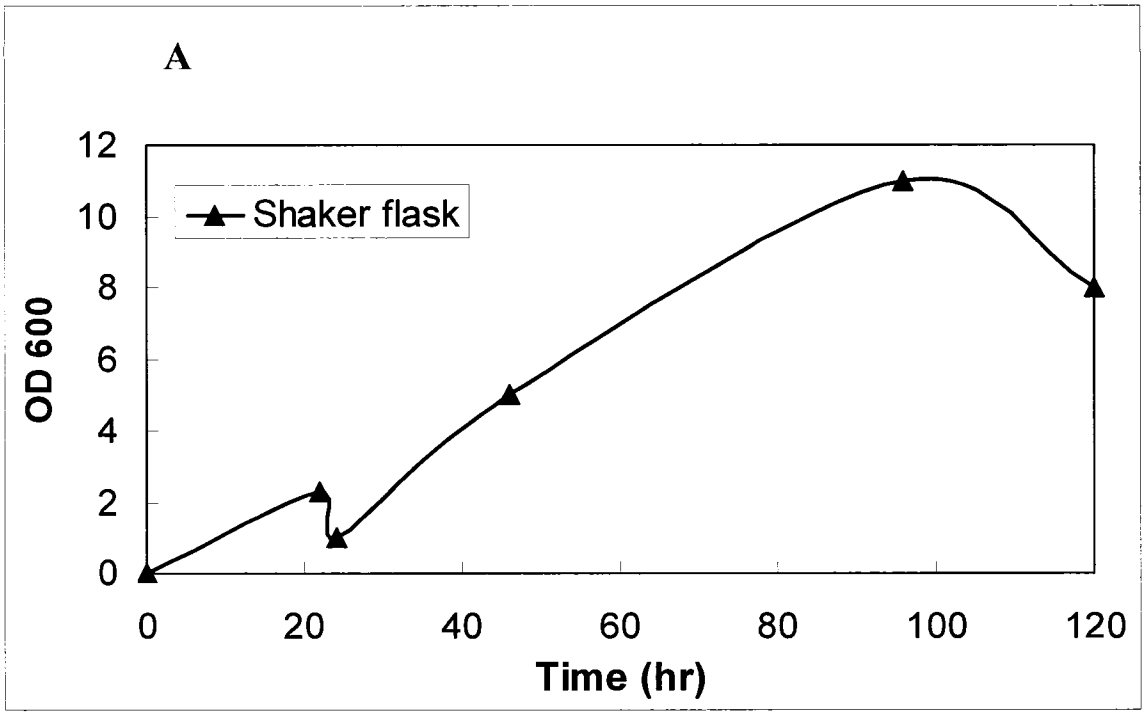

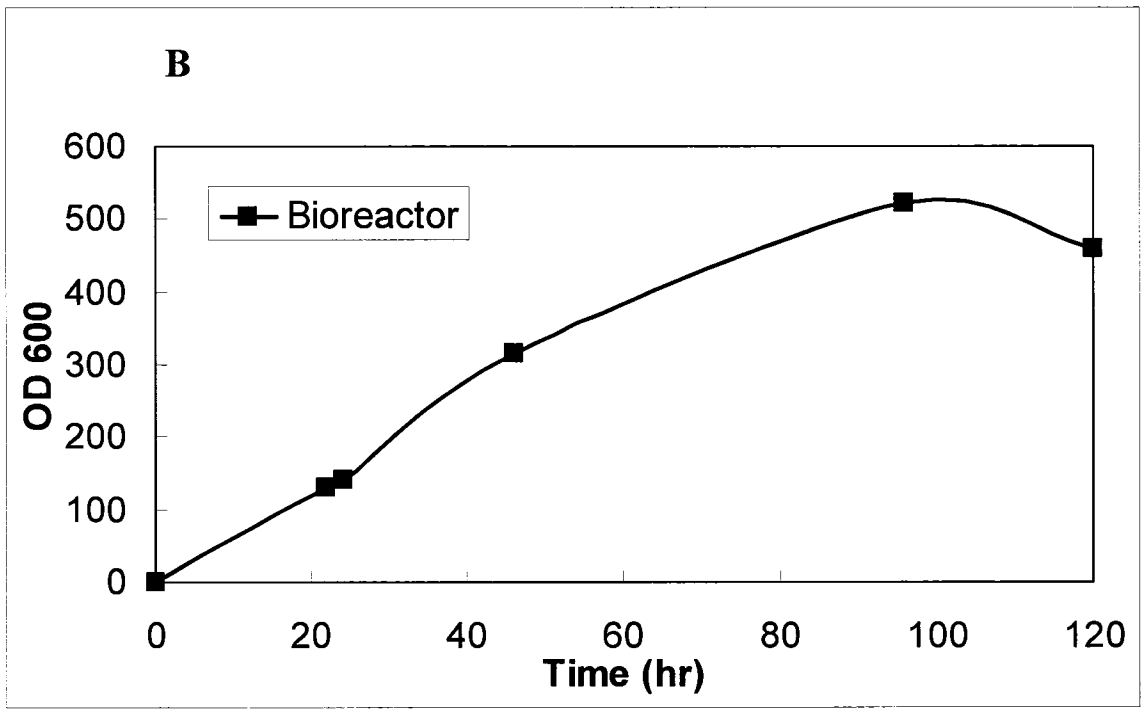

Figure 2.2: Pichia growth curve in shaker flask (A) and bioreactor (B).

A recombinant *P. pastoris* expressing the major structural protein of AeDNV was obtained by optimizing the VP gene from the infectious clone of AeDNV pUCA. Custom gene synthesis was performed by GenScript Corporation (Piscataway, NJ). GenScript used a proprietary algorithm to optimize codon usage for protein expression. The optimized VP gene was cloned into the vector pPICZA resulting in plasmid PIC-VPO shown in Figure 2.1. pPICZA shares sequence homology with *P. pastoris* in the alcohol oxidase region of the genome. The linearized plasmid was incorporated into the chromosome of *P. pastoris* by homologous recombination. Expression of the VP gene was upregulated in the presence of methanol. The structural proteins self assemble inside the yeast to form capsids that are recognized by polyclonal AeDNV antiserum as shown in Figure 2.3 (A) dot blot. The blot shows yeast cell lysate from colonies that contain the optimized gene as well as negative control with no gene and positive control AeDNV harvested from C6/36 cells transfected with pUCA. This antiserum recognizes only assembled particles and not denatured VPs.

AeDNV and VLP show similar size and morphology as shown by transmission electron microscopy. The VLPs have a dark center showing that the empty capsid absorbed the stain and therefore lacks a genome. Figure 2.3 (C) shows a transmission electron micrograph with 50000X magnification. The bar shows 50 nm as a reference. This analysis confirmed the VLPs are icosahedral and approximately 20 nm in diameter. Figure 2.3 (B) shows a western blot stained with α-VP2. As shown,

AeDNV from C6/36 cell culture has 2 bands, VP1 and VP2 with sizes 40 kDa and 38 kDa respectively. Only one band appears in the Pichia sample with size 40 kDa.

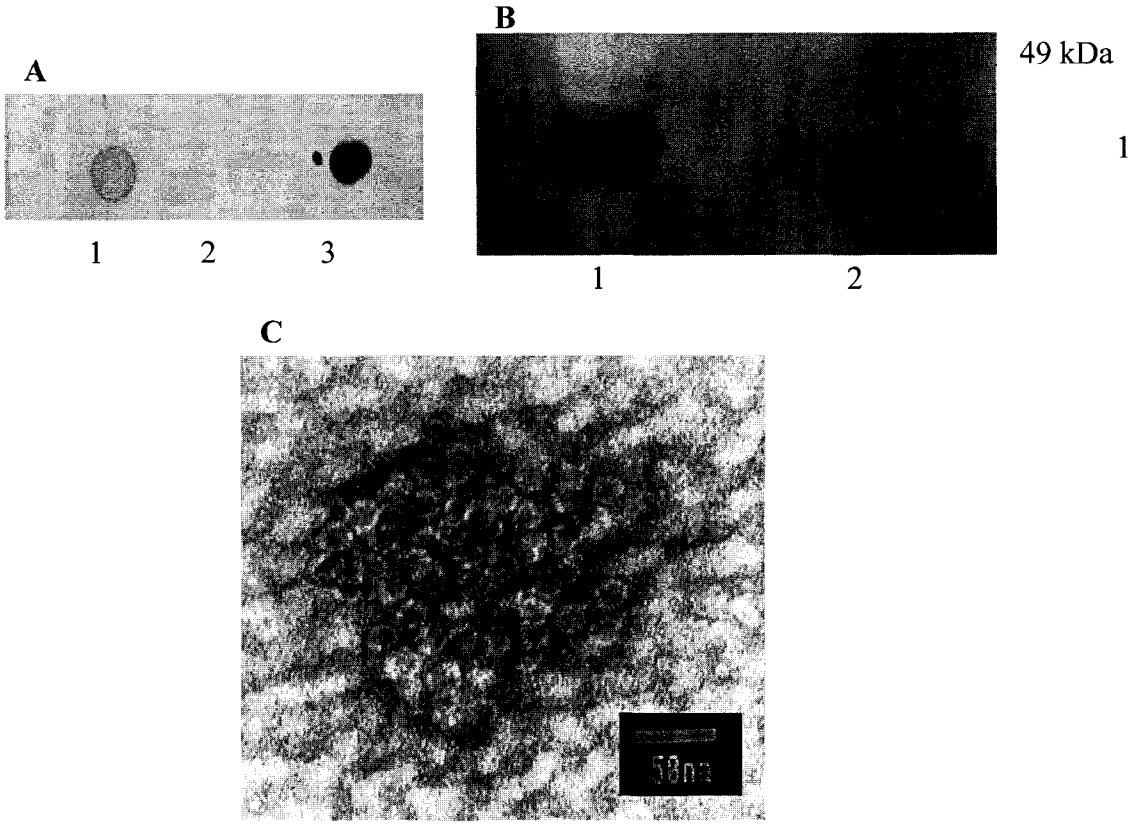

Figure 2.3: (A) Shows a dot blot to confirming expression and self assembly of VLP. (B) Western blot using a polyclonal VP2 oligopeptide antiserum. Column 1 shows VP1 and VP2 in native AeDNV with molecular weights of 40 and 38 kDa respectively, column 2 shows VP1 expressed in *Pichia pastoris*, VP1 is not cleaved to form VP2. (C) Transmission electron micrograph of VLP empty capsids (50000X magnification).

Figure 2.4 shows that little expression of VP1 is observed in the *P. pastoris* strain that has the native VP gene sequence from pUCA.

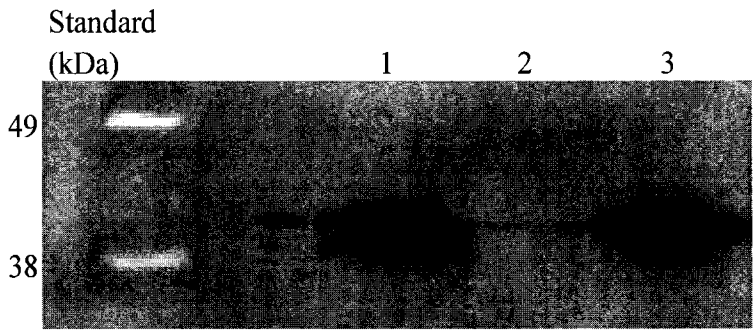

Figure 2.4: Expression of AeDNV structural protein, by optimization of codon usage. Western blot using polyclonal polypeptide specific to VP2. Molecular weight makers 49 kDa and 38 kDa are shown, followed by lane 1 that shows AeDNV particles isolated after transfection of C6/36 cells. Lane 2 shows no expression in *Pichia pastoris* when plasmid PIC-VPN containing native VP gene codon usage is used. Lane 3 shows VP expression in *Pichia pastoris* when plasmid PIC-VPO containing optimized VP gene is used, Pichia was grown under controlled growth conditions in a bioreactor.

The antigenticity of the VLPs was compared to AeDNV using polyclonal AeDNV antiserum in an enzyme-linked immunosorbant assay (ELISA). The AeDNVLPs were recognized by polyclonal AeDNV antiserum, showing similar absorption values compared to AeDNV across a range of antigen dilutions shown in Figure 2.5. This results shows that the immunodominant epitopes on the AeDNV capsid surface are also present on the VLPs. ELISA was also used to quantitate the increase in protein expression when *P. pastoris* was grown in a bioreactor compared to a shaker flask. A standard ELISA curve used to quantitate VLPs is shown in Appendix A.2.

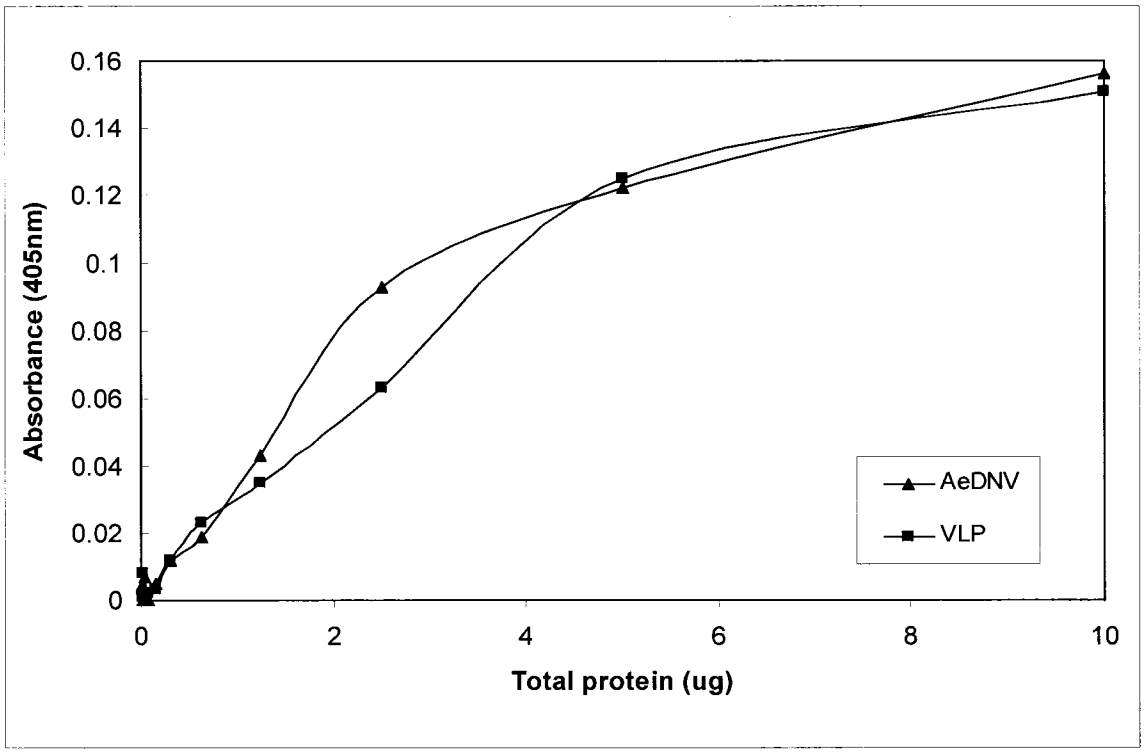

Figure 2.5: Antigenic comparison of AeDNV and VLPs. The plot shows absorbance at 405 nm as a function of increasing amounts of particles expressed as total protein in an ELISA using polyclonal AeDNV capsid antiserum. Negative controls have been subtracted from the total absorbance.

The AeDNV empty capsids were purified in order to perform transmission electron microscopy. Continuous sucrose gradients were ultracentrifudged, fractions were collected in 0.75 ml volumes. The fractions were analyzed using dot blot to find the VLP. The dot is shown in Figure 2.6 (A). The fraction D3 contains most of the VLP and was analyzed by TEM. SDS-PAGE was used to determine the purity of the D3 fraction. The resulting silver stained gel is shown in Figure 2.6 (B). The denatured VLP is shown as the AeDNV major structural protein VP1 having approximate molecular weight 40.5 kDa.

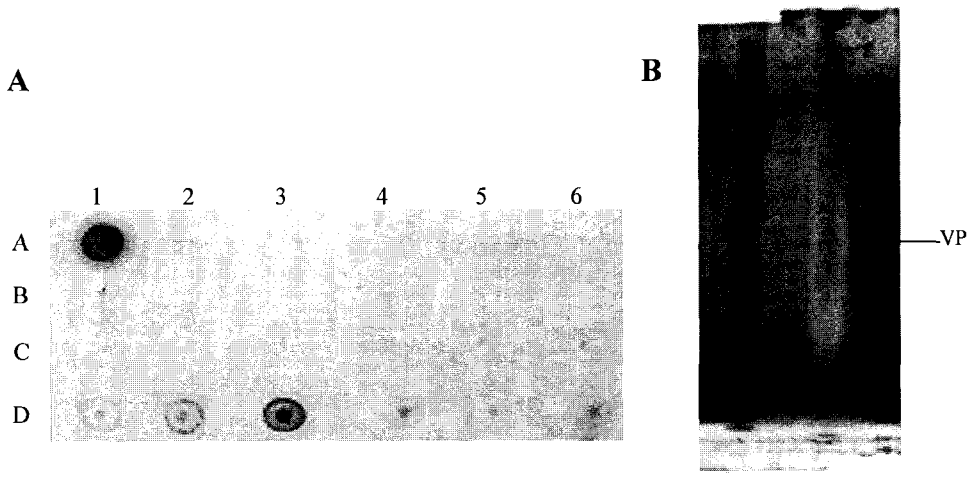

Figure 2.6: Purification of VLP from P. pastoris. (A) Dot blot of the sucrose density gradient ultracentrifugation of VLPs using polyclonal AeDNV antiserum, The left top dot (A1) shows VLP before the sucrose gradient. Ten microliters of gradient fractions from bottom to top fraction were applied from A2 to D6. Most of the VLP is present in the D3 fraction. (B) silver stained SDS-PAGE of fraction D3.

Indirect fluorescent antibody (IFA) assay was used to demonstrate that every transformed yeast cell is expressing the optimized VP gene. IFA was preformed according to protocols described by Hasek, 2006. Figure 2.8 shows the resulting IFA. Figure 2.7 (A) shows a micrograph of pPIC-VPO transformed yeast stained with DAPI, (B) shows the same yeast cells stained with a polyclonal antibody raised in rabbits against AeDNV capsids detected using FITC anti-rabbit polyclonal antibody. Figure 2.7 (C) shows yeast that was transformed with pPIC-VPN expressing the VP gene using the native gene sequence and stained with AeDNV capsid polyclonal antibody used in (B). No VLPs were detected in the yeast strain encoding the native gene sequence.

Figure 2.7: Immunofluorescence assay. Indirect fluorescent antibody (IFA) assay of *P. pastoris* transformed with pPIC-VPO (A) and (B) and pPIC-VPN (C) were fixed, permeabilized, and stained with the polyclonal antibody raised against AeDNV, followed by DAPI to visualize the nucleus. (A) shows *P. pastoris* cells strained with DAPI to visualize the cells, (B) shows VLPs expressed by Pichia and (C) shows cells transformed with pPIC-VPN.

2.4 Discussion

Table 2.2 shows a comparison of codon usage for native AeDNV VP gene and the new codon optimized VP gene. The native and optimized genes share approximately 80% sequence homology. The most abundant amino acid encoded in the gene is threonine in the native VP gene 4 different codons are used, the codon usage in the optimized gene was reduced to one preferred codon. The native gene uses up to five different codons for a single amino acid. While the maximum codons used in the optimized gene is two.

Figure 2.4 shows a western blot detecting the VP protein from *P. pastoris* transformed with pPIC-VPN and pPIC-VPO. The blot shows there is little to no expression of the VP protein in *P. pastoris* transformed with the native VP gene. Growth in the bioreactor resulted in higher expression of VP gene compared to a shaker flask. Codon optimization is essential to protein expression in *P. pastoris*.

Previous work has shown the native AeDNV structural proteins can be expressed in a double subgenomic Sindbis virus (TE/3'2J/VP) forming empty capsid. The RNA was transfected into BHK-21 cells and C6/36 *A. albopictus* (Allen-Miura et al., 1999). The resulting transfection and infection rates were similar to those observed in C6/36 cells, between one and two percent of the cells express the VP protein using the Sindbis virus expression system. By transforming *P. pastoris* using homologous recombination all of the yeast express the VP protein as demonstrated in Figure 2.7, all cells that are stained with DAPI are positive for AeDNV empty capsid. The yeast cells were also stained with polyclonal antibody raised in chicken against VP protein; this serum only recognizes VP protein, not capsids. There is very little VP protein detected in the yeast demonstrating that most of the VP protein expressed is self-assembling into empty capsids. High-cell density fermentation produced over 300 grams of yeast; all cells have VLP as shown by IFA. The Pichia expression system has a higher expression rate when compared to transfection of the TE/3'2J/VP plasmid into C6/36 cells and is more efficient for the sole production of VLPs.

2.5 Conclusions

Codon optimization is essential to AeDNV major structural protein expression in the methyltropic yeast *P. pastoris*. As observed in many other parvoviruses, only the major structural protein is required for capsid self assembly. *P. pastoris* is a low cost alternative to baculovirus protein expression systems as it is easily grown to very high cell densities. The high cell density makes it difficult to purify the VLP because of

the high levels of host cell protein present in the cell lysate. Empty AeDNV capsids can be used as a tool to gain further insight into mechanisms of infection.

References

Acosta-Rivero, N., Aguilar, J.C., Musacchio, A., Falcon, V., Vina, A., de la Roas, M.C., and Morales, J. (2001). Characterization of the HCV core virus-like particles produced in the methylotrophic yeast *Pichia pastoris*. *Biochem. Biophy. Resear. Commun.* 287, 122-125.

Afanasiev, B.N., Kozlov Y.V., Carlson J.O., Beaty B.J. (1994). Densovirus of *Aedes aegypti* as an expression vector in mosquito cells. *Experimental Parasitology*. 79, 332-339.

Allen-Miura, T., Afanasiev, B.N., Olsen, K.E., Beaty, B.J., Carlson, J.O. (1999). Packaging of AeDNV-GFP transducing virus by expression of densovirus structural proteins from a Sindbis virus expression system. *Virology*. 257, 54-61.

Bisht, H., Chugh, D.A., Swaminathan, S., Khanna N. (2001). Expression and purification of dengue virus type 2 envelope protein as a fusion with hepatitis B surface antigen in Pichia pastoris. *Protein Express. Pur*. 23, 84-96.

Brumfield S., Willits D., Tang, L., Johnson, J.E., Douglas T., Young, M. (2004). Heterologous expression of the modified coat protein of Cowpea chlorotic mottle bromovirus results in the assembly of protein cages with altered architectures and function . *J. Gen. Vir*. 85, 1049-1053.

Couderc, R. and Baratti, J. (1980). Oxidation of methanol by yeast, *Pichia pastoris*. Purification and properties of the alcohol oxidase. *Agric. Biol. Chem*. 44, 2279-2289.

Cregg, J.M., Barringer K.J., Hessler, A.Y., Madden, K.R. (1985). Pichia-pastoris as a host system for transformations. *Molecular and Cellular Biology* 5, 3376-3385.

Cregg, J.M., Tschopp, J.F., Stillman, C., Siegel, R., Akong, M., Craig, W.S., Buckholz, R.G., Madden, K.R., Kellaris, P.A., Davis, G.R., Smiley, B.L., Cruze, J., Torregrossa, R., Velicelibi, G., Thill, G.P. (1987). High level expression and efficient assembly of hepatitis B surface antigen in the methylotropic yeast, Pichia pastoris. *Bio/Technology*. 5, 479-485.

Cregg, J.M., Maddn, K.R., Barringer, K.J., Thill, G.P., Stillman, C.A. (1989). Functional characterization of the two alcohol oxidase genes from the yeast *Pichia pastoris*. *Molecular and Cellular Biology*. 9, 1316-1323.

Cregg, J.M.Vedvick, T.S., Raschke, W.C. (1993). Recent advances in the expression of foreign genes in Pichia-pastoris. *Bio-Technology* 11, 905-910.

Dale, C., Allen, A., Fogerty, S. (1999). *Pichia pastoris*: A Eukaryotic system for the large-scale production of biopharmaceuticals. *BioPharm.* 12(11): 36-42.

Falcon, V., Garcia, M., de la Rosa, M.C., Menendez, I., Seoane, J., Grillo J.M. (1999). Ultrastructural and immunocytochemical evidences of core-particles formation in the methylotrophic *Pichia pastoris* yeast when expressing HCV structural proteins (core-E1). *Tissue & Cell*. 31, 117-125.

Hasek, J. (2006). Yeast Fluorescence Microscopy. In W. Xiao (Eds). Methods in Molecular Biology vol. 313. Human Press, Totowa, NJ. pp. 85-96.

Higgins, D.R. and Cregg, J.M. (1998). Introduction to *Pichia pastoris*. In DR Higgins and JM Cregg (Eds). Methods in Molecular Biology: Pichia Protocols. Humana Press: Totowa, NJ. pp. 1-18.

Li, Z.J., Xiong, F., Lin, Q.S., d'Anjou, M., Daugulis, A.J., Yang, D.S.C., Hew, C.L., (2001). Low-temperature increases the yield of biologically active herring antifreeze protein in *Pichia pastoris*. *Protein Expression and Purification.* 21, 438-445.

Massaer, M., Mazzu, P., Haumont, M., Magi, M., Daminet, V., Bollen, A., Jacquet A. (2001). High-level expression in mammalian cells of recombinant house dust mite allergen ProDer p1 with optimized codon usage. *International Archieves of Allergy and Immunology.* 125, 32-43.

Moriyama, E.N. and Powell, J.R. (1997). Codon usage bias and tRNA abundance in Drosophila. *J. Mol. Evol.* 45, 514-523.

Paterson, A., Robinson, E., Suchman, E., Afanasiev, B, Carslon J. (2005). Mosquito densonucleosis viruses causes dramatically different infection phenotypes in C6/36 *Aedes albopictus* cell line. *Virology*. 337, 253-261.

Sambrook, J., Fritsch, E.F., and Maniatis, T. (1989). In Molecular Cloning, A Laboratory Manual, 2nd Ed. Cold Spring Harbor Laboratory Press, Cold Springs Harbor, NY.

Schilling, B.M., Goodrick, J.C., Wan, N.C. (2001). Scale-up of a high cell density continuous culture with *Pichia pastoris* X-33 for the constitutive expression of rh-chitinase. *Biotechnology Progress.* 17, 629-633.

Sinclair, G., Choy, F.Y.M. (2002). Synonymous codon usage bias and the expression of human glucocerebrosidase in the methylotrophic yeast, *Pichia pastoris. Protein Expression and Purification.* 26, 96-105.

Stratton, J., Chiruvolu, V., Meagher, M. (1998). High cell-density fermentation. In DR Higgins and JM Cregg (Eds). Methods in Molecular Biology: Pichia Protocols. Humana Press: Totowa, NJ.

Sugrue, R.J., Fu, J., Howe, J., Yow-Cheong, C. (1997). Expression of the dengue virus structural proteins in *Pichia pastoris* leads to the generation of virus-like particles. *Journal of General Virology.* 78, 1861-1866.

Woo, J.H., Liu, Y.Y., Mathias, A. (2002). Gene optimization is necessary to express a bivalent anti-human anti-T cell immunotoxin in *Pichia pastoris. Protein Expression and Purification.* 25, 270-282.

Yadava, A., Ockenhouse, C.F. (2003). Effect of codon optimization on expression levels of a functionally folded malaria vaccine candidate in prokaryotic and eukaryotic expression systems. *Infection and immunity.* 71, 4961-4969.

Zhu, X., Wu, S., Letchworth, G.J. (1997). Yeast-secreted bovine herpesvirus type 1 glycoprotein D has authentic conformational structure and immunogenicity. *Vaccine.* 15, 679-688.

Chapter 3

Identification of mosquito virus binding proteins using AeDNV empty capsids produced in *Pichia pastoris*

3.1 Introduction

Empty parvovirus capsids produced in natural infection of animals and tissue culture were first described by Richards et al. in 1977. Cotmore and Tattersall purposed capsid formation proceeds DNA insertion in 1987.

B19 parvovirus capsids were produced in baculovirus system by Kajigaya et al., 1991. VLPs were constructed because B19 lacks a good model cell culture system. B19 parvovirus required the expression of empty capsids for the development of serological assays and vaccine. Empty B19 capsids were expressed in recombinant baculovirus expression system. Plasmid constructs were made containing either the major VP2 or minor VP1 structural. Coexpression of VP2 and VP1 plasmids resulted in empty B19 capsids. Expression of VP2 alone resulted in VLP formation as well. Capsids were examined by electron microscopy and detected by anti-B19 parvovirus antiserum. The empty capsids are antigenically similar to native B19 capsids expressed in humans. The empty capsids were used in clinical assays for human

antibody to B19 parvovirus, results were identical to antigen from human infected sera.

Expression of VP2 major structural protein resulted in the formation of empty capsids as determined by electron microscopy and immunofluorescent assay. Rabbits were injected with high doses of VP1 and VP2 capsids and capsids made of only VP2. In both cases, the rabbits produced antibodies to capsid antigen. Only the empty capsids from the coexpression of VP1 and VP2 proteins resulted in neutralizing antibodies. Immunization with capsids containing only VP2 did not result in neutralizing antibody.

Table 3.1 summarizes parvovirus-like particles that have previously been expressed. The empty capsids have been developed as vaccines for animals and have been used as tools to better understand virus formation and structure. The viruses were all expressed in baculovirus expression system. Previous studies have shown only the major structural protein is required for capsid assembly.

Virus	Expression system	Structural proteins expressed	Reference
Human parvovirus B19	Baculovirus	VP1 and VP2	Brown et al., 1991, Kajigaya et al., 1991
Junonia coenia densovirus	Baculovirus	VP1, VP2, VP3 and VP4	Croizier et al., 2000
Canine parvovirus	Baculovirus	VP1 and VP2	Saliki et al., 1992
Minute virus of mice	Baculovirus	VP1 and VP2	Hernando et al., 2000
Adeno-associated virus type 2	Baculovirus	VP1 and VP2	Ruffing et al., 1992

Table 3.1: Parvoviridae empty capsids previous expressed

Empty parvovirus capsids have been used to investigate protein requirements for capsid formation and stability. Deletion mutants have been used to identify essential domain sites in porcine parvovirus and canine parvovirus. Chimeric canine parvovirus-like particles were made by Rueda et al. in 1999. These authors investigated the effects of inserting the poliovirus C3:B epitope so it was presented on the surface of a canine parvovirus empty capsid expressed in an baculovirus expression system. By targeting the correct placement of the epitope on the surface of the capsid the chimeric C3:B CPV VLP is able to elicit an immune response.

VLPs can also be used as a tool for identification of virus binding receptors in cells as demonstrated previously by Tamura et al., 2000. Previous work has identified many cellular receptors for several parvoviruses and is summarized in a review by Vihinen-Ranta et al., 2004. The receptors for AeDNV unknown in cell culture and in mosquitoes.

In this chapter, AeDNVLPs were used to identify putative virus binding proteins in mosquito tissue culture cells. This work is the first description of *Densovirinae* cellular binding proteins. Because of their high specificity for mosquitoes, AeDNV-like particles may have use as a vehicle for packaging and delivery of molecules to mosquitoes.

The technique of VOPBA has been used effectively in the identification of virus binding proteins in C6/36 cells by Salas-Benito and Del Angel, 1997; Munoz et al., 1998; Chu and Ng, 2003. *A. albopictus* C6/36 and *A. aegypti* ATC-10 cells were both investigated. Two different treatments were studied to find virus binding proteins in C6/36.

3.2 Methods and Materials

3.2.1 Virus-cell binding assay

AeDNV empty capsid binding assays were carried out at 4 °C to prevent virus uptake so that only virus binding is detected. Briefly, the C6/36 cells were seeded into a 12 well plate at 80% confluency, approximately $8x10^5$ cells per well and incubated at 4° C for one hour. Cells were then incubated with increasing amount of VLPs to give 1:5000 and 1:10000 cells per empty capsid ratios. Infection assays using C6/36 cells are typically preformed at 1:10000 cells per virus ratio. After incubation, medium and VLPs are removed, cells were washed three times with PBS and fixed with acetone/ethanol fixative. Fixed cells were incubated with primary polyclonal antibody against AeDNV whole capsids made in rabbit. Polyclonal secondary antibody was FITC labeled anti-rabbit raised in goat. Cells are washed with PBS and examined using an epifluorescence inverted microscope (Nikon, Diaphot 200). Images were collected using a CoolSnap camera and software.

3.2.2 Preparation of total cell proteins

C6/36 cellular proteins were isolated by harvesting 1 x 10^6 cells that were grown in L-15 medium supplemented with 10% fetal bovine serum and 1% penicillin/streptomycin incubated at 28°C. Medium was removed from the cells and washed once with PBS, the washed cells were incubated for one minutes in RSB-NP40 (1.5 mmol MgCl, 10 mmol Tris HCl, 10 mmol NaCl, and 1% NP-40) with 2 mmol protease inhibitor phenylmethyl sulfonyl fluoride (PMSF). Nuclei and debris were removed by centrifugation.

3.2.3 Biotinylation of AeDNVLPs

Biotinylated VLPs were prepared using a EZ-Link Sulfo-NHS-Biotin protein labeling kit (Pierce) according to the manufactures instructions. Sulfo-NHS-Biotin reacted with primary amino groups on the surface of the VLP to form stable amine bonds. The reaction was controlled by limiting the concentration of Sulfo-NHS-biotin to VLP to prevent excess biotinylation. Biotin labeling did not interfere with the binding characteristics of the VLP. Biotin labeling was confirmed using streptavidin conjugated to HRP.

3.2.4 Virus overlay protein-binding assay

To identify cellular proteins involved in virus binding, a virus overlay protein-binding assay (VOPBA) was carried out. VOPBA was preformed as previously described by Uwatoko et al. 1996 and Chu et al. 2005 with some modifications. Proteins were separated by SDS-PAGE using a Novex 12-4% Bis-Tris polyacrylamide gels (Invitrogen Corp) and transferred electrophoretically to nitrocellulose membranes

using a NOVEX blotting module (Invitrogen). The membranes were stained with Panceau S to verify complete protein transfer. Blots were incubated overnight in 1X Uniblock diluted in PBS/0.1% Tween 20 at 4°C. The blots were washed once with PBS/0.1% Tween 20 and incubated with 1X Uniblock diluted in PBS/0.1% Tween 20 with 50 μL biotinylated AeDNVLPs for one hour. The blots were then washed three times in PBS/0.1% Tween 20 to remove unbound particles. The blots were then incubated with an avidin-biotin complex (ABC) conjugated with horseradish peroxidase for 30 minutes. The blot was washed three times and the bound VLPs were detected with a Vector VIP enhanced staining kit according to the manufacturers blot protocol. Blots were imaged using a BioRad VersaDoc system.

3.2.5 Isolation of virus binding proteins

Live C6/36 cells were counted using a hemocytometer and cellular protein was extracted as previously describe in total preparation of cell proteins methods sections (3.2.2). Cell proteins were incubated with biotinylated VLPs for one hour. Virus protein complexes were isolated using streptavidin magnetic beads. Streptavidin magnetic beads are 1 μm supermagnetic beads covalently coupled to a highly pure form of streptavidin purchased from New England Biolabs (Ipswich, MA, USA). The streptavidin forms an avidin-biotin complex (ABC) with the biotinylated VLPs that are bound to virus binding proteins. A magnetic separation rack is used to remove the magnetic bead virus protein complex from solution. The complexes are washed and proteins are separated on a SDS-PAGE is preformed using a 12-4% Bis-Tris polyacrylamide gel (Invitrogen).

3.2.6 Protein Identification

Virus binding proteins isolated using the magnetic bead pull-down assay was separated using SDS-PAGE and stained with Coomassie Blue. Macromolecular Resources at Colorado State University performed protein identification. The proteins of interest were excised from the gel and delivered to Macromolecular Resources. The protein identification consists of MALDI-TOF/TOF mass spectrometry analysis of peptides resulting from the typsin enzymatic digestion of the target protein. The MASCOT search engine was used to search the experimental mass spectrometry data against the sequence databases to obtain a protein identification (Macromolecular Resources, 1/30/06.).

3.3 Results

3.3.1 Analysis of densovirus-like particles binding to mosquito cells

When C6/36 cells are infected with AeDNV, a persistent infection is established in which a low percentage of the cells (0.5-3%) show antigen production (Paterson et al., 2005). Is this because only a few cells are susceptible to infection, or are all cells infectable, with only a few capable of sustaining a productive infection? In order to determine the fraction of cells that were capable of binding virus particles, C6/36 cells were seeded at 80% confluency in a 12 well tissue culture plate and refrigerated for one hour prior to incubation with AeDNV empty capsids. Cells were incubated with 5000 and 10000 VLPs per cell at 4°C to inhibit virus uptake into the cells. Bound VLPs were detected using IFA and are shown in Figure 3.1 and Figure 3.2

Cells were also incubated with yeast lysate from the strain transformed with parental plasmid as a control.

Figure3.1: VLP binding to C6/36 cells. The cell to empty capsid ratio is 1:5000

Figure 3.2: VLP binding to C6/36 cells. The cell to empty capsid ratio is 1:10000

The total number of cells that bind AeDNVLPs was calculated by dividing the number of positive cells by the total number of cells in the micrograph. Results are summarized in Table 3.2. Cells incubated with 5000 VLPs per cell showed 1.52% bound virus particles. Cells incubated with 10000 VLPs per cell showed 2.13% bound virus particles. The number of positive cells is similar to AeDNV infection rates in C6/36 as reported by Paterson et al., 2005, suggesting that only a small fraction of cells are capable of binding virus particles to initiate an infection.

Cell to virus ratio	1:5000	1:10000
Percent positive cells	1.52%	2.13%

Table 3.2: Empty virus capsid binding to C6/36 cells

3.3.2 Analysis of densovirus-like particles binding to mosquito cells

In this study, 1×10^6 C6/36 cells were incubated with 25 µL biotinylated AeDNVLPs for varying amounts of time 5, 15, 30, or 60 minutes. The VLPs were then detected using a streptavidin label FITC and examined by florescent microscopy. The cells that were exposed to VLPs for 5 minutes showed the least amount of viral absorption, while the cells exposed for 60 minutes showed the greatest viral uptake. Figure 3.3 shows a immuno-fluorescent micrograph of C6/36 cells with biotinylated VLPs. Figure 3.3 demonstrates that biotinylation does not interfere with virus/cell interactions.

Figure 3.3: Cell binding assay. C6/36 cells were incubated with biotinylated VLPs for one hour. Binding of VLPs was detected with streptavidin labeled FITC. Results show VLPs were adsorbed by C6/36 cells.

3.3.3 Virus overlay protein-binding assay

Little is known about how densoviruses bind and enter host cells. In an attempt to identify potential receptors, a virus overlay protein-binding assay (VOPBA) was used to identify virus-binding proteins. Uninfected *A. albopictus* C6/36 cells were lysed using NP-40 detergent or freeze-thaw. The cellular proteins were then separated by SDS-PAGE and transferred to a nitrocellulose membrane. The membrane was incubated with 2×10^9 VLPs/ml, the bound VLPs were detected using a avidin-biotin complex labeled with horseradish peroxidase (ABC-HRP) and the HRP was detected using a colorimetric assay. The resulting blot is shown in Figure 3.4. A VLP-binding band was observed at an approximate molecular mass of 110 kDa in the freeze thaw lysate. Four bands were detected in the NP-40 lysate with approximate molecular masses of 220, 140, 110, and 67 kDa. *A. aegypti* larvae and the *A. aegypti* ATC-10

cell line were also investigated for binding proteins. No binding proteins were observed in larvae, but ATC-10 cell culture gave the similar results observed for *A. albopictus* C6/36 cells, with virus binding proteins observed to have approximate molecular masses of 220, 110, and 67 kDa. Figure 3.5 demonstrates how VersaDoc (BioRad) software was used to determine the molecular weight of the proteins.

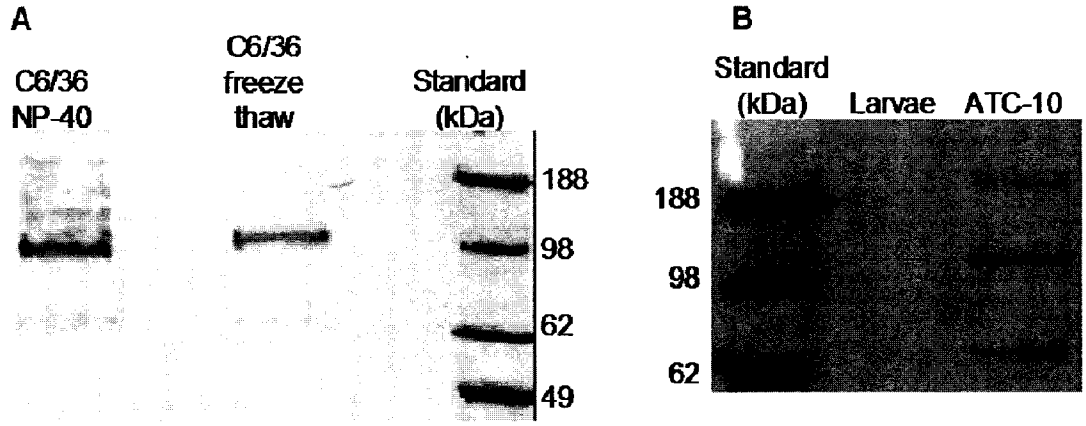

Figure3.4: A. AeDNVLPs binds to C6/36 cellular protein using VOPBA. Cellular proteins were isolated from C6/36 cells using freeze thaw to lyse cells and nonidet –P 40 to dissolve membrane proteins. Proteins were separated by SDS-PAGE and transferred to a nitrocellulose membrane. Biotinylated VLPs binding to the cellular protein was detected by binding the biotin on the VLP to an avidin-biotin complex labeled with horseradish peroxidase. VLPs bind toC6/36 cellular proteins isolated using freeze thaw with approximate molecular weights of 110 kDa, cellular proteins isolated using NP-40 developed protein bands with molecular weights of 220, 140, 110, and 67 kDa. Molecular weight is given by the ladder shown on the right of the blot.

B. VOPBA for *A. aegypti* larvae and *A. aegypti* mosquito tissue culture ATC-10 cells. No proteins are visible using VOPBA technique for mosquito proteins. ATC -10 cells show the same three virus binding proteins as *A. albopictus* C6/36 cells with approximate molecular masses of 220, 110, and 67 kDa.

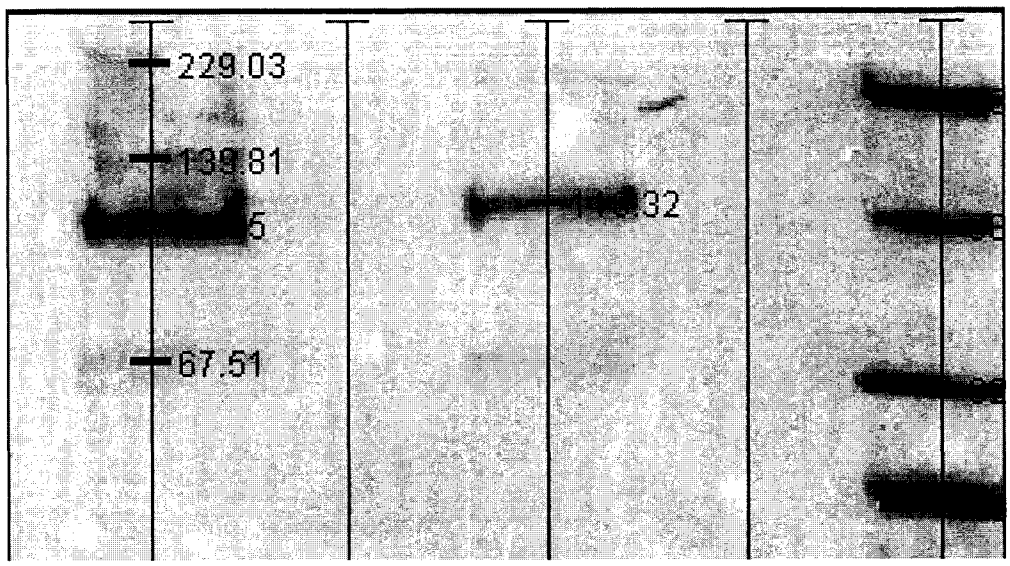

Figure3.5: Molecular weight determination using VersaDoc imaging system

Other parvoviruses, such as canine parvovirus, have been previously identified to bind to streptavidin receptors. To insure we did not misidentified virus binding proteins a control blot was first exposed to biotin followed by an ABC-HRP. Specificity of the virus binding proteins observed was confirmed by two separate assays. In the first assay, a C6/36 protein blot was incubated with biotin, washed and developed with peroxidase conjugated avidin-biotin complex. The resulting blot is shown in Figure 3.6. The same blot was incubated with biotinylated VLPs and developed, the virus binding proteins were detected. This confirms the cellular proteins were interacting with the biotinylated VLP capsids and not biotin or streptavidin.

In the second assay, VOPBA blots were preincubated with AeDNV to compete for virus binding sites before incubation with biotinylated VLPs. Figure 6 shows membranes incubated with 5000 and 10000 virus particles per cell, washed and

incubated with biotinylated VLPs. A ratio of 10000 AeDNV particles per C6/36 cell was needed to inhibit VLP binding. In a similar assay, a cell to virus ratio of 1:5000 was needed to saturate C6/36 with West Nile virus as reported by Chu et al., 2005.

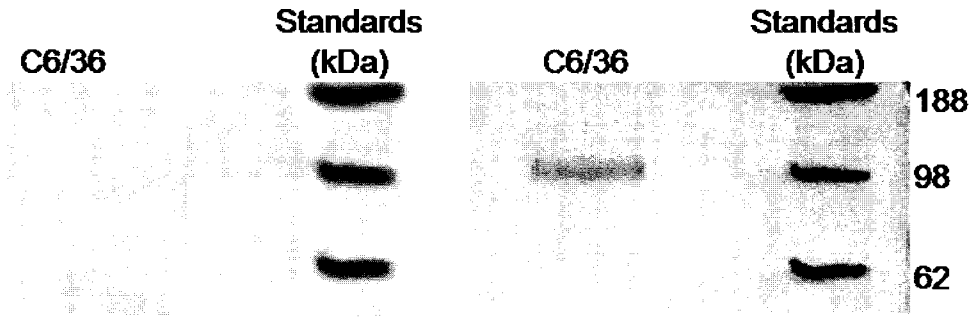

Figure 3.6: Cellular proteins do not bind biotin or avidin. C6/36 cellular proteins were separated by SDS-PAGE and transferred to a nitrocellulose membrane, incubated with biotin followed by washing and detection of bound biotin using an ABC labeled with horseradish peroxidase shown in (A), the blot was then washed and incubated with biotinylated VLP.

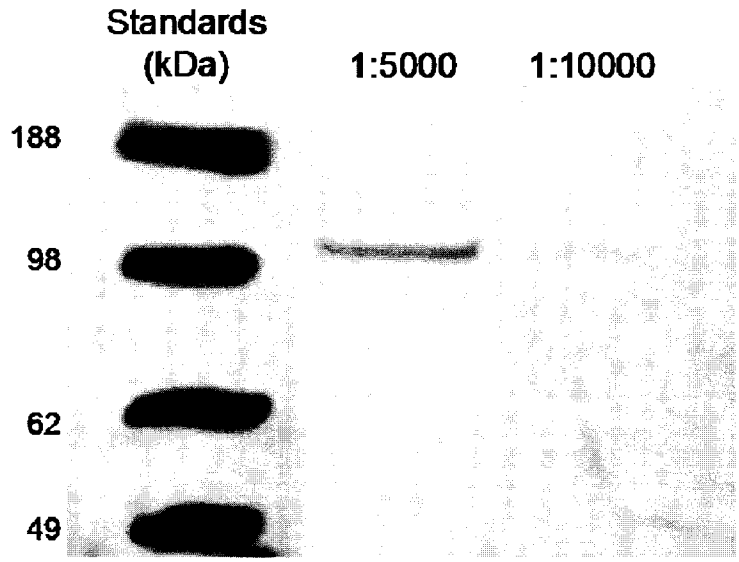

Figure 3.7: AeDNV saturation blot. Decreasing amounts of C6/36 cellular protein were incubated first with AeDNV followed by biotinylated AeDNVLPs. A cell to virus ratio of 1:5000 block VLPs from binding, while a ratio of 1:10000 shows complete saturation of the virus binding proteins

3.3.4 Isolation of binding proteins

Biotinylated densovirus-like particles were incubated with C6/36 cellular lysate. A one hour incubation allowed cellular receptor/VLP complexes to form. The complexes were isolated from the solution using streptavidin magnetic beads. The biotinylated VLPs bound to the streptavidin, the beads were then removed from the solution along with proteins that strongly bound to the VLPs. The cellular protein-VLP complex was separated by boiling in SDS followed by electrophoresis. The proteins were then transferred to a membrane, a VOPBA was then performed. Figure shows the resulting blot. Three strong bands are shown in the sample with magnetic beads protein isolation step. The three bands were previously identified as 220, 140 and 110 kDa; the band with an approximate molecular weight of 67 kDa does not appear in the magnetic bead sample.

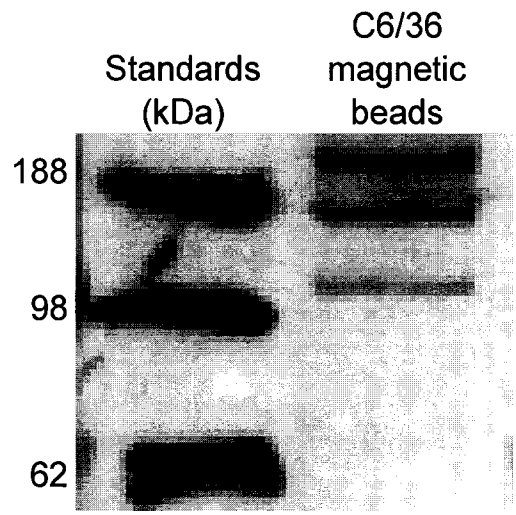

Figure3.8: Magnetic beads isolate cellular binding proteins. The blot shows C6/36 incubated with biotinylated VLPs followed by incubation with streptavidin coated magnetic beads C6/36 cellular protein without treatment. Approximate molecular mass is given at left. Incubation with biotinylated VLP followed by magnetic beads isolated proteins that specifically bind to AeDNV, the protein bands are distinct and the 67 kDa protein is no longer visible on the blot.

The virus binding protein with apparent molecular mass of 110 kDa was digested, the peptides resulting from the digestion were analyzed using MALDI-TOFF and gave two different protein identification results. The results are shown in Appendix 3. The first protein identification was match based on the peptide sequences that match to isoform C protein in the Drosophila melanogaster protein library. The second protein that has a match to other peptide sequences found in the 110 kDa protein is a match to putative mucin-like protein in *Aedes aegypti*. Isoform C protein in Drosophila has been identified as Isoleucyl-tRNA synthetase, which is a cytoplasmic protein. The putative mucin-like protein has been previously identified as AeIMUC1 for *A. aegypti* intestinal mucin 1 (Raymes-Keller et al. 2000). Ae1MUC1 was identified using an *A. aegypti* larval cDNA library. Ae1MUC1 is upregulated in the presence of heavy metals. Current proteomics studies are continuing to further identify mosquito proteins. It is possible the 110 kDa protein observed in this paper is a putative mucin-like protein if alternative splicing mechanisms are considered. A novel mucin-like class I integral membrane glycoprotein, HAVcr-1, has been identified as a virus receptor for hepatitis A virus in African green monkey kidney cells (Kaplan et al., 1996).

Isolating cellular proteins using NP-40 showed more bands in VOPBA as compared to freeze thaw treatment. This is likely caused by cellular proteins being removed by centrifugation with the cellular debris. NP-40 appears to solublize the cellular protein better then freeze thawing. The 220, 110, and 67 kDa are present in blots of C6/36 and ATC-10 cell line. The presence of the virus binding proteins in both cell lines

indicates they may play a critical role in infection. The lack of binding proteins to be identified in *A. aegypti* larvae is an unexpected result due to previous studies that have reported identification of dengue virus binding proteins in both cell culture and mosquitoes (Mendoza et al., 2002).

3.4 Discussion

The AeDNVLPs were used to initiate investigation of the initial events of virus infection. Incubation of C6/36 cells with a large excess of VLPs resulted in particles binding to only a small fraction (1-2%) of cells. This suggests that there is only a small fraction of cells that are receptive to AeDNV binding and infection. This agrees well with the low number of antigen producing cells when persistently infected C6/36 cells are stained with antibody to AeDNV.

Production of large quantities of coat proteins is relatively inexpensive because growth of the yeast on methanol results in high levels of recombinant gene expression. All of the yeast express the VP protein as shown in Figure 3; all cells that are stained with DAPI are positive for AeDNV empty capsid VLPs. VLPs such as these can be used for structural studies and to determine the effects of various mutations on particle assembly and architecture (Brumfield et al., 2004). Mutations that cannot be propagated by virus can easily be studied in the VLPs. VLPs can potentially be used for nanotechnology applications, as immunological epitope

delivery vehicles or perhaps for targeted delivery of anything packaged in the particles.

The technique of VOPBA has been used effectively in the identification of virus binding proteins in C6/36 cells for dengue viruses (Salas-Benito and Del Angel, 1997; Munoz et al., 1998) and West Nile virus (Chu and Ng, 2003). VLPs were used in a VOPBA to AeDNV binding proteins in *A. albopictus* C6/36 and *A. aegypti* ATC-10 cells. Two different cellular treatments were investigated to identify virus binding proteins in C6/36. Preparing cellular proteins with NP-40 showed more bands in VOPBA as compared to freeze thaw preparations. NP-40 appears to solublize the cellular protein better then freeze thawing. The 220, 110, and 67 kDa are present in blots of C6/36 and ATC-10 cell line. To insure we did not misidentify putative virus binding proteins a control blot was first exposed to biotin followed by an ABC-HRP. The results confirm the specificity of the virus binding proteins as no proteins were visualized on the blot. The presence of similar-sized virus binding proteins in both cell lines may indicate that they play a critical role in infection. The nature of the role will require further investigation.

3.5 Conclusions

The technique of VOPBA was used to identify mosquito proteins that may be involved in AeDNV infection using a biotinylated VLPs produced in *P. pastoris*. Biotinylation of the virus has some advantages over labeling with radioisotopes, as

there is no need for specialized equipment need to work with biotin labeled virus capsids as compared to radioactive virus capsids. While the binding proteins were not fully identified, the VOPBA demonstrates a powerful application using VLPs. The VLPs could be used in future work to further the understanding of infection mechanisms in mosquitoes. Protein identification will be simplified with the development of a more extensive *A. aegypti* proteomic database.

References

Brown, C.S., van Lent, J.W.M., Vlak, J.M., Spaan, W.J.M. (1991). Assembly of empty capsids by using baculovirus recombinants expressing human parvovirus B19 structural proteins. *J. Viology.* 65, 2702-2706.

Brumfield, S., Willits, D., Tang, L., Johnson, J.E., Douglas T., Young, M. (2004). Heterologous expression of the modified coat protein of Cowpea chlorotic mottle bromovirus results in the assembly of protein cages with altered architectures and function . *J Gen. Vir.* 85, 1049-1053.

Chu, J.J.H., Ng, M.L. (2003). Characterization of a 105 kDa plasma membrane associated glycoprotein that is involved in West Nile virus binding and infection. *Virology.* 312, 458-469.

Chu, J.J.H., Leong, P.W.H., Ng, M.L. (2005). Characterization of plasma membrane-associated proteins from *Aedes albopictus* mosquito (C6/36) cells that mediate West Nile virus binding and infection. *Virology.* 339, 249-260.

Cotmore, S.F. and Tattersall, P. (1987). The autonomously replicating parvoviruses of vertebrates. *Adv. Virus Res.* 33, 91−174.

Croizier, L., Jousset, F., Veyrunes, J., Lopez-Ferber, M., Bergoin, M., Croizier, M. (2000). Protein requirements for assembly of virus-like particles of Junonia coenia densovirus in insect cells. *J. Gen. Virol.* 81, 1605-1613.

Hernando, E., Llamas-Saiz, A.L., Foces-Foces, C., McKenna R., Portman, I., Agbandie-McKenna, M., Almendral, J.M. (2000). Biochemical and physical characterization of parvovirus minute virus of mice virus-like particles. *J. Virology.* 267, 299-309.

Kajigaya, S., Fujii, H., Field, A., Anderson S., Rosenfeld, S., Anderson L., Shimada, T., and Young, N.S. (1991). Self-assembled B19 parvovirus capsids, produced in a baculovirus system, are antigenically and immunogenically similar to native virions. *Proc. National Acad. Sci. USA.* 88, 4646-4650.

Kaplan, G., Totsuka, A., Thompson, P., Akatsuka, T., Moritsugu Y., and Feinstone, S.M. (1996). Identification of a surface glycoprotein on African green monkey kidney cells as a receptor for hepatitis A virus. *The EMBO Journal*. 15, 4281-4296.

Macromolecular Resources. Proteomics Services: Protein Identification. Retrieved 1/30/06, from http://macromolecular.colostate.edu/proteomics.service.html.

Mendoza, Y.M., Salas-Benito, J., Lanz-Mendoza, H., Hernandez-Martinez, S., del Angel, R.M. (2002). Putative receptor for dengue virus in mosquito tissues: localization of a 45-kDa glycoprotein. *Am. J. Trop. Med. Hyg*. 67, 76-84.

Munoz, M.L., Cisneros, A., Cruz, J., Das, P., Tovar, R., Ortega, A. (1998). Putative dengue virus receptors from mosquito cells. *FEMS Microbiology Letters*. 168, 251-258.

Moriyama, E.N. and Powell, J.R. (1997). Codon usage bias and tRNA abundance in Drosophila. *J. Mol. Evol.* 45, 514-523.

Paterson, A., Robinson, E., Suchman, E., Afanasiev, B, Carslon, J. (2005). Mosquito densonucleosis viruses causes dramatically different infection phenotypes in C6/36 *Aedes albopictus* cell line. *Virology*. 337, 253-261.

Raymes-Keller, A., McGaw, M., Oray, C., Carlson, J.O., Beaty, B.J. (2000). Molecular cloning and characterization of a metal responsive *Aedes aegypti* intestinal mucin cDNA. *Insect Molecular Biology*. 9, 419-426.

Richards, R., Linser, P., Armentrout, R.W. (1977). Kinetics of assembly of a parvovirus, minute virus of mice, in synchronized rat brain cells. *J. Virol*. 22, 778-73.

Rueda, P., Hurtado, A., del Barrio, M., Martinez-Torrecuadrada, J.L., Kamstrup, S., Leclerc, C., Casal, J.I. (1999). Minor displacements in the insertion site provoke major differences in the induction of antibody responses by chimeric parvovirus-like particles. *Virology*. 263, 89-99.

Ruffing, M., Zentgraf, H., and Kleinschmidit, J.A. (1993). Assembly of virus-like particles by recombinant structural protein of adeno-associated virus type 2 in insect cells. *J. Virol.* 66, 6922-6930.

Salas-Benito, J.S., del Angel, R.M. (1997). Identification of two surface proteins from C6/36 cells that bind dengue type 4 virus. *J. Virol.* 71, 7246-7252.

Saliki, J.T., Mizak, B., Flore, H.P., Gettig, R.R., Burand, J.P., Carmichael, L.E., Wood, H.A., Parrish, C.R. (1992). Canine parvovirus empty capsids produced by expression in a baculovirus vector: Use in analysis of viral properties and immunization of dogs. *J. Gen. Virol.* 73, 369-374.

Tamura, M., Natori, K., Kobayashi, M., Miyamura, T., and Takeda, N. (2000). Interaction of recombinant Norwalk virus particles with the 105-kilodalton binding protein, a candidate receptor molecule for virus attachment. *J. Virol.* 74, 11589-11597.

Uwatoko, K., Kano, R., Sunairi, M., Nakajima, M., Yamaura, K. (1996). Canine parvovirus binds to multiple cellular membrane proteins from both permissive and nonpermisive cell lines. *Vet. Micro.* 51, 267-273.

Vihinen-Ranta, M., Suikkanen, S., and Parrish, C.R. (2004). Pathways of cell infection by parvoviruses and adeno-associated viruses. *J. Virol.* 78, 6709-6714.

Chapter 4

Investigation of Performance Differences between Anion Exchange Resin and Membrane Adsorbers for Trace Impurity Removal in a Biomanufacturing Processes

4.1 Introduction

The purification of biological products produced using recombinant DNA technology is critical to the safety of patients receiving biopharmaceutical derived therapeutics. Chromatography is the most commonly implemented high-resolution separation technique used in protein purification (Ghosh, 2002). In this role, packed beds are traditionally used because of their high selectivity. However, packed bed chromatography does have some disadvantages such as high-pressure drops, potential channeling of fluid around beads, column packing, and large buffer consumption (Specht et al., 2004, Zhou and Tressel, 2006). The challenges associated with packed bed chromatography may be eliminated using membrane chromatography. Ion exchange membranes have a lower pressure drop across the bed, are sold as sterile prepackaged single use devices requiring no column packing, use less buffer, eliminate the capital investment in columns, and require less manufacturing space.

Recombinant monoclonal antibodies (MAb) have proven to be successful in treating a variety of human diseases and are the protein product of interest in the evaluation of the chromatography devices. The most commonly used chromatographic steps used in MAb purification manufacturing processes are protein A and ion exchange columns. The typical yields and purity values for a standard three-step antibody recovery process are summarized in Table 4.1. Protein A affinity chromatography selectively captures MAb while impurities pass through the column. Cation exchange chromatography uses a negatively charged group to bind MAbs which typically have an isoelectric point (p*I*) at or above 8 while host cell proteins (HCP), DNA, and leached protein A pass through the column. MAb is eluted from the column with a step gradient to high salt. Anion exchange chromatography uses a positively charged group (typically quaternary amine) to bind trace impurities with a *pI* below 8. The MAb flows through the column while trace impurities are bound to the column (Fahrner et al., 2001).

MAb pool	Yield (%)	Host cell proteins (ng/mg)	DNA (pg/mg)	Protein A (ng/mg)
Harvest cell culture fluid	-	250,000-1,000,000	100,000-1,500,000	-
Protein A	>95	200-3000	100-1000	3-35
Cation	75-90	25-150	<10	<2
Anion	>95	<5	<10	<2

Table 4.1: Typical yield and purity values for a three-step antibody purification process (Fahrner, 2001).

It has been reported that anion exchange packed beds used for MAb manufacturing processes are sized for throughput not binding capacity (Fahrner et al., 2001, Knudsen et al., 2001, Zhou and Tressel, 2006, Zhou et al., 2006). Anion exchange membranes may provide an alternative processing step to anion exchange columns to

remove trace impurities. Commercially available flat sheet ion exchange membranes have a lower total protein binding capacity compared to commercially available ion exchange resins (Ghosh, 2002, Specht, 2004, Amersham Bioscience, 2006). Anion exchange columns, however, are not operated in bind and elute mode. Therefore, there may be an opportunity to replace anion exchange packed beds with anion exchange membranes.

Protein transport in membrane chromatography is dominated by convective flow (Charcosset, 2006). Transport phenomena dominated by convective flow shows a lack of flowrate dependence. The lack of pore diffusion in membrane chromatography was investigated by Charcosset et al., 1995 using the first Damkohler number, Da_I, the ratio of the characteristic times for convection and for protein adsorption in the membrane. The characteristic time for convection is defined as the mean residence time, τ, and is given by $\varepsilon V/Q$, where ε is the membrane porosity, V is the membrane total volume and Q is the volumetric flow rate. The characteristic time for protein adsorption, τ_R, is given by $1/kQ_m$ where k is the rate constant of protein binding to the ligand and Q_m is the maximum protein binding capacity determined using a Langmuir type isotherm. Da_I is defined as τ / τ_R, therefore Da_I greater than one shows that transport is dominated by convective flow and not adsorption time. Da_I has previously been calculated by Charcosset et al., 1995 and Specht et al., 2004 for a MAb binding to protein A, immobilized on a hollow fiber membrane and AeDNV in flat sheet anion exchange membrane system, respectively. Charcosset determined Da_I to be from 2 to 170 depending on the

flowrate, a higher flowrate gave a lower Da_I. Specht et al., 2004 determined the Da_I to be 14. Both of the studies determined that transport is dominated by convective flow.

Membrane manufacturers emphasize this lack of flowrate dependence as an important processing feature as demonstrated in Figure 4.1. In a conventional ion exchange bead, the target molecules must first diffuse into the pore to bind to an ion exchange ligand. Knudsen et al., 2001 showed, in their study, that flow rate does not significantly affect HCP removal for anion exchange membranes. However, for current manufacturing facilities, higher achievable flow rates would not be a significant advantage for membranes because the anion exchange step is not rate limiting in the process. A standard anion exchange resin process also requires over one hour for column cleaning and regeneration that are not required for a single use membrane device; therefore a single use membrane device would not require reuse validation studies.

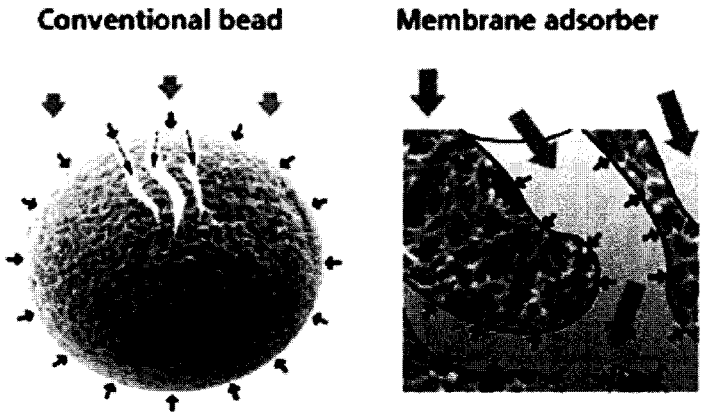

Figure 4.1: A depiction of transport differences between conventional ion exchange bead and membrane adsorber. Transport of proteins is dominated by diffusive transport in the

conventional bead while convective flow dominates protein transport in a membrane adsorber (Gottschalk, 2004).

In previous work at Genentech anion exchange membranes were evaluated for DNA, host cell protein, and virus removal (Knudsen et al., 2001; Philips et al., 2005). To be competitive a single-use membrane is required to process the same volume at equivalent cost to a multiple-use ion exchange resin. Anion exchange columns typically process load densities of 50-100 g antibody/ l resin (Fahrner et al., 2001). The load density for a membrane adsorber would have to be significantly higher than that for the resin because the membrane is expensive and will only be single-use (Zhou and Tressel, 2006). Previous target membrane load densities have been determined based on an economic analysis of a single-use membrane compared to a multiple-use Q-Sepharose column. Zhou and Tressel, 2006, report that a single-use Q-membrane device at a load density of 10.7 kg/l would have an overall cost cheaper than that of a Q-column.

In order to consider incorporating ion exchange membranes as a chromatography step, the performance differences between packed beds and membranes need to be better understood. In this study, the performance of ion exchange membranes and resins were evaluated on the basis of several factors: (1) Load density – the amount of target protein loaded per device (or column) volume. (2) Concentration of host cell protein (HCP) in the feedstock and (3) residence time. In addition, the strength of binding of model proteins to the anion exchange membrane devices and an anion

exchange resin was evaluated to determine whether strength of binding could be used as a predictor of HCP removal performance.

4.2 Methods and Materials

4.2.1 Materials

Commercially available anion exchange membranes were purchased from the respective suppliers. Sartobind Q membrane devices (Sartorius, Goettingen, Germany) were purchased in 3 layer and 15 layer device formats. Mustang Q coins (Pall, East Hills, NY, USA) were purchased in a 16 layer device. Q-Sepharose Fast Flow (QSFF) anion-exchange resin was purchased from GE HealthCare (Piscataway, NJ, USA). The QSFF resin was packed in a 25 x 0.66 cm column with a bed height of 19 cm and a 2 x 0.66 cm column with a 0.5 cm bed height, both columns are from Omnifit (Cambridge, UK). All devices were connected to a 0.2 μm low protein binding filter, either a Sterivex filter (Millipore, Bedford, MA, USA) or Fluorodyne EX filter (Pall, East Hills, New York, USA). Load material was two different recombinant humanized monoclonal antibodies (IgG_1) produced in Chinese hamster ovary cells, manufactured by Genentech, Inc. (South San Francisco, CA, USA). MAb 1 feedstock is a pool that was harvested and processed through protein A and cation exchange chromatography. The average HCP level in the MAb 1 pool is approximately 22 ng/mg. MAb 2 feedstock is a pool that was harvested and processed through protein A chromatography. The average HCP level in the MAb 2 pool is approximately 1880 ng/mg. Model Protein B (MPB) is a protein produced and

fully purified by Genentech, Inc and bovine serum albumin (BSA) was purchased from Calbiochem (La Jolla, CA, USA).

4.2.2 Instruments

Chromatography was performed on an AKTA Explorer equipped with Unicorn v5.10 software (GE HealthCare). A UV Spectrophotomer (Model UV-1601, Shimadzu, Columbia, MD, USA) was used to measure monoclonal antibody concentration.

4.2.3 Methods

ELISA

Host cell protein levels were determined by an enzyme-linked immunosorbent assay (ELISA) developed by Genentech. The assay was developed to detect Chinese hamster ovary cell proteins (CHOP). For the ELISA, affinity purified goat anti-CHOP antibodies were immobilized on microtiter plate wells. Samples were diluted to fall within the assay range of the standard curve (5-320 ng/ml) and incubated in the antigen-coated wells. Unbound CHOP was removed by washing the wells; bound CHOP was detected using a peroxidase-conjugated goat anti-CHOP antibodies. Unbound anti-CHOP antibody is removed by washing and horseradish peroxidase (HRP) activity was quantified with the substrate *o*-phenylenediamine by measuring the absorbance at 492 nm. The limit of detection for the assay is 10 ng/ml because samples have to be diluted a minimum of 2-fold. Samples that were assumed to have HCP levels less than detectable were first concentrated using a Millipore Amicon ultra membrane centrifuge device with a molecular weight cutoff of 10 kDa.

Chromatography

Columns were operated in five phases shown in Figure 4.2 at 0.57 ml/min.

1. **Equilibration:** Equilibrates column with equilibration buffer (pH 8, conductivity 7 mS/cm).
2. **Load**: Column is loaded with a calculated amount of feed. The MAb feed volume is calculated by mass MAb/device volume. Feed is adjusted to pH 8 using 1.5 *M* Tris base; conductivity is adjusted to 7 mS/cm or 4 mS/cm. At pH 8, the MAb is positively charged. The MAb flows through the column while trace impurities with a negative charge are bound to the column. Fraction collection is started when the UV absorbance at 280 nm reaches 100 mAU.
3. **Wash:** Wash flushes the remaining load through the column. Fraction collection is stopped when the absorbance at 280 nm reaches 100 mAU.
4. **Regeneration:** Trace impurities that were bound during the load phase are removed.
5. **Storage:** Column is placed in storage buffer for future use.

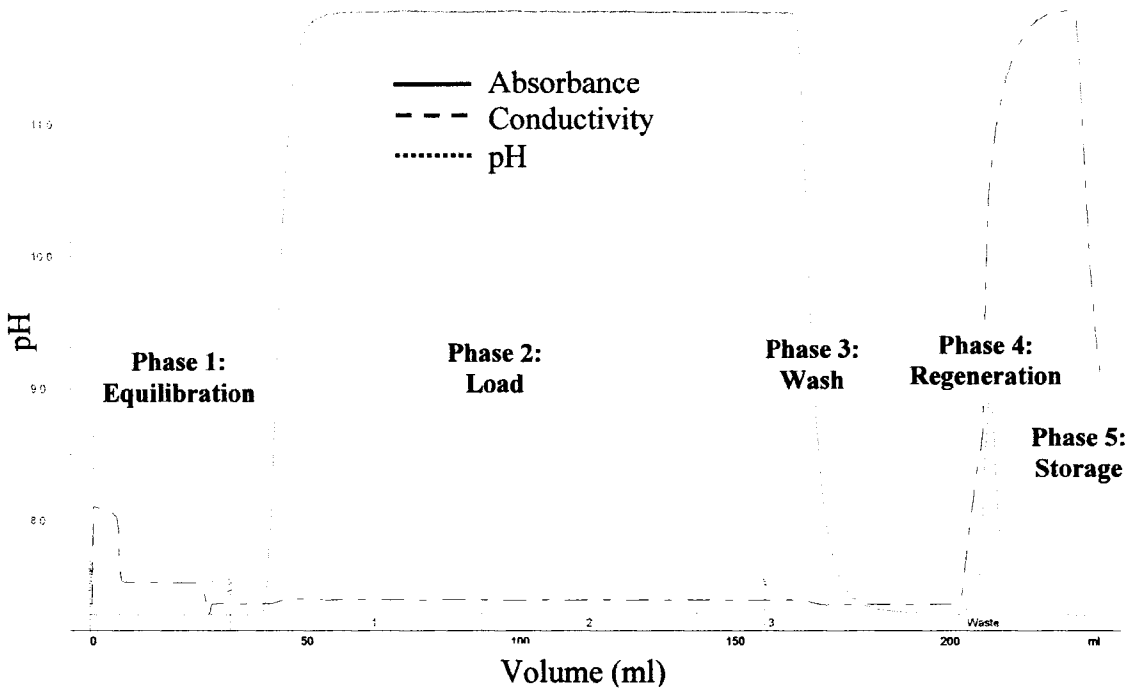

Figure 4.2: Chromatogram of a typical Q Sepharose Fast Flow (QSFF) chromatography run (0.66 x 19 cm column). The five phases of a QSFF process are shown: equilibration, load, wash, regeneration, and storage.

Membrane devices were operated with the same phases as the resin with operating flow rates of 10 ml/min for Sartobind Q and 3.5 ml/min for Mustang Q. The Mustang Q coin is a single use device and the method ends after washing is complete. The Sartobind Q membrane device is regenerated with 0.2 N NaOH and stored in 1 M KCl with 20% ethanol.

Strength of binding

The strength of binding was measured on a 19 cm QSFF column and on the Sartobind Q and Mustang Q devices. The device (or column) was equilibrated to 7 mS/cm, pH 8 using equilibration buffer. Next, a 500 µl pulse of model protein was injected into the device. Two model proteins were used, bovine serum albumin (BSA) and Model

Protein B (MPB) (p*I* 6.8, Genentech, Inc.). The concentration of protein was 5 mg/ml for BSA and 1 mg/ml for MPB followed by a wash to remove unbound protein. Both proteins were dissolved in equilibration buffer at pH 8, conductivity 7 mS/cm. A linear gradient of 1 M salt and equilibration buffer was passed through the device. The linear salt elution was 10 column volumes for the QSFF column and Sartobind Q and ~72 CVs for the Mustang Q membrane device. The absorbance at 280 nm and conductivity were recorded. The absorbance and conductivity data were plotted as absorbance as a function of conductivity. A sample chromatogram showing the linear salt gradient and protein elution peak is shown in Figure 4.3.

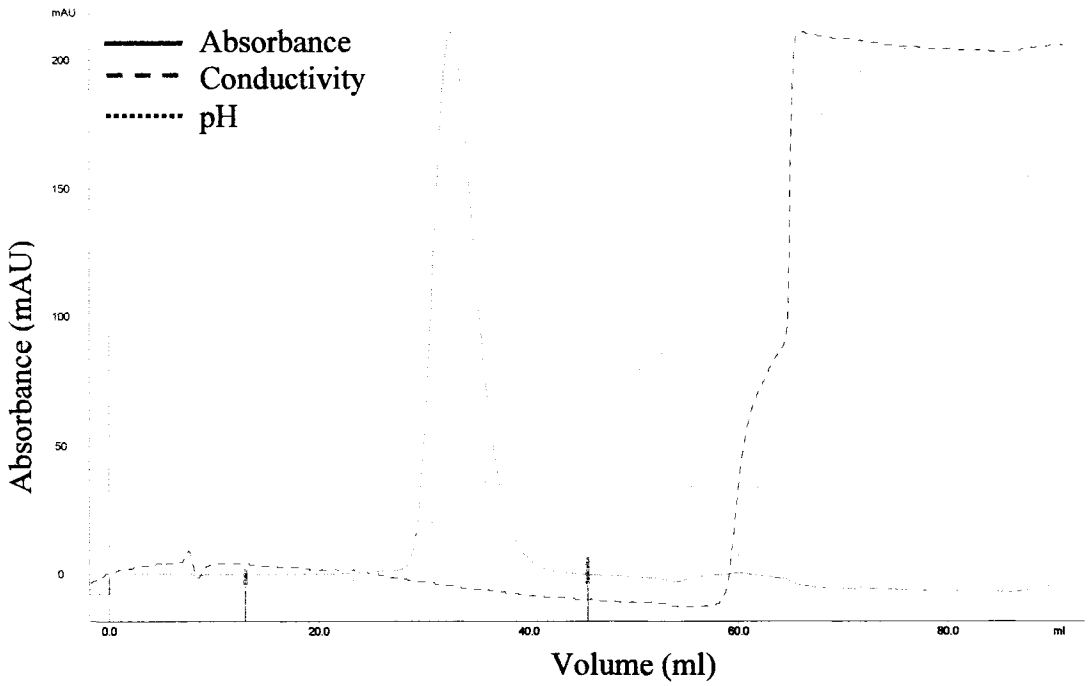

Figure 4.3: Chromatogram showing absorbance at 280 nm (mAU) as a function of volume (ml). Strength of binding chromatogram showing linear salt elution gradient and BSA protein peak for a QSFF 19 cm column operated at 400 cm/hr.

4.3 Results and Discussion

Flow-through anion exchange chromatography was performed using MAb 1 and MAb 2 feedstock. The host cell protein removal by a Q-Sepharose Fast Flow column and a Sartobind Q device with a load density of 100 g/l are summarized in Table 4.2. MAb 1 feedstock is a cation exchange pool adjusted to pH 8 and conductivity 7 mS/cm; MAb 2 feedstock is a protein A pool adjusted to pH 8 and conductivity 4 mS/cm. The QSFF column and Sartobind Q membrane device show similar HCP removal for both MAb 1 and MAb 2 feedstock.

Antibody	Anion Exchanger	Conductivity (mS/cm)	Load HCP (ng/mg)	Pool HCP (ng/mg)
Cation exchange pool (MAb 1)	Q-Sepharose Fast Flow	7	17	<0.64
Cation exchange pool (MAb1)	Sartobind Q	7	20	0.29
Protein A pool (MAb 2)	Q-Sepharose Fast Flow	4	1950	95
Protein A pool (MAb 2)	Sartobind Q	4	1950	76

Table 4.2: Trace impurity removal for Q-Sepharose fast flow resin and Sartobind Q host cell protein levels (ng/mg) in load and collected pool at load density 100 g/l.

Results for Sartobind Q membrane device loaded to a load density of 10000 g/l using MAb 1 and MAb 2 feedstock are shown in Figure 4.4. The host cell protein level (ng/mg) as a function of MAb1 loaded (kg/l) is shown in Figure 4.4 A. The HCP level remains nearly constant between 2 ng/mg and 3 ng/mg over the entire experiment. The HCP level as a function of MAb 2 loaded is shown in Figure 4.4 B. The HCP level remains constant until a load density of 2 kg/l when the HCP begins to

breakthrough the device until 6 kg/l where the HCP level remains constant in the fractions, but still below the level in the feed.

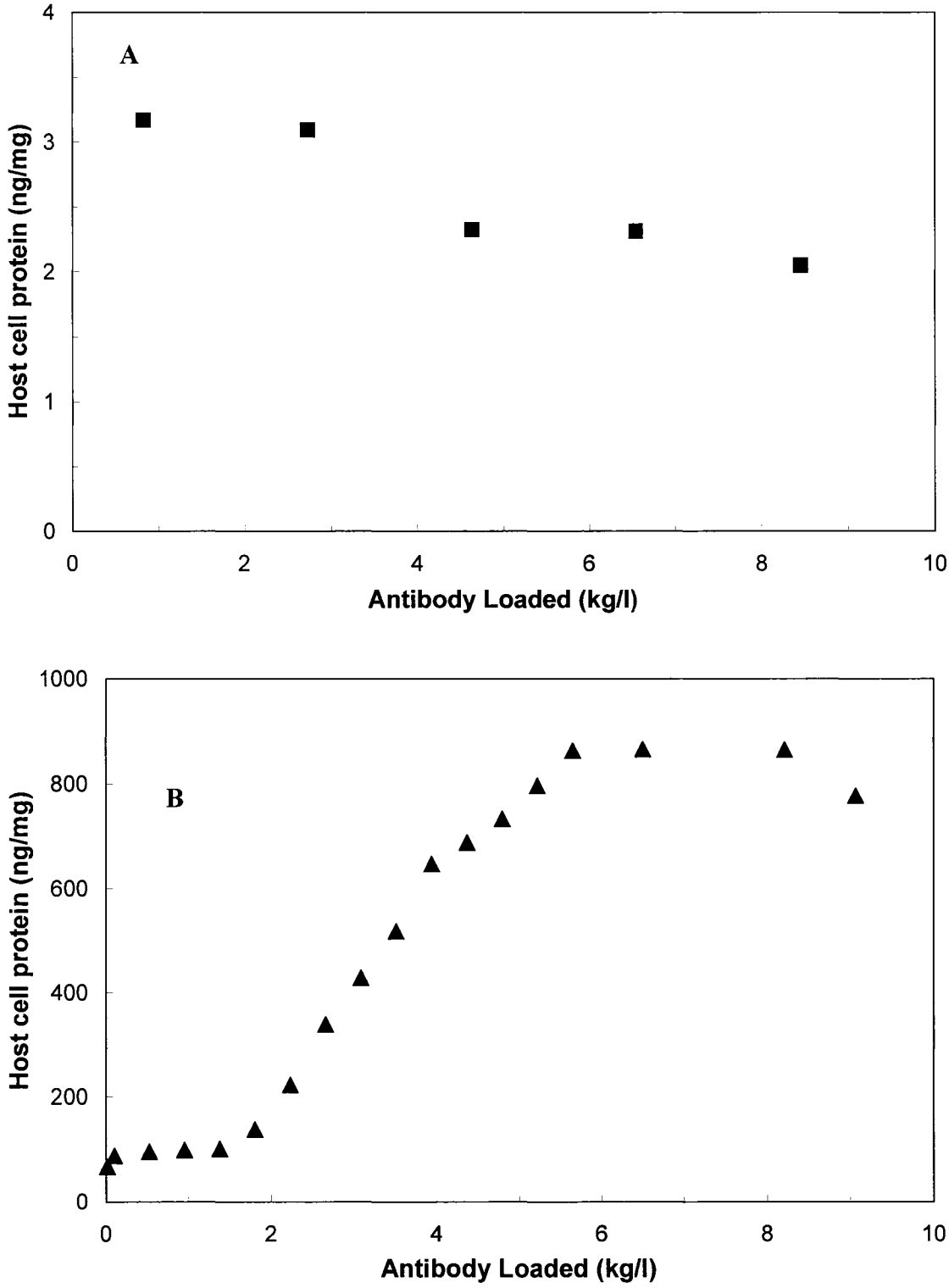

Figure 4.4: Host cell protein (ng/mg) as a function of antibody loaded (kg/l) for Sartobind Q membrane device loaded with MAb 1 (A) and MAb 2 (B).

The effect of residence time on HCP removal in anion exchange columns and membranes was also explored. The residence time in a packed bed is much longer than in a membrane device because of the differences in bed height and total bed size. The anion exchange step removes trace impurities; therefore, a long residence time may not be required. To determine the effect of residence time, HCP removal on a QSFF column with a bed height of 0.5 cm was compared to that for a 19 cm bed height column. Both columns were operated at a flow rate of 0.57 ml/min. The residence times for the 19 cm and 0.5 cm column are 11.4 minutes and 0.29 minutes, respectively. As shown in Figure 4.A, the bed height does not significantly impact HCP removal for MAb 1 with a low HCP level in the load. The amount of HCP present in the feed is very low and removed quickly because the proteins do not have a large diffusion path length before being bound to a free ion exchange site. MAb 2 feedstock was processed with the same columns and a significant difference in HCP removal was observed as shown in Figure 4.5B. Similar HCP removal is seen until a load density of approximately 800 g/l is reached; the 0.5 cm column then shows a rapid breakthrough of HCP in the following fractions. These results show that residence time in a QSFF column can be a factor in HCP removal when the feedstock has higher levels of HCP.

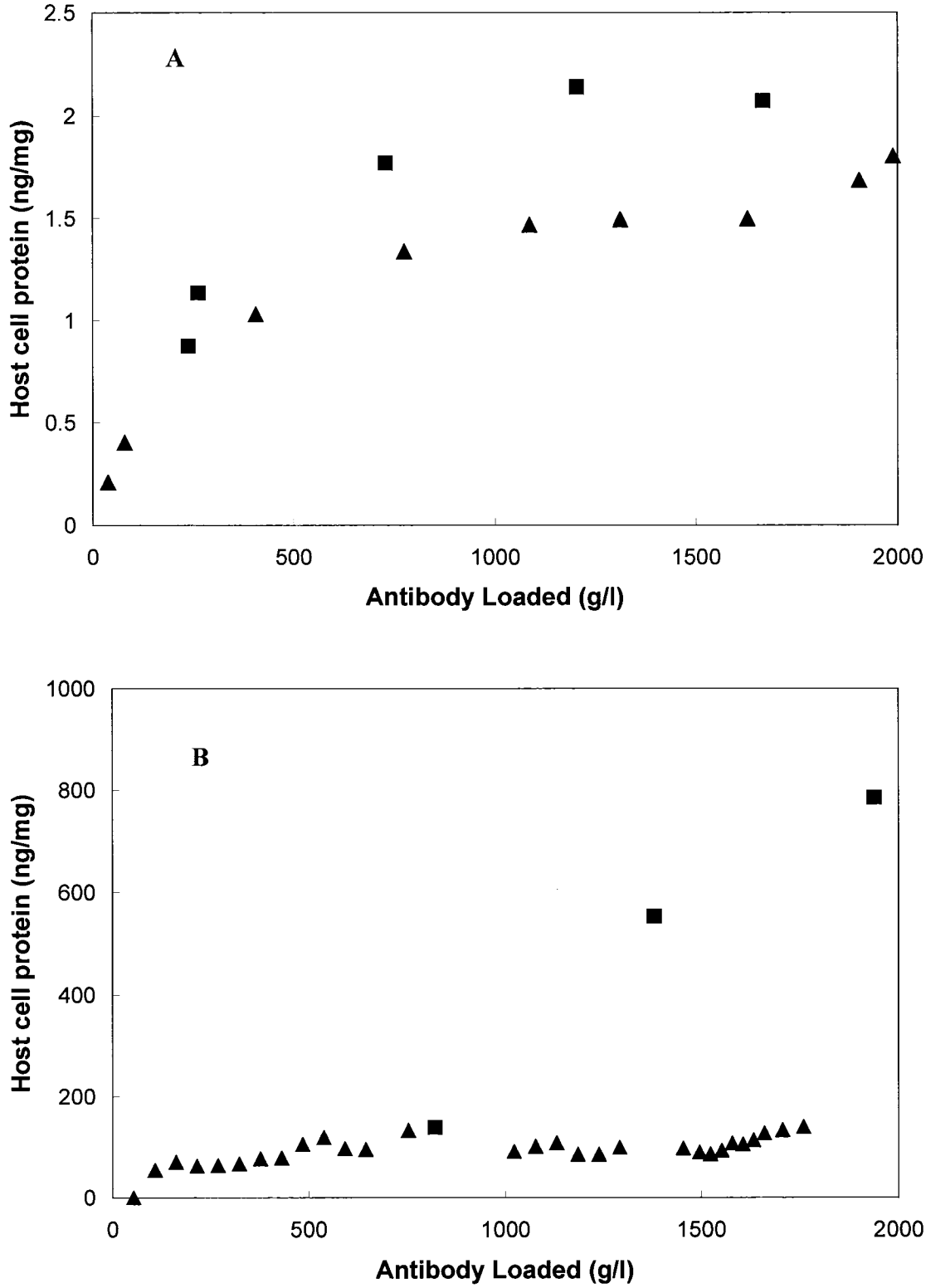

Figure 4.5: Host cell protein (ng/mg) as a function of antibody loaded for Q-Sepharose Fast Flow columns with a bed height of 19 cm (▲) and 0.5 cm (■). Effect of bed height for MAb 1 (A) and MAb 2 (B). Host cell protein is ng HCP/ mg antibody. Antibody loaded is g antibody/l.

Previous results have demonstrated that the performance of membrane adsorbers is not significantly affected by flowrate (Knudsen et al., 2001, Zhou and Tressel, 2006). MAb1 and MAb 2 feedstocks were processed using a Sartobind Q device at several different load flowrates to determine the effect of residence time on performance. The HCP levels in the fractions collected are shown in Figure 4.6. The run with the longest residence time (0.21 min) has the lowest level of HCP in the pool. However, the HCP levels for the 0.1 min. and 0.05 min. residence times are very similar. Overall, there appears to be no significant effect of residence time on HCP removal. Results for MAb 2 are shown in Figure 4.6B. There is no apparent trend in HCP removal with changing residence time. The HCP used in this study is made up of many different proteins, the rate constant and maximum protein binding capacity required to calculate the Da_I can not be determined. Results shown for both MAb 1 and MAb 2 in Figure 4.6 verify that changing residence time does not significantly impact HCP removal in membrane adsorbers.

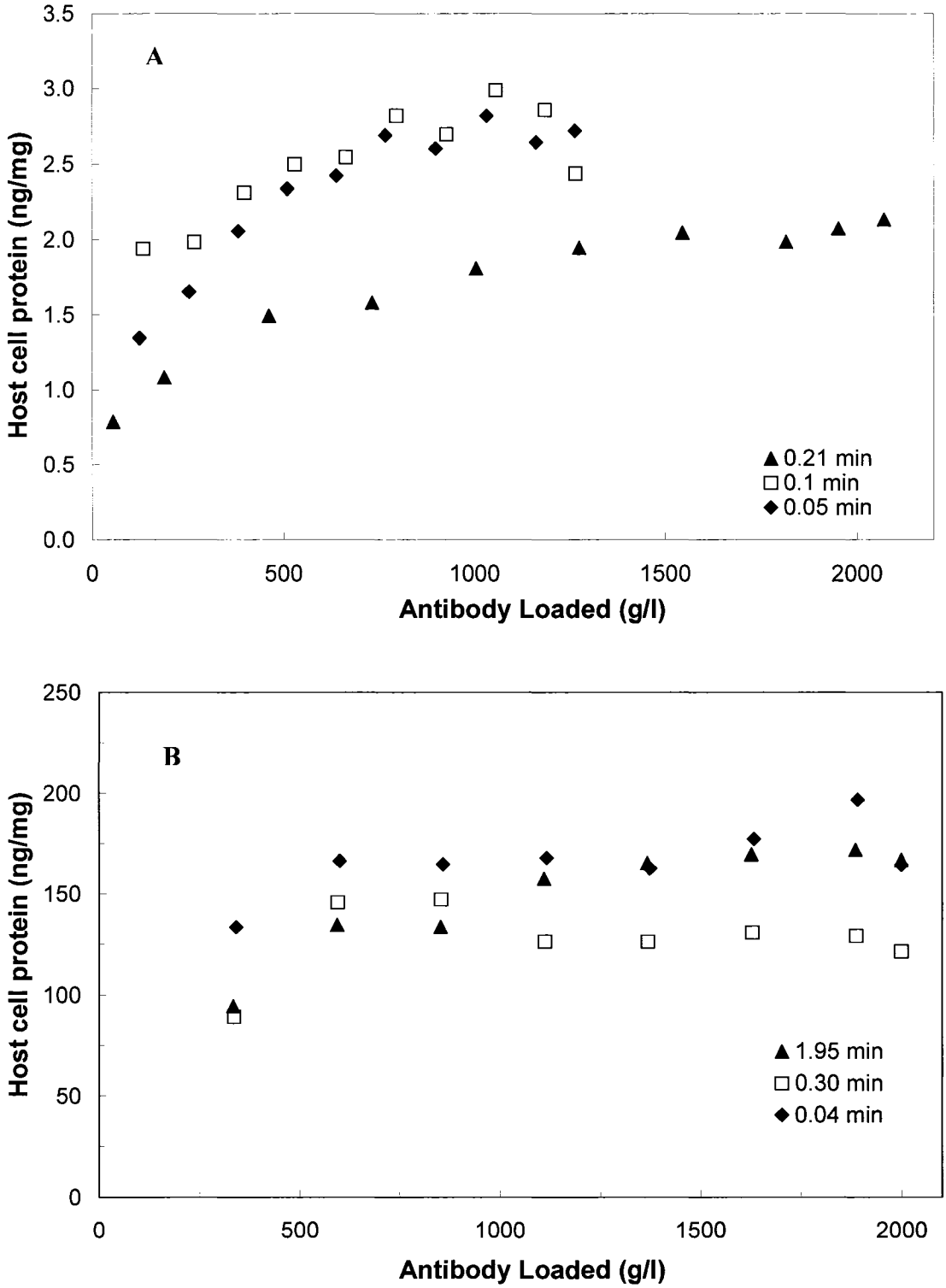

Figure 4.6: Host cell protein level (ng/mg) as a function of antibody loaded (g/l) for Sartobind Q membrane device operated at different flowrates MAb 1 (A) and MAb 2 (B).

HCP removal by a 19 cm QSFF column and a Sartobind Q membrane device is compared in Figure 4.7. The column and membrane device were loaded to equal load density with MAb 1 and MAb 2 feedstock. Figure 4.7A shows the HCP level as a function of MAb 1 loaded. The Sartobind Q membrane device shows slightly higher HCP levels in the fractions collected compared to the 19 cm QSFF column, but the difference falls within the uncertainty of the ELISA assay used to measure HCP. There is also very little difference in HCP removal between the Sartobind Q membrane device and the 19 cm QSFF column for MAb 2.

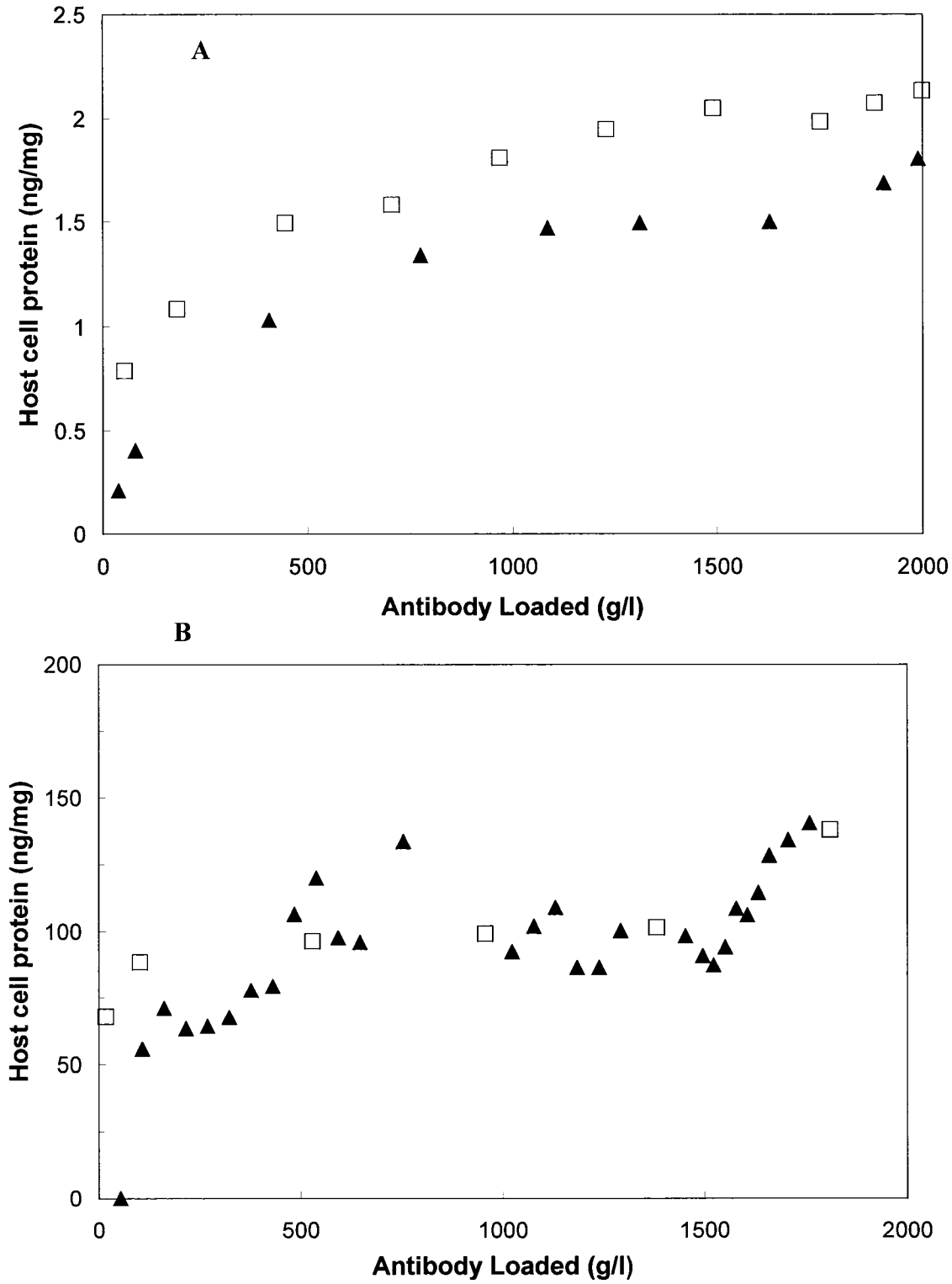

Figure 4.7: Host cell protein level (ng/mg) as a function of antibody loaded MAb 1 (A) and MAb 2 (B). Comparison between a Q-Sepharose FF column (▲) and a Sartobind Q membrane device (□).

Two different commercially available anion exchange membranes were evaluated for their ability to remove HCP. Both membranes were operated at nearly equal residence time. Figure 4.8 shows HCP levels (ng/mg) as a function of antibody loaded per membrane volume. Both devices were loaded to 2000 g/l with MAb 1 and MAb 2. Sartobind Q has a lower HCP level in the collected fractions compared to Mustang Q. Sartorius reports a total BSA protein binding capacity of dynamic 29 mg/ml for their device, half the total BSA binding capacity (50-60 mg/ml) reported by Pall for the Mustang Q device. When comparing the two membrane devices there is a significant difference in HCP removal. The HSA dynamic binding capacity of QSFF resin is 120 mg/ml, The Sartobind Q membrane removes HCP to similar levels as the QSFF resin, even though the total protein binding capacity of the membrane is much less than the resin. This result implies that the BSA binding capacity of a chromatography resin or membrane device may not predict HCP removal performance for flow-through applications.

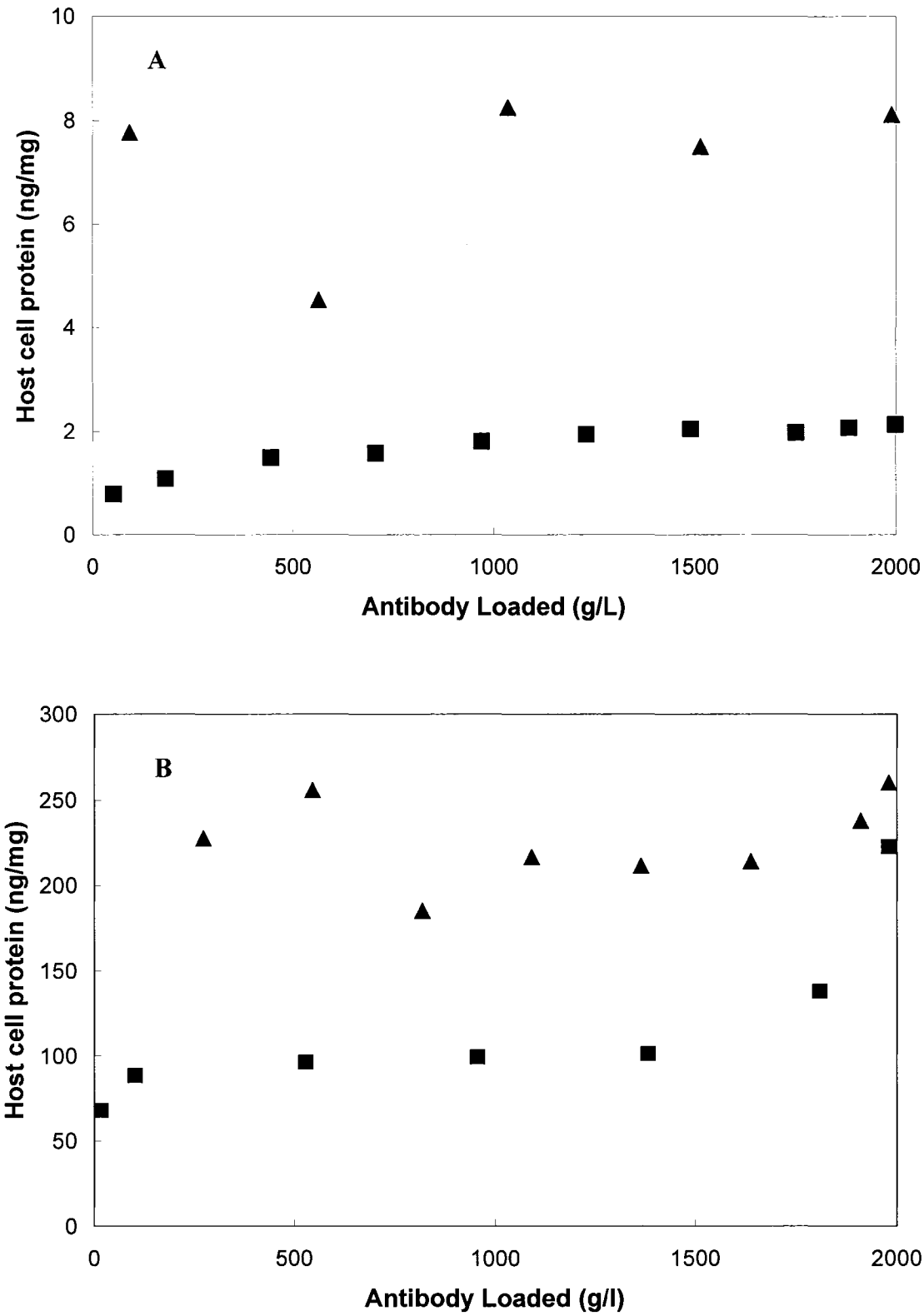

Figure 4.8: Host cell protein level (ng/mg) as a function of antibody loaded (g/l) MAb 1 feedstock (A) and MAb 2 feedstock (B) on a Sartobind Q device (■) and a Mustang Q device (▲).

To explain the performance differences observed between anion exchange membranes and Q Sepharose Fast Flow, the strength of binding was evaluated with two model proteins, BSA and MPB, on each membrane device and QSFF. Strength of binding, the conductivity at which the protein elutes from a device (or resin), is a measure of how strongly proteins are bound to the ion exchanger. BSA was chosen as a model protein because it is a very often used by ion exchange membrane developers to measure the total protein binding capacity. MPB was chosen as a model protein because it has a higher p*I* and is therefore expected to bind more weakly. Some host cell proteins may have an isoelectric point near the MAb and are very difficult to remove as HCP that is present in a cation exchange pool has already undergone a charged-based separation. These difficult-to-remove species may be breaking through at high load densities. A membrane with a higher strength of binding for the model proteins may also bind HCP more tightly and delay breakthrough.

Results for BSA (p*I*=4.9) and MPB (p*I*=6.8) are shown in Figure 4.9 and 4.10. Both proteins have a negative charge in a pH 8 solution. The QSFF column requires the highest conductivity to elute BSA. Mustang Q needs the lowest conductivity to elute BSA. The same linear gradient method was repeated using MPB. At pH 8 MPB does not bind to Mustang Q. MPB elutes at a lower conductivity compared to BSA for both Sartobind Q membrane device and the QSFF column. This result is expected because MPB has a higher isoelectric point than BSA and therefore the protein is more weakly bound at pH 8. The fact that MPB does not bind to the Mustang Q

device is unexpected and gives insight into the differences in performance previously shown in Figure 4.8. HCP is made up of proteins with a range of isoelectric points and Mustang Q membrane device may not be able to capture some HCP proteins with p*I* of 6.8 or greater and those that are captured may be bound more weakly and breakthrough sooner.

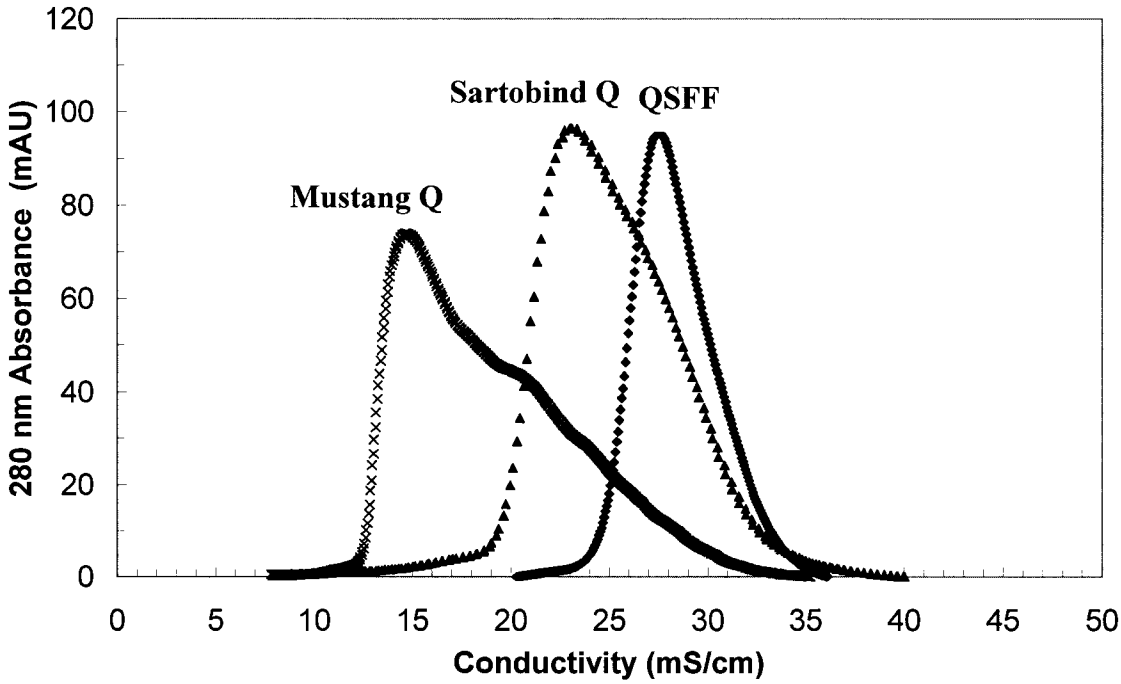

Figure 4.9: Absorbance at 280 nm as a function of conductivity (mS/cm). Strength of bovine serum albumin binding for Mustang Q, Sartobind Q, and Q-Sepharose Fast Flow column.

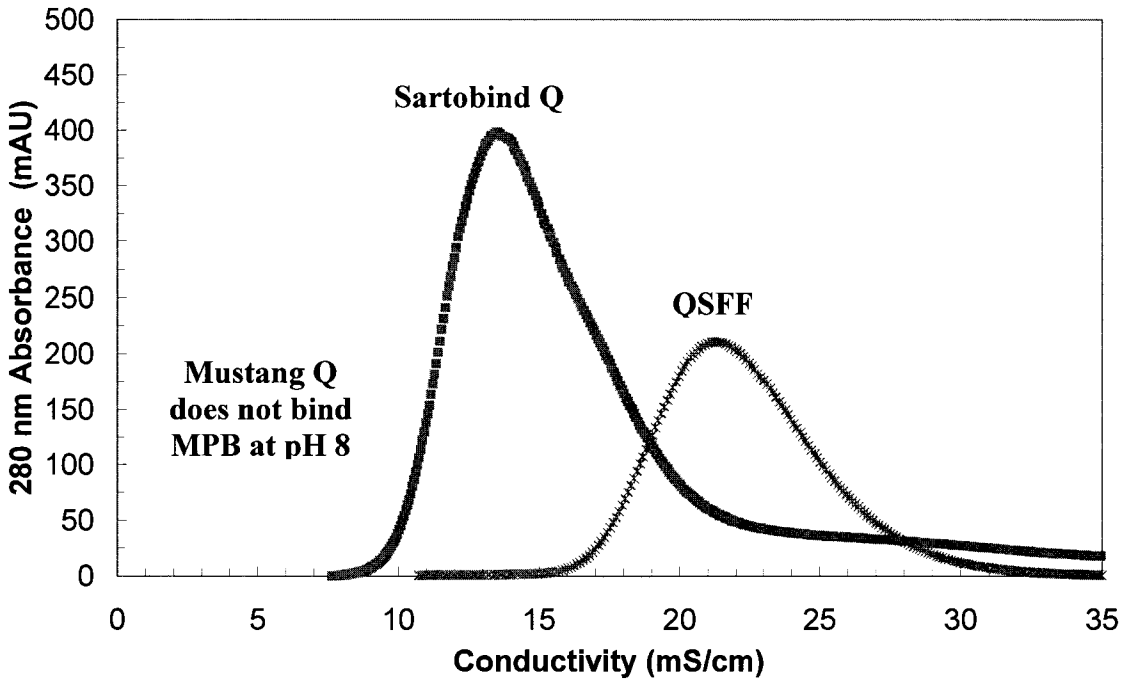

Figure 4.10: Absorbance at 280 nm as a function of conductivity (mS/cm). Strength of Model Protein B (MPB) binding for Mustang Q, Sartobind Q and Q-Sepharose Fast Flow column.

4.4 Conclusions

The ability of anion exchange membranes and resins to remove HCP from MAb feedstocks was evaluated and compared based on several factors: load density, HCP level in the feedstock, and residence time. Due to the smaller size of an anion exchange membrane, the membrane device needs to be loaded to a higher load density than a QSFF column in order to purify the same quantity of feedstock and so the two devices are typically compared with different load densities. However, there is no significant difference in HCP removal between Sartobind Q membrane device and QSFF column when loaded to equal load densities, independent of the HCP level in the feedstock. When comparing the effect of residence time on the devices, the performance of the QSFF column is found to be dependent on the flow rate when the feedstock contains a high level of HCP. No correlation could be established for HCP removal performance versus residence time for the membrane devices. The membrane device and QSFF column perform similarly except when QSFF is run at short residence time with a high level of HCP in the feed in which case the membrane device performs better. When comparing membrane devices, a difference in HCP removal was observed between the Mustang Q and Sartobind Q. The Sartobind Q removed more HCP than the Mustang Q. This result is consistent with using the strength of binding as a performance evaluation characteristic, since the Sartobind Q has a larger binding strength than the Mustang Q. The strength of binding of the Sartobind Q device is closer to that of QSFF, which may explain why they show similar HCP removal. QSFF and Sartobind Q show similar performance,

demonstrating the possibility of the implementation of membrane chromatography for protein purification.

References

Amersham Bioscience. (2006). Sepharose Fast Flow ion exchangers. http://www4.gelifesciences.com/APTRIX/upp00919.nsf/Content/WD:Sepharose+Fast+(187853951-P516).

Charcosset, C., Su, Z., Karoor, S., Daun, G., and Colton, C. (1995). Protein A immunoaffininty hollow fiber membranes for immunoglobulin G purification: experimental characterization. *Biotechnology and Bioengineering*. 48, 415-427.

Charcosset, C. (2006). Membrane processes in biotechnology: An overview. *Biotechnology Advances*. 24, 482-492.

Fahrner, R.L., Knudsen, H.L., Basey, C.D., Galan, W., Feuerhlm, D., Vanderlaan, M., Blank, G.S. (2001). Industrial Purification of Pharmaceutical Antibodies: Development, Operation, and Validation of Chromatography Processes. *Biotechnology and Genetic Engineering Reviews*. 18, 301-327.

Ghosh, R. (2002). Protein separation using membrane chromatography: opportunities and challenges. *J. Chromatography A*. 952, 13-27.

Gottschalk U., Fischer-Frueholz S., Reif O. (2004). Membrane adsorbers a cutting edge process technology at the threshold. *BioProcess International*, 2, 56-65.

Knudsen, H.L., Fahrner, R.L., Xu, Y., Norling, L.A., Blank, G.S. (2001). Membrane ion-exchange chromatography for process-scale antibody purification. *J. Chromatography A*. 907, 145-154.

Philips, M., Cormier, J., Ferrence, J., Dowd, C., Kiss, R., Lutz, H., Carter, J. (2005). Performance of a membranes adsorber for trace impurity removal in biotechnology manufacturing. *J. Chromatography A*. 1078, 74-82.

Specht, R., Han, B., Wickramasinghe, S.R., Carlson, J.O., Czermak, P., Wolf, A. Oscar-Werner Reif, O.W. (2004). Densonucleosis virus purification by ion exchange membranes. *Biotechnology and Bioprocessing.* 88, 465-473.

Zhou, J.X. and Tressel, T. (2006). Basic concepts in Q membrane chromatography for large-scale antibody production. *Biotechnol. Prog.* 22, 341-349.

Zhou, J.X., Tressel, T., Gottschalk, U., Solamo F., Pastor A., Dermawan S., Hong T., Reif O., Mora J., Hutchinton F., Murphy M. (2006). New Q membrane scale-down model for process-scale antibody purification. *J. Chromatography A.* 1134, 66-73.

Chapter 5

Conclusions and Future Work

5.1 Ultrafiltration of AeDNV

Future work in AeDNV purification should include the development of a multi-step purification process such as using direct virus capture and charged based separation and filtration. Purification of AeDNV is challenging because of the small size of the virus. Mosquito cell culture was performed using two different growth medium, with and without fetal bovine serum. Tangential flow ultrafiltration was used to fractionate the virus particles produced in serum free medium cell culture, the 100 kDa MWCO membrane showed the best performance. Higher cell densities can be reached using the serum free medium in a bioreactor compared to a spinner flask. Yet, for a cell culture production process to be feasible for virus production a much greater percentage of the cells have to be infected which would give a higher virus titer. The two growth medias have different separation characteristics, which shows the importance of selecting cell growth conditions before purification development.

5.2 Expression of AeDNV empty capsids in Pichia pastoris

Pichia pastoris methylotrophic yeast was used to express the major AeDNV structural protein VP1. Codon optimization was necessary to have detectable levels

of protein expression in the yeast. The VP1 protein self assembles intracellularly to form a virus-like particle. Western blot analysis showed the VP1 protein is not cleaved to form VP2 in the yeast. These results show an alternative economic method to produce parvovirus empty capsids. Previously parvovirus-like particles have been produced using baculovirus. Future work of interest in the *P. pastoris* expression system is to improve VLP recovery. The high cell density fermentation led to a large amount of host cell proteins in the cell lysate making VLP recovery very challenging. Cell lysis optimization is of particular interest as the cells were lysed using acid washed glass beads and a small vortex machine. This process is only appropriate for small amounts of cells. The VLPs can potentially be designed to have foreign epitopes on the surface of the capsid that could be used to deliver to mosquitoes. The expression system could also be used to investigate virus assembly. Structural studies using the VLP are also of great interest.

5.3 Identification of AeDNV binding proteins in mosquito tissue culture

Virus-overlay protein binding assay (VOPBA) was used to identify proteins from *A. albopictus* C6/36 cells that bind AeDNV. Low infections rates are observed in C6/36 cells, the VLPs bind to the C6/36 cell surface at low rates. Therefore, the low infection rates may be caused by a low level of virus binding protein interactions. The use of VOPBA is one example of using the VLPs as a tool. Future work with VLPs may include further identification of the proteins cited in this work. This

research has presented several unanswered questions. Why is the protein with approximate molecular weight of 140 kDa not found in the *A. aegypti* ATC-10 mosquito tissue culture VOPBA? Why is the 67 kDa protein not present on the VOPBA when the C6/36 virus binding proteins are isolated using the magnetic beads pull-down assay? The answer to these questions may be found by making polyclonal antibodies against the virus binding proteins. The identification of virus binding proteins in mosquitoes using VOPBA should be further investigated. As the proteomics of mosquitoes becomes more available, the identification of the virus binding proteins will become more obvious.

5.4 Evaluation of performance differences between anion exchange resin and membranes

The ability of anion exchange membranes and resins to remove HCP from MAb feedstocks was evaluated and compared based on several factors: load density, HCP level in the feedstock, and residence time. Due to the smaller size of an anion exchange membrane, the membrane device needs to be loaded to a higher load density than a QSFF column in order to purify the same quantity of feedstock and so the two devices are typically compared with different load densities. However, there is no significant difference in HCP removal between Sartobind Q membrane device and QSFF column when loaded to equal load densities, independent of the HCP level in the feedstock. When comparing the effect of residence time on the devices, the performance of the QSFF column is found to be dependent on the flow rate when the

feedstock contains a high level of HCP. No correlation could be established for HCP removal performance versus residence time for the membrane devices. The membrane device and QSFF column perform similarly, except when QSFF is run at short residence time with a high level of HCP in the feed in which case the membrane device performs better. When comparing membrane devices, a difference in HCP removal was observed between the Mustang Q and Sartobind Q. The Sartobind Q removed more HCP than the Mustang Q. This result is consistent with using the strength of binding as a performance evaluation characteristic, since the Sartobind Q has a larger binding strength than the Mustang Q. The strength of binding of the Sartobind Q device is closer to that of QSFF, which may explain why they show similar HCP removal. QSFF and Sartobind Q show similar performance, demonstrating the possibility of the implementation of membrane chromatography for protein purification.

Appendix A.1: DNA sequence of AeDNV VP and yeast optimized VP

```
  1  A T G G C T G A C T C T A C T T C T A T  yeast optimized VP
  1  A T G G C A G A C A G C A C T T C A A T  AeDNV VP

 21  G G A C C A T G A C G G A G A G C A A A  yeast optimized VP
 21  G G A C C A T G A C G G A G A A C A A C  AeDNV VP

 41  G A G G A A C T A A A A G A A A A A G A  yeast optimized VP
 41  G A G G A A C A A A A A C G A A A A A C G A  AeDNV VP

 61  G A C G C T G G T G C T G G A G G T T C  yeast optimized VP
 61  G A C G C A G G C G C T G G A G G A T C  AeDNV VP

 81  T G G T G C T G G A A T C G G T A A A G  yeast optimized VP
 81  A G G T G C T G G A A T T G G C A A A G  AeDNV VP

101  G A A C T T C T A A C T A C G T T A A A  yeast optimized VP
101  G A A C A A G C A A C T A C G T A A A A  AeDNV VP

121  G A A G G A T A C G G A C C A A A C A T  yeast optimized VP
121  G A A G G A T A T G G A C C T A A T A T  AeDNV VP

141  G T C T G A G A T G G T T C C A A G A A  yeast optimized VP
141  G A G C G A A A T G G T A C C A A G A A  AeDNV VP

161  A C A T C A T G A A C A A G G G T A A C  yeast optimized VP
161  A C A T T A T G A A T A A A G G C A A C  AeDNV VP

181  C A T A C T G T T T A C C A T G T T G T  yeast optimized VP
181  C A C A C G G T A T A T C A T G T A G T  AeDNV VP

201  T A A G C A A C A A A A G T A C T T G G  yeast optimized VP
201  A A A G C A G C A A A A A T A C T T G G  AeDNV VP

221  A C T T C A A C T A C G T T T C T A A C  yeast optimized VP
221  A C T T C A A C T A C G T A T C A A A T  AeDNV VP

241  C A A A A C C C A T A C A T T A T C C C  yeast optimized VP
241  C A A A A C C C A T A T A T T A T T C C  AeDNV VP

261  A T A C C A A A C T G C T G G A T T C T  yeast optimized VP
261  A T A T C A A A C G G C A G G A T T C T  AeDNV VP

281  G G G C T T C T A T G T G G G A C C A A  yeast optimized VP
281  G G G C A T C A A T G T G G G A C C A A  AeDNV VP

301  A C T G A C A T C G G A T C T A A C A A  yeast optimized VP
301  A C A G A C A T C G G A T C G A A T A A  AeDNV VP
```

```
321  C A C T A T C A A C A T C A T G A A G G  yeast optimized VP
321  C A C C A T T A A T A T A A T G A A A G  AeDNV VP

341  C T T T G A A C A A C G T T T C T G T T  yeast optimized VP
341  C A C T A A A T A A C G T A T C A G T A  AeDNV VP

361  G G T G T T A C T T G G A T C A A G G G  yeast optimized VP
361  G G G G T A A C A T G G A T C A A A G G  AeDNV VP

381  A G A G A T C A C T T T C G A G G T T T  yeast optimized VP
381  A G A A A T C A C G T T C G A A G T A T  AeDNV VP

401  A C G C T G T T A C T A G A C A A A G A  yeast optimized VP
401  A T G C A G T A A C A A G A C A A C G C  AeDNV VP

421  T T G T T G A C T G G T A C T A C T A A  yeast optimized VP
421  T T G C T A A C G G G G A C A A C A A A  AeDNV VP

441  C C A A A C T A C T T G G G A C T T C G  yeast optimized VP
441  C C A A A C T A C A T G G G A C T T T G  AeDNV VP

461  A G A C T T C T C A A A A C A T G T T C  yeast optimized VP
461  A A A C A A G T C A A A A C A T G T T C  AeDNV VP

481  A T C G C T G A T G C T G A C A G A G A  yeast optimized VP
481  A T C G C A G A T G C A G A C A G A G A  AeDNV VP

501  A C C A G A A A A T T T C A A C T T G G  yeast optimized VP
501  A C C A G A A A A T T T C A A C T T G G  AeDNV VP

521  C T A C T G C T G C T G C T A C T G G A  yeast optimized VP
521  C A A C A G C A G C A G C A A C T G G A  AeDNV VP

541  C C A T T G G C T C A A C A A A C T A C  yeast optimized VP
541  C C A C T T G C A C A A C A A A C A A C  AeDNV VP

561  T C A A A C T T T G T T G T T C A A C G  yeast optimized VP
561  A C A A A C A C T A C T A T T C A A T G  AeDNV VP

581  C T A A C A A C G A C A G A T A C A C T  yeast optimized VP
581  C A A A C A A C G A C A G A T A T A C A  AeDNV VP

601  A A G T A C G A G T T G C C A C A A A G  yeast optimized VP
601  A A A T A T G A A T T A C C A C A A A G  AeDNV VP

621  A A A C C A A T A C A C T A G A G A G T  yeast optimized VP
621  A A A C C A G T A T A C A A G A G A A T  AeDNV VP

641  A C G A C T T C C A A C A A T T G A C T  yeast optimized VP
641  A T G A C T T C C A A C A A C T T A C A  AeDNV VP

661  A A C A A C T A C A T G T G G A A A C C  yeast optimized VP
661  A A T A A C T A C A T G T G G A A A C C  AeDNV VP

681  A A C T G A C A T C T C T G C T G C T G  yeast optimized VP
```

```
681  A A C A G A C A T T A G C G C T G C A G  AeDNV VP

701  C T A A C T T T A G A A G A T T G A T C  yeast optimized VP
701  C A A A C T T T A G A A G A T T G A T C  AeDNV VP

721  C C A A T G G C T G A A G G A G T T T A  yeast optimized VP
721  C C A A T G G C G G A A G G A G T A T A  AeDNV VP

741  C A C T A C T A C T G C T G C T A C T A  yeast optimized VP
741  T A C A A C A A C A G C G G C A A C A A  AeDNV VP

761  C T A A G A T G G C T G A G T T G A C T  yeast optimized VP
761  C T A A A A T G G C A G A A T T A A C A  AeDNV VP

781  G A A C A A A A A G T C T G T T T A C G C  yeast optimized VP
781  G A A C A A A A A A T C A G T A T A T G C  AeDNV VP

801  T G G A T C T G G T A A A A C T A C T G  yeast optimized VP
801  A G G A T C A G G C A A A A C A A C A G  AeDNV VP

821  A G G C T T C T T T G T T C A G A A A C  yeast optimized VP
821  A A G C A T C A C T A T T C A G A A A T  AeDNV VP

841  A G A A C T T C T T A C C C A A G A A T  yeast optimized VP
841  A G A A C A T C A T A T C C T A G A A T  AeDNV VP

861  G C A T A T G G C T C A A C C A C A A G  yeast optimized VP
861  G C A T A T G G C A C A A C C A C A A G  AeDNV VP

881  T T C C A G A C G A G A C T G G A T A C  yeast optimized VP
881  T T C C A G A T G A A A C C G G A T A C  AeDNV VP

901  A T G A A G T T C A G A T A C C A A G T  yeast optimized VP
901  A T G A A A T T C A G A T A C C A A G T  AeDNV VP

921  T A G A A T G T C T A C T A A G T T G C  yeast optimized VP
921  A C G A A T G A G T A C A A A A C T A C  AeDNV VP

941  A T T T G G T T T T C C A T T T G T A C  yeast optimized VP
941  A C C T C G T A T T T C A T C T A T A C  AeDNV VP

961  C C A G A C T A C T C T A C T T C T A C  yeast optimized VP
961  C C A G A T T A T A G T A C A T C A A C  AeDNV VP

981  T A A C A T C G A G T A C A T G G G T A  yeast optimized VP
981  A A A C A T A G A A T A C A T G G G G A  AeDNV VP

1001 G A C A A G T T T T G G A A T T G C C A  yeast optimized VP
1001 G A C A A G T A T T G G A A T T A C C A  AeDNV VP

1021 G A A G T T A C T G C T A C T G G A G G  yeast optimized VP
1021 G A A G T A A C A G C A A C A G G A G G  AeDNV VP

1041 T G T T G T T A C T T G T A T G C C A T  yeast optimized VP
1041 A G T G G T A A C A T G T A T G C C G T  AeDNV VP
```

```
1061  A C G A G A T C A A G A C T T A A        yeast optimized VP
1061  A T G A A A T C A A A A C T T A A        AeDNV VP
```

Appendix A.2 ELISA standard curve

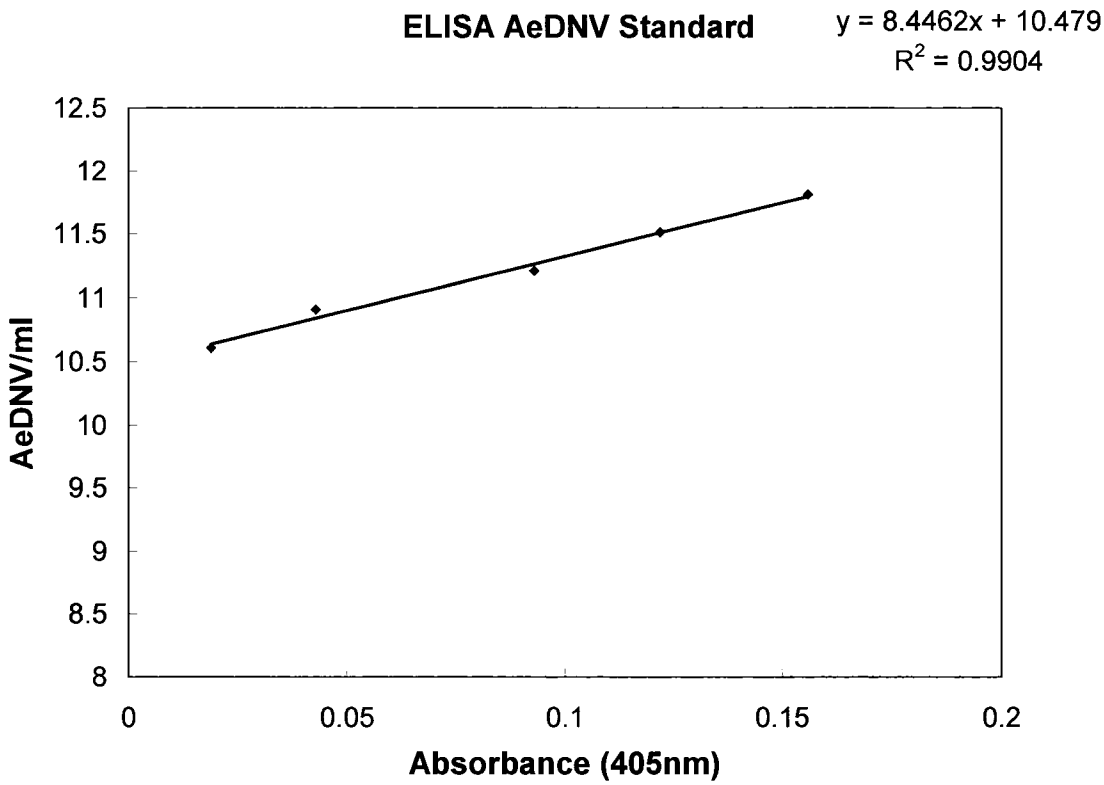

Appendix A.3 MALDI-TOFF peptide identification report

140 kDa band

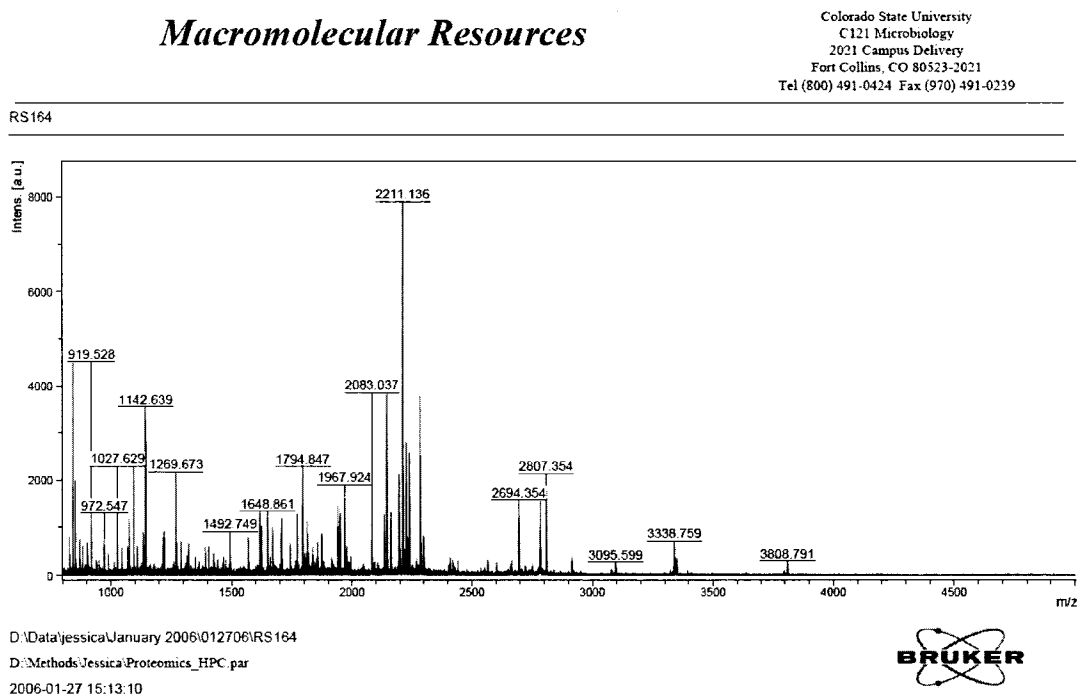

{MATRIX} {SCIENCE} Mascot Search Results

```
User            : Jessica
Email           : jprenni@colostate.edu
Search title    : RS164
MS data file    : DATA.TXT
Database        : NCBInr 20050618 (2521256 sequences; 854568500 residues)
Taxonomy        : Drosophila (fruit flies) (56063 sequences)
Timestamp       : 27 Jan 2006 at 22:41:36 GMT
Warning         : A Peptide summary report will usually give a much clearer picture of MS/MS se
Top Score       : 94 for gi|7301076, CG5394-PA, isoform A [Drosophila melanogaster]
```

Probability Based Mowse Score

Ions score is -10*Log(P), where P is the probability that the observed match is a random event.
Protein scores greater than 60 are significant (p<0.05).
Protein scores are derived from ions scores as a non-probabilistic basis for ranking protein hits.

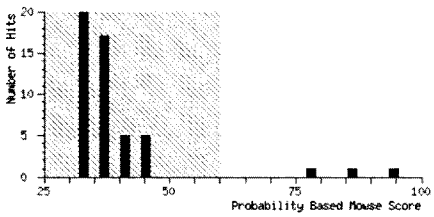

Protein Summary Report

Format As | Protein Summary (deprecated) | Help

Significance threshold p< 0.05 Max. number of hits 20
Standard scoring ◉ MudPIT scoring ○ Ions score cut-off 0 Show sub-sets ☐
Show pop-ups ◉ Suppress pop-ups ○ Sort unassigned Decreasing Score Require bold red ☐

Re-Search All | Search Unmatched

Index

	Accession	Mass	Score	Description
1.	gi|7301076	189293	94	CG5394-PA, isoform A [Drosophila melanogaster]
2.	gi|54638528	189830	87	GA18849-PA [Drosophila pseudoobscura]
3.	gi|1871360	189080	80	glutamyl-prolyl-tRNA synthetase
4.	gi|25009699	82488	46	AT04516p [Drosophila melanogaster]
5.	gi|24581168	82515	46	CG3210-PA [Drosophila melanogaster]
6.	gi|67098438	41164	45	Extracellular ligand-binding receptor [Burkholderia cenocepacia
7.	gi|24655082	70627	44	CG10924-PA [Drosophila melanogaster]
8.	gi|25012603	107900	43	RE41560p [Drosophila melanogaster]
9.	gi|24638806	110423	42	CG11059-PB, isoform B [Drosophila melanogaster]
10.	gi|67098245	84828	42	conserved hypothetical protein [Burkholderia cenocepacia HI2424
11.	gi|16769274	91789	42	LD22423p [Drosophila melanogaster]
12.	gi|23171292	100837	40	CG7292-PA [Drosophila melanogaster]
13.	gi|16183135	49345	39	GH18370p [Drosophila melanogaster]
14.	gi|67103454	30160	38	hypothetical protein Bcen2424DRAFT_5621 [Burkholderia cenocepac
15.	gi|54644304	82207	38	GA16678-PA [Drosophila pseudoobscura]
16.	gi|45550545	15719	38	CG13297-PA [Drosophila melanogaster]
17.	gi|24585079	105136	37	CG18398-PA [Drosophila melanogaster]
18.	gi|7301553	68550	37	CG5889-PA [Drosophila melanogaster]
19.	gi|29336005	8950	37	GM07658p [Drosophila melanogaster]
20.	gi|7300484	52842	36	CG11779-PA, isoform A [Drosophila melanogaster]

Results List

1. gi|7301076 **Mass:** 189293 **Score:** 94 **Expect:** 2e-005 **Queries matched:** 19

CG5394-PA, isoform A [Drosophila melanogaster]

Observed	Mr(expt)	Mr(calc)	Delta	Start		End	Miss	Ions	Peptide
870.58	869.58	869.53	0.04	522	-	530	0	---	R.VIVNVAGAK.V
903.52	902.51	902.46	0.05	1706	-	1712	0	---	K.FYTLFGR.S
1026.58	1025.57	1025.63	-0.06	521	-	530	1	---	K.RVIVNVAGAK.V
1070.67	1069.66	1069.62	0.04	673	-	681	1	---	K.KGDIIQLQR.R
1075.68	1074.67	1074.58	0.09	59	-	68	1	---	R.ALARAAPDYK.L
1142.64	1141.63	1141.60	0.03	1345	-	1353	0	12	R.LNQWNNVVR.W
1143.56	1142.56	1142.59	-0.04	1200	-	1211	1	---	K.EPAADASGAVKK.Q
1289.65	1288.64	1288.62	0.02	1276	-	1285	0	---	K.ECYFPIFVSK.A + Carbamidomet
1425.70	1424.69	1424.62	0.07	346	-	358	1	---	R.AKIDMSSPNGCMR.D + Oxidation
1569.81	1568.81	1568.77	0.04	1263	-	1275	1	---	K.TWFDAEITRMGVK.E + Oxidation
1616.81	1615.80	1615.88	-0.08	193	-	207	1	---	K.FVDLPGAEMGKVVVR.F
1623.86	1622.86	1622.82	0.04	208	-	222	0	33	R.FPPEASGYLHIGHAK.A
1670.87	1669.86	1669.91	-0.05	1585	-	1599	1	---	R.DTVEKITIPLADVEK.K
1707.84	1706.84	1706.82	0.02	1222	-	1235	0	---	K.EDNLPDWYSQVITK.G
1772.90	1771.90	1771.92	-0.02	1276	-	1290	1	---	K.ECYFPIFVSKAVLEK.E
1949.96	1948.95	1948.92	0.03	1417	-	1435	0	---	K.FAGGDYTTTVEAFISASGR.A
1967.92	1966.92	1966.88	0.04	1236	-	1251	0	---	K.GEMIEYYDVSGCYILR.Q + Carbam
1977.94	1976.94	1976.93	0.01	444	-	460	0	---	K.LTWFVDSGLVDGWDDPR.F
2694.35	2693.35	2693.32	0.03	379	-	401	0	---	K.VYPTYDFACPIVDAIENVTHTLR.T +

No match to: 828.51, 842.56, 852.49, 882.38, 919.53, 972.55, 989.52, 1027.63, 1045.58, 1094.56, 1109.57, 1133.63, 1140.58, 1216.75, 1220.60, 1269.67, 1320.67, 1390.76, 1403.74, 1492.75, 1648.86, 1705.88, 1742.93, 1794.85, 1813.94, 1837.90, 1856.97, 1873.95, 1940.96, 2083.04, 2135.10, 2145.16, 2161.17, 2196.09, 2211.14, 2225.14, 2230.23, 2239.15, 2283.18, 2286.18, 2298.20, 2779.81, 2782.39, 2807.35, 2914.52, 3095.60, 3338.76, 3348.59, 3808.79

2. gi|54638528 **Mass:** 189830 **Score:** 87 **Expect:** 0.00012 **Queries matched:** 18

GA18849-PA [Drosophila pseudoobscura]

Observed	Mr(expt)	Mr(calc)	Delta	Start		End	Miss	Ions	Peptide
852.49	851.48	851.43	0.05	1345	-	1350	0	---	K.WIQSYR.D
870.58	869.58	869.53	0.04	527	-	535	0	---	R.VIVNVAGAK.V

903.52	902.51	902.46	0.05	1717 - 1723	0	---	K.FYTLFGR.S
989.52	988.51	988.54	-0.03	1532 - 1540	1	---	R.AQLLDACKK.L
1026.58	1025.57	1025.63	-0.06	526 - 535	1	---	K.RVIVNVAGAK.V
1045.58	1044.57	1044.55	0.03	781 - 789	1	---	K.EQVDAEVKK.L
1070.67	1069.66	1069.62	0.04	678 - 686	1	---	K.KGDIIQLQR.R
1075.68	1074.67	1074.58	0.09	59 - 68	1	---	R.ALARAAPDYK.L
1142.64	1141.63	1141.60	0.03	1356 - 1364	0	12	R.LNQWNNVVR.W
1289.65	1288.64	1288.62	0.02	1287 - 1296	0	---	K.ECYFPIFVSK.A + Carbamidomet
1425.70	1424.69	1424.62	0.07	351 - 363	1	---	R.AKIDMSSPNGCMR.D + Oxidation
1623.86	1622.86	1622.82	0.04	213 - 227	0	33	R.FPPEASGYLHIGHAK.A
1772.90	1771.90	1771.90	-0.00	131 - 145	0	---	R.YEFLASQGIPQHVQR.W
1856.97	1855.96	1856.00	-0.04	510 - 525	1	---	K.LIDPIAPRYTALEQEK.R
1949.96	1948.95	1948.92	0.03	1428 - 1446	0	---	K.FAGGDYTTTVEAFISASGR.A
1967.92	1966.92	1966.88	0.04	1247 - 1262	0	---	K.GEMIEYYDVSGCYILR.H + Carbam
1977.94	1976.94	1976.93	0.01	449 - 465	0	---	K.LTWFVDSGLVDGWDDPR.F
2694.35	2693.35	2693.32	0.03	384 - 406	0	---	K.VYPTYDFACPIVDAIENVTHTLR.T +

No match to: 828.51, 842.56, 882.38, 919.53, 972.55, 1027.63, 1094.56, 1109.57, 1133.63, 1140.58, 1143.56, 1216.75, 1220.60, 1269.67, 1320.67, 1390.76, 1403.74, 1492.75, 1569.81, 1616.81, 1648.86, 1670.87, 1705.88, 1707.84, 1742.93, 1794.85, 1813.94, 1837.90, 1873.95, 1940.96, 2083.04, 2135.10, 2145.16, 2161.17, 2196.09, 2211.14, 2225.14, 2230.23, 2239.15, 2283.18, 2286.18, 2298.20, 2779.81, 2782.39, 2807.35, 2914.52, 3095.60, 3338.76, 3348.59, 3808.79

3. gi|1871360 **Mass:** 189080 **Score:** 80 **Expect:** 0.00059 **Queries matched:** 16

glutamyl-prolyl-tRNA synthetase

Observed	Mr(expt)	Mr(calc)	Delta	Start	End	Miss	Ions	Peptide
870.58	869.58	869.53	0.04	522 - 530	0	---	R.VIVNVAGAK.V
903.52	902.51	902.46	0.05	1706 - 1712	0	---	K.FYTLFGR.S
1026.58	1025.57	1025.63	-0.06	521 - 530	1	---	K.RVIVNVAGAK.V
1070.67	1069.66	1069.62	0.04	673 - 681	1	---	K.KGDIIQLQR.R
1075.68	1074.67	1074.58	0.09	59 - 68	1	---	R.ALARAAPDYK.L
1142.64	1141.63	1141.60	0.03	1344 - 1352	0	12	R.LNQWNNVVR.W
1289.65	1288.64	1288.62	0.02	1275 - 1284	0	---	K.ECYFPIFVSK.A + Carbamidomet

110 kDa band Mosquito Results

Peptide Summary Report (../data/20060314/F003557.dat)

Mascot Search Results

User	:
Email	:
Search title	:
MS data file	: T:\Macromolecular\Data\Jessica\RS505_2.mgf
Database	: NCBInr 20050618 (2521256 sequences; 854568500 residues)
Taxonomy	: Mosquito (8812 sequences)
Timestamp	: 14 Mar 2006 at 16:10:49 GMT
Significant hits:	gi|19335684 putative mucin-like protein [Aedes aegypti]
	gi|67102604 Filamentation induced by cAMP protein Fic [Burkholderia cenocepacia HI2424]
	gi|67104283 AMP-dependent synthetase and ligase [Burkholderia cenocepacia HI2424]
	gi|67093100 Protein-glutamate O-methyltransferase [Burkholderia cenocepacia AU 1054]
	gi|67103284 Acyl-CoA dehydrogenase, C-terminal:Acyl-CoA dehydrogenase, central region [Burkholderia cenocepacia
	gi|67102699 Glycoside hydrolase, family 31 [Burkholderia cenocepacia HI2424]
	gi|67102636 Aldehyde dehydrogenase [Burkholderia cenocepacia HI2424]
	gi|67104843 Cold-shock protein, DNA-binding [Burkholderia cenocepacia HI2424]
	gi|67095676 hypothetical protein BcenDRAFT_4841 [Burkholderia cenocepacia AU 1054]
	gi|67100595 regulatory protein, LuxR:Response regulator receiver [Burkholderia cenocepacia HI2424]
	gi|67095675 Intradiol ring-cleavage dioxygenase:Catechol dioxygenase, N-terminal [Burkholderia cenocepacia AU 1
	gi|67101046 Peptidase M48, Ste24p [Burkholderia cenocepacia HI2424]

Probability Based Mowse Score

Ions score is -10*Log(P), where P is the probability that the observed match is a random event.
Individual ions scores > 30 indicate identity or extensive homology (p<0.05).
Protein scores are derived from ions scores as a non-probabilistic basis for ranking protein hits.

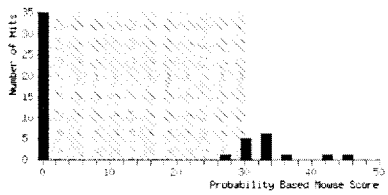

Peptide Summary Report

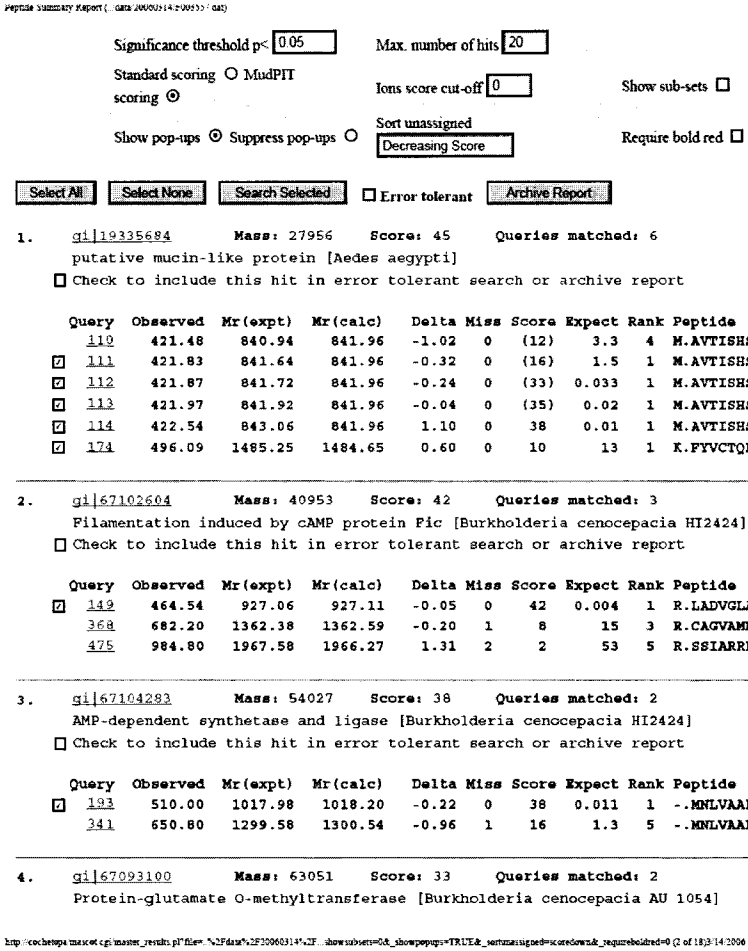

Peptide Summary Report (...data/20060314/...dat)

Significance threshold p< 0.05 Max. number of hits 20

Standard scoring ○ MudPIT scoring ◉ Ions score cut-off 0 Show sub-sets ☐

Show pop-ups ◉ Suppress pop-ups ○ Sort unassigned Decreasing Score Require bold red ☐

Select All | Select None | Search Selected | ☐ Error tolerant | Archive Report

1. gi|19335684 Mass: 27956 Score: 45 Queries matched: 6
putative mucin-like protein [Aedes aegypti]
☐ Check to include this hit in error tolerant search or archive report

	Query	Observed	Mr(expt)	Mr(calc)	Delta	Miss	Score	Expect	Rank	Peptide
	110	421.48	840.94	841.96	-1.02	0	(12)	3.3	4	M.AVTISHSK.V
☑	111	421.83	841.64	841.96	-0.32	0	(16)	1.5	1	M.AVTISHSK.V
☑	112	421.87	841.72	841.96	-0.24	0	(33)	0.033	1	M.AVTISHSK.V
☑	113	421.97	841.92	841.96	-0.04	0	(35)	0.02	1	M.AVTISHSK.V
☑	114	422.54	843.06	841.96	1.10	0	38	0.01	1	M.AVTISHSK.V
☑	174	496.09	1485.25	1484.65	0.60	0	10	13	1	K.FYVCTQEGPVER.S + Carbamidomethyl (C)

2. gi|67102604 Mass: 40953 Score: 42 Queries matched: 3
Filamentation induced by cAMP protein Fic [Burkholderia cenocepacia HI2424]
☐ Check to include this hit in error tolerant search or archive report

	Query	Observed	Mr(expt)	Mr(calc)	Delta	Miss	Score	Expect	Rank	Peptide
☑	149	464.54	927.06	927.11	-0.05	0	42	0.004	1	R.LADVGLALR.D
	368	682.20	1362.38	1362.59	-0.20	1	8	15	3	R.CAGVAMNERQVK.V + Carbamidomethyl (C)
	475	984.80	1967.58	1966.27	1.31	2	2	53	5	R.SSIARRLGVDIGALAPVDR.H

3. gi|67104283 Mass: 54027 Score: 38 Queries matched: 2
AMP-dependent synthetase and ligase [Burkholderia cenocepacia HI2424]
☐ Check to include this hit in error tolerant search or archive report

	Query	Observed	Mr(expt)	Mr(calc)	Delta	Miss	Score	Expect	Rank	Peptide
☑	193	510.00	1017.98	1018.20	-0.22	0	38	0.011	1	-.MNLVAALDR.A + Oxidation (M)
	341	650.80	1299.58	1300.54	-0.96	1	16	1.3	5	-.MNLVAALDRAAR.A

4. gi|67093100 Mass: 63051 Score: 33 Queries matched: 2
Protein-glutamate O-methyltransferase [Burkholderia cenocepacia AU 1054]

http://cochetopa.matrixscience.com/cgi-bin/mascot/cgi/master_results.pl?file=%2Fdata%2F20060314%2F...showsubsets=0&_showpopups=TRUE&_sortunassigned=scoreDown&_requirebold=0 (2 of 18)3/14/2006 2:14:59 AM

☐ Check to include this hit in error tolerant search or archive report

	Query	Observed	Mr(expt)	Mr(calc)	Delta	Miss	Score	Expect	Rank	Peptide
☑	231	551.08	1100.14	1099.21	0.93	0	33	0.032	1	R.QADAGAGAVALR.A
	455	567.33	1698.97	1697.83	1.14	2	2	32	8	R.DAGVPAARADGVRTDAR.R

---

5. gi|67103284 **Mass:** 66338 **Score:** 33 **Queries matched:** 2

Acyl-CoA dehydrogenase, C-terminal:Acyl-CoA dehydrogenase, central region [Burkholderia cenocepacia

☐ Check to include this hit in error tolerant search or archive report

	Query	Observed	Mr(expt)	Mr(calc)	Delta	Miss	Score	Expect	Rank	Peptide
☑	179	487.44	972.86	972.11	0.75	1	33	0.037	1	R.IGATVERAR.A
	411	738.50	1474.98	1475.63	-0.64	1	3	27	9	K.IPDEHGRLQPGTR.G

---

6. gi|67102699 **Mass:** 90730 **Score:** 32 **Queries matched:** 3

Glycoside hydrolase, family 31 [Burkholderia cenocepacia HI2424]

☐ Check to include this hit in error tolerant search or archive report

	Query	Observed	Mr(expt)	Mr(calc)	Delta	Miss	Score	Expect	Rank	Peptide
	292	601.40	1200.78	1201.33	-0.55	0	9	13	4	R.QGGHCTWSLR.G + Carbamidomethyl (C)
	296	602.86	1203.70	1202.38	1.32	1	19	0.68	3	R.ADTRGFLVAPR.I
☑	342	651.68	1301.34	1300.65	0.70	0	32	0.033	1	R.LCANIKPCLLR.D + Carbamidomethyl (C)

---

7. gi|67102636 **Mass:** 51903 **Score:** 32 **Queries matched:** 2

Aldehyde dehydrogenase [Burkholderia cenocepacia HI2424]

☐ Check to include this hit in error tolerant search or archive report

	Query	Observed	Mr(expt)	Mr(calc)	Delta	Miss	Score	Expect	Rank	Peptide
☑	357	665.71	1329.40	1329.52	-0.11	1	32	0.034	1	R.AGVEVAKAAADTVK.R
☑	358	665.73	1329.44	1329.52	-0.07	1	(20)	0.58	1	R.AGVEVAKAAADTVK.R

---

8. gi|67104843 **Mass:** 18870 **Score:** 32 **Queries matched:** 2

Cold-shock protein, DNA-binding [Burkholderia cenocepacia HI2424]

☐ Check to include this hit in error tolerant search or archive report

	Query	Observed	Mr(expt)	Mr(calc)	Delta	Miss	Score	Expect	Rank	Peptide
☑	274	583.58	1165.14	1165.27	-0.13	0	32	0.034	1	R.QGFTTGASLAGR.G
	383	699.56	1397.10	1397.58	-0.47	2	9	6	2	R.HPKCADRNSLTR.C

---

9. gi|67095676 **Score:** 32 **Queries matched:** 1

hypothetical protein BcenDRAFT_4841 [Burkholderia cenocepacia AU 1054]
☐ Check to include this hit in error tolerant search or archive report

Query	Observed	Mr(expt)	Mr(calc)	Delta	Miss	Score	Expect	Rank	Peptide
231	551.08	1100.14	1100.24	-0.10	0	32	0.04	2	R.SLVSASHFPR.I

Proteins matching the same set of peptides:
gi|67101712 **Score:** 32 **Queries matched:** 1

---

10. gi|67100595 **Mass:** 24098 **Score:** 32 **Queries matched:** 1
regulatory protein, LuxR:Response regulator receiver [Burkholderia cenocepacia HI2424]
☐ Check to include this hit in error tolerant search or archive report

Query	Observed	Mr(expt)	Mr(calc)	Delta	Miss	Score	Expect	Rank	Peptide
☑ 289	597.07	1192.12	1192.34	-0.21	1	32	0.037	1	R.EDQYAVRALK.A

---

11. gi|67095675 **Mass:** 32949 **Score:** 31 **Queries matched:** 3
Intradiol ring-cleavage dioxygenase:Catechol dioxygenase, N-terminal [Burkholderia cenocepacia AU 1
☐ Check to include this hit in error tolerant search or archive report

Query	Observed	Mr(expt)	Mr(calc)	Delta	Miss	Score	Expect	Rank	Peptide
127	436.04	870.06	871.04	-0.98	0	(16)	1.4	2	K.QAIDALLK.T
☑ 128	436.12	870.22	871.04	-0.82	0	31	0.044	1	K.QAIDALLK.T
182	503.49	1004.96	1004.07	0.90	1	8	8.5	8	R.SIRTDAEGR.Y

Proteins matching the same set of peptides:
gi|67101002 **Mass:** 32975 **Score:** 31 **Queries matched:** 3
Intradiol ring-cleavage dioxygenase:Catechol dioxygenase, N-terminal [Burkholderia cenocepacia HI24

---

12. gi|67101046 **Mass:** 46764 **Score:** 31 **Queries matched:** 1
Peptidase M48, Ste24p [Burkholderia cenocepacia HI2424]
☐ Check to include this hit in error tolerant search or archive report

Query	Observed	Mr(expt)	Mr(calc)	Delta	Miss	Score	Expect	Rank	Peptide
☑ 87	368.88	735.74	735.90	-0.15	0	31	0.041	1	R.IESLMK.R + Oxidation (M)

---

13. gi|60460225 **Mass:** 10741 **Score:** 30 **Queries matched:** 3
putative 7.8 kDa acidic protein [Aedes aegypti]
☐ Check to include this hit in error tolerant search or archive report

Query	Observed	Mr(expt)	Mr(calc)	Delta	Miss	Score	Expect	Rank	Peptide

	Query	Observed	Mr(expt)	Mr(calc)	Delta	Miss	Score	Expect	Rank	Peptide
☑	144	456.09	910.16	911.04	-0.88	1	32	0.031	1	K.YLDCKGGR.V
☑	145	456.13	910.24	911.04	-0.80	1	(23)	0.21	1	K.YLDCKGGR.V
	164	480.02	958.02	957.07	0.95	0	0	66	6	K.MGESFAATK.F + Oxidation (M)

14. gi|67038006 **Mass:** 86696 **Score:** 29 **Queries matched:** 2
PAS:GGDEF [Burkholderia cenocepacia HI2424]
☐ Check to include this hit in error tolerant search or archive report

	Query	Observed	Mr(expt)	Mr(calc)	Delta	Miss	Score	Expect	Rank	Peptide
	275	584.14	1749.40	1749.98	-0.59	0	2	63	6	K.LATEATGVGIWEFDLK.T
☑	452	829.44	2485.30	2486.07	-0.78	0	29	0.13	1	R.SQLLVYALFGLLCMAGLIIYQR.Q

15. gi|67039803 **Mass:** 31241 **Score:** 28 **Queries matched:** 1
2-hydroxy-3-oxopropionate reductase [Burkholderia cenocepacia HI2424]
☐ Check to include this hit in error tolerant search or archive report

	Query	Observed	Mr(expt)	Mr(calc)	Delta	Miss	Score	Expect	Rank	Peptide
☑	234	646.87	1937.59	1936.25	1.34	0	28	0.15	1	K.LVIDMSSISPLDTQAFAK.Q

16. gi|67100846 **Mass:** 124465 **Score:** 0 **Queries matched:** 5
Beta-mannosidase [Burkholderia cenocepacia HI2424]
☐ Check to include this hit in error tolerant search or archive report

	Query	Observed	Mr(expt)	Mr(calc)	Delta	Miss	Score	Expect	Rank	Peptide
☑	154	470.00	937.98	939.06	-1.07	0	25	0.16	1	R.DAGFNMIR.V + Oxidation (M)
	277	586.43	1170.84	1171.28	-0.43	1	9	8.5	4	R.SDRGVPSAVAGR.R
	283	592.19	1182.36	1183.40	-1.03	1	12	6.5	4	R.TPVARAGCPVR.I + Carbamidomethyl (C)
	298	603.70	1205.38	1206.33	-0.94	2	18	0.79	8	R.DRRAGTFDLR.A
	410	738.33	1474.64	1474.73	-0.09	1	13	4.9	2	R.GRPVHVLQVSARR.A

17. gi|67034041 **Mass:** 175735 **Score:** 0 **Queries matched:** 8
hypothetical protein BcenDRAFT_2976 [Burkholderia cenocepacia AU 1054]
☐ Check to include this hit in error tolerant search or archive report

	Query	Observed	Mr(expt)	Mr(calc)	Delta	Miss	Score	Expect	Rank	Peptide
	118	428.85	855.68	856.89	-1.21	1	15	1.7	3	R.DARDQPR.R
	122	440.66	879.30	878.02	1.29	1	8	9	3	R.TLAMRDR.E + Oxidation (M)
	187	506.57	1011.12	1010.12	1.00	1	2	32	5	R.IDHVGGRTR.M
☑	260	564.64	1127.26	1127.26	0.01	1	14	2.2	1	R.FMGGGRDECR.I
	306	612.00	1221.98	1223.38	-1.40	2	11	4.3	5	R.MRAQARGDFR.R + Oxidation (M)
	312	614.00	1225.98	1225.29	0.69	2	17	1.2	3	R.ADHATDRQRR.I

	Query	Observed	Mr(expt)	Mr(calc)	Delta	Miss	Score	Expect	Rank	Peptide
[x]	216	620.10	1238.18	1238.44	-0.25	2	15	1.6	1	R.VGHGRMRAQAR.G
	254	561.96	1682.86	1682.84	0.02	2	3	51	3	R.DARQFADSVMQRSR.E + Oxidation (M)

18. gi\|40988981 **Mass:** 279060 **Score:** 0 **Queries matched:** 7

target of rapamycin [Aedes aegypti]

☐ Check to include this hit in error tolerant search or archive report

	Query	Observed	Mr(expt)	Mr(calc)	Delta	Miss	Score	Expect	Rank	Peptide
	128	436.12	870.22	870.06	0.16	0	13	3.4	9	R.QIDLLIR.Q
[x]	140	452.23	902.44	902.11	0.34	1	15	2.3	1	K.IPFRLTR.M
	193	510.00	1017.98	1017.10	0.88	0	15	2	9	K.ISYTEYNK.L
	207	528.50	1054.98	1054.34	0.65	1	9	13	3	R.LLARCYMK.L + Carbamidomethyl (C)
	299	604.91	1207.80	1209.28	-1.48	0	7	18	5	K.SPSSEVWFDR.R
	331	640.51	1279.00	1277.53	1.48	0	3	56	4	M.STVVLQFVSGLK.S
[x]	388	706.49	1410.96	1411.64	-0.68	2	8	10	1	K.FASLCRKSDSLK.L + Carbamidomethyl (C)

19. gi\|67091544 **Score:** 0 **Queries matched:** 6

ABC transporter [Burkholderia cenocepacia AU 1054]

☐ Check to include this hit in error tolerant search or archive report

	Query	Observed	Mr(expt)	Mr(calc)	Delta	Miss	Score	Expect	Rank	Peptide
[x]	71	595.91	594.90	594.73	0.17	0	4	8.7	1	K.STLMK.I + Oxidation (M)
	144	456.09	910.16	909.06	1.10	2	22	0.28	2	R.AHRKELR.V
	145	456.13	910.24	909.06	1.18	2	(1)	37	7	R.AHRKELR.V
	189	507.05	1012.08	1012.17	-0.09	0	10	5.4	6	R.AGIGILPESR.K
	261	565.47	1128.92	1129.24	-0.31	1	14	2.6	5	R.DAKGGGVADALR.T
	296	602.86	1203.70	1203.42	0.28	0	9	6.5	8	R.TEKPMDTILR.L

Proteins matching the same set of peptides:

gi\|67100502 **Score:** 0 **Queries matched:** 6

20. gi\|67092400 **Mass:** 103752 **Score:** 0 **Queries matched:** 4

ATP-dependent DNA ligase:ATP-dependent DNA ligase [Burkholderia cenocepacia AU 1054]

☐ Check to include this hit in error tolerant search or archive report

	Query	Observed	Mr(expt)	Mr(calc)	Delta	Miss	Score	Expect	Rank	Peptide
	159	474.79	947.56	947.11	0.46	2	15	1.9	4	K.LDPYRRK.R
[x]	201	517.38	1032.74	1032.27	0.47	2	23	0.32	1	R.RKVTLMTR.E
	258	563.95	1125.88	1125.38	0.50	2	6	12	7	R.ILARIAGKGAR.R
	343	652.14	1302.26	1303.31	-1.04	0	13	5	7	R.AEDDASGPDTLGR.V

110 kDa band Drosophila Results

Peptide Summary Report (RS105-2)

Mascot Search Results

User	:
Email	:
Search title	: RS105-2
MS data file	: T:\Macromolecular\Data\Jessica\RS505_2.mgf
Database	: NCBInr 20050618 (2521256 sequences; 854568500 residues)
Taxonomy	: Drosophila (fruit flies) (56063 sequences)
Timestamp	: 14 Mar 2006 at 17:16:53 GMT
Significant hits:	gi|24668547 CG11471-PC, isoform C [Drosophila melanogaster]
	gi|54637236 GA19824-PA [Drosophila pseudoobscura]
	gi|54640849 GA10407-PA [Drosophila pseudoobscura]
	gi|54645657 GA20110-PA [Drosophila pseudoobscura]
	gi|54636375 GA18543-PA [Drosophila pseudoobscura]
	gi|51951082 CG41114-PB.3 [Drosophila melanogaster]
	gi|21429196 SD07726p [Drosophila melanogaster]
	gi|24639438 CG14422-PA [Drosophila melanogaster]
	gi|24652184 CG1625-PA [Drosophila melanogaster]
	gi|24586163 CG12836-PA [Drosophila melanogaster]
	gi|54641577 GA21977-PA [Drosophila pseudoobscura]
	gi|67102604 Filamentation induced by cAMP protein Fic [Burkholderia cenocepacia HI2424]
	gi|54640407 GA14391-PA [Drosophila pseudoobscura]

Probability Based Mowse Score

Ions score is -10*Log(P), where P is the probability that the observed match is a random event.
Individual ions scores > 40 indicate identity or extensive homology (p<0.05).
Protein scores are derived from ions scores as a non-probabilistic basis for ranking protein hits.

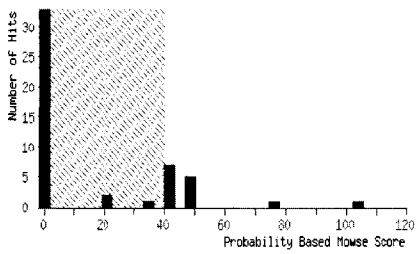

Peptide Summary Report

Format As | Peptide Summary | Help

Standard scoring ○ MudPIT scoring ◉ Ions score cut-off [0] Show sub-sets ☐

Show pop-ups ◉ Suppress pop-ups ○ Sort unassigned [Decreasing Score] Require bold red ☐

Select All | Select None | Search Selected | ☐ Error tolerant | Archive Report

1. gi|24668547 Mass: 141099 Score: 104 Queries matched: 3
CG11471-PC, isoform C [Drosophila melanogaster]
☐ Check to include this hit in error tolerant search or archive report

Query	Observed	Mr(expt)	Mr(calc)	Delta	Miss	Score	Expect	Rank	Peptide
☑ 280	587.96	1173.90	1173.42	0.48	0	(38)	0.097	1	R.LYLINSPVVR.A
☑ 281	588.10	1174.18	1173.42	0.76	0	58	0.00098	1	R.LYLINSPVVR.A
☑ 403	727.98	1453.94	1454.65	-0.70	0	84	2.1e-006	1	K.FIDQLTNWYVR.L

Proteins matching the same set of peptides:
gi|54641154 Mass: 140829 Score: 104 Queries matched: 3
GA11021-PA [Drosophila pseudoobscura]

---

2. gi|54637236 Mass: 133026 Score: 74 Queries matched: 1
GA19824-PA [Drosophila pseudoobscura]
☐ Check to include this hit in error tolerant search or archive report

Query	Observed	Mr(expt)	Mr(calc)	Delta	Miss	Score	Expect	Rank	Peptide
☑ 231	551.08	1100.14	1099.34	0.80	1	74	2.2e-005	1	R.EGTIGLKILR.R

---

3. gi|54640849 Mass: 42613 Score: 51 Queries matched: 2
GA10407-PA [Drosophila pseudoobscura]
☐ Check to include this hit in error tolerant search or archive report

Query	Observed	Mr(expt)	Mr(calc)	Delta	Miss	Score	Expect	Rank	Peptide
☑ 340	650.70	1299.38	1298.59	0.79	2	51	0.0073	1	K.LKASRALLAEVK.T
☑ 122	434.23	1299.67	1298.59	1.07	2	(19)	12	1	K.LKASRALLAEVK.T

---

4. gi|54645657 Mass: 91019 Score: 49 Queries matched: 1
GA20110-PA [Drosophila pseudoobscura]
☐ Check to include this hit in error tolerant search or archive report

Query	Observed	Mr(expt)	Mr(calc)	Delta	Miss	Score	Expect	Rank	Peptide
☑ 236	553.36	1104.70	1103.35	1.35	1	49	0.0066	1	R.LMRDQLLAK.L + Oxidation (M)

---

5. gi|54636375 Score: 48 Queries matched: 1
GA18543-PA [Drosophila pseudoobscura]
☐ Check to include this hit in error tolerant search or archive report

Query	Observed	Mr(expt)	Mr(calc)	Delta	Miss	Score	Expect	Rank	Peptide
231	551.08	1100.14	1099.34	0.80	0	48	0.0085	2	R.LSGSLLQLIR.R

---

6. gi|51951082 Mass: 34373 Score: 47 Queries matched: 1
CG41114-PB.3 [Drosophila melanogaster]
☐ Check to include this hit in error tolerant search or archive report

Query	Observed	Mr(expt)	Mr(calc)	Delta	Miss	Score	Expect	Rank	Peptide
☑ 96	396.82	791.62	790.87	0.75	0	47	0.012	1	R.WTVSGGGK.C

---

7. gi|21429196 Mass: 134919 Score: 46 Queries matched: 1
SD07726p [Drosophila melanogaster]
☐ Check to include this hit in error tolerant search or archive report

Query	Observed	Mr(expt)	Mr(calc)	Delta	Miss	Score	Expect	Rank	Peptide
☑ 438	783.37	1564.72	1564.71	0.01	0	46	0.013	1	R.SSGEGVGPQEYTLIK.M

Proteins matching the same set of peptides:
gi|28574733 Mass: 134873 Score: 46 Queries matched: 1
CG33123-PA [Drosophila melanogaster]

---

8. gi|24639438 Mass: 33854 Score: 43 Queries matched: 1
CG14422-PA [Drosophila melanogaster]
☐ Check to include this hit in error tolerant search or archive report

Query	Observed	Mr(expt)	Mr(calc)	Delta	Miss	Score	Expect	Rank	Peptide
☑ 333	643.12	1284.22	1285.47	-1.24	2	43	0.054	1	R.QKELNEQLRK.Q

---

9. gi|24652184 Mass: 128846 Score: 43 Queries matched: 1
CG1625-PA [Drosophila melanogaster]
☐ Check to include this hit in error tolerant search or archive report

Query	Observed	Mr(expt)	Mr(calc)	Delta	Miss	Score	Expect	Rank	Peptide
☑ 298	603.70	1205.38	1205.49	-0.10	2	43	0.032	1	K.MKKAISVGSLR.E + Oxidation (M)

---

10. gi|24586163 Mass: 30306 Score: 42 Queries matched: 2
CG12836-PA [Drosophila melanogaster]
☐ Check to include this hit in error tolerant search or archive report

	Query	Observed	Mr(expt)	Mr(calc)	Delta	Miss	Score	Expect	Rank	Peptide
	272	582.62	1163.22	1162.41	0.82	1	7	1.2e+002	7	R.MCHLMDEKR.D
☑	377	692.93	1383.84	1383.61	0.24	0	42	0.029	1	R.MNALLSHSMLSR.R + 2 Oxidation (M)

Proteins matching the same set of peptides:
gi|54635360 Mass: 19615 Score: 42 Queries matched: 2
GA11842-PA [Drosophila pseudoobscura]

---

11. gi|54641577 Mass: 92597 Score: 42 Queries matched: 2
GA21977-PA [Drosophila pseudoobscura]
☐ Check to include this hit in error tolerant search or archive report

	Query	Observed	Mr(expt)	Mr(calc)	Delta	Miss	Score	Expect	Rank	Peptide
	215	534.03	1066.04	1066.19	-0.15	1	5	1.7e+002	5	K.ETDKMLDSK.K
☑	224	544.17	1086.32	1087.30	-0.98	0	42	0.07	1	R.TVCPLLTNAR.L

---

12. gi|67102604 Mass: 40953 Score: 42 Queries matched: 1
Filamentation induced by cAMP protein Fic [Burkholderia cenocepacia HI2424]
☐ Check to include this hit in error tolerant search or archive report

	Query	Observed	Mr(expt)	Mr(calc)	Delta	Miss	Score	Expect	Rank	Peptide
☑	149	464.54	927.06	927.11	-0.05	0	42	0.032	1	R.LADVGLALR.D

---

13. gi|54640407 Mass: 75839 Score: 40 Queries matched: 2
GA14391-PA [Drosophila pseudoobscura]
☐ Check to include this hit in error tolerant search or archive report

	Query	Observed	Mr(expt)	Mr(calc)	Delta	Miss	Score	Expect	Rank	Peptide
☑	233	552.55	1103.08	1102.34	0.74	2	40	0.052	1	R.RKSVASTILK.I
☑	390	707.98	1413.94	1412.60	1.35	0	16	13	1	K.SCAQVMLNFEDR.L

---

14. gi|54635799 Mass: 244390 Score: 40 Queries matched: 3
GA18514-PA [Drosophila pseudoobscura]
☐ Check to include this hit in error tolerant search or archive report

	Query	Observed	Mr(expt)	Mr(calc)	Delta	Miss	Score	Expect	Rank	Peptide
☑	210	530.17	1058.32	1059.18	-0.86	0	(24)	2.5	1	K.VDLDIDIEK.E
☑	212	530.97	1059.92	1059.18	0.74	0	40	0.064	1	K.VDLDIDIEK.E
☑	213	531.02	1060.02	1059.18	0.84	0	(32)	0.71	1	K.VDLDIDIEK.E

---

15. gi|21357303 Mass: 64851 Score: 36 Queries matched: 2
CG9389-PA [Drosophila melanogaster]
☐ Check to include this hit in error tolerant search or archive report

Query	Observed	Mr(expt)	Mr(calc)	Delta	Miss	Score	Expect	Rank	Peptide
☑ 164	480.02	958.02	957.10	0.93	0	8	94	1	K.AGAIALAENK.E
☑ 285	595.68	1189.34	1188.41	0.94	1	36	0.14	1	R.AMSMKMSQAR.L + 3 Oxidation (M)

16. gi|17737290 Mass: 28407 Score: 22 Queries matched: 1
CG10944-PB, isoform B [Drosophila melanogaster]
☐ Check to include this hit in error tolerant search or archive report

Query	Observed	Mr(expt)	Mr(calc)	Delta	Miss	Score	Expect	Rank	Peptide
☑ 440	784.13	1566.24	1567.67	-1.43	2	22	2.8	1	R.SASIRESKSSVSSDK.K

Proteins matching the same set of peptides:
gi|24640435 Mass: 28672 Score: 22 Queries matched: 1
CG10944-PC, isoform C [Drosophila melanogaster]
gi|24640437 Mass: 24696 Score: 22 Queries matched: 1
CG10944-PA, isoform A [Drosophila melanogaster]

17. gi|24651928 Score: 18 Queries matched: 1
CG13745-PA [Drosophila melanogaster]
☐ Check to include this hit in error tolerant search or archive report

Query	Observed	Mr(expt)	Mr(calc)	Delta	Miss	Score	Expect	Rank	Peptide
☑ 71	595.91	594.90	594.68	0.22	0	18	3.2	1	K.STMTR.S

18. gi|54638570 Mass: 95208 Score: 0 Queries matched: 2
GA19045-PA [Drosophila pseudoobscura]
☐ Check to include this hit in error tolerant search or archive report

Query	Observed	Mr(expt)	Mr(calc)	Delta	Miss	Score	Expect	Rank	Peptide
☑ 306	612.00	1221.98	1221.44	0.55	0	39	0.061	1	R.SGVELMELSIK.Q + Oxidation (M)
☑ 320	622.47	1864.39	1865.04	-0.66	1	30	1.1	1	R.VACTCPNCTDGEKRSDK.K + Carbamidomethyl (C)

19. gi|62471695 Score: 0 Queries matched: 5
CG33549-PB, isoform B [Drosophila melanogaster]
☐ Check to include this hit in error tolerant search or archive report

Query	Observed	Mr(expt)	Mr(calc)	Delta	Miss	Score	Expect	Rank	Peptide
97	368.88	735.74	734.96	0.79	1	26	1.3	4	K.IKSLMK.D + Oxidation (M)
132	443.13	884.24	885.07	-0.83	1	31	0.74	6	K.LENLKLR.S
292	601.40	1200.78	1200.36	0.42	0	12	65	6	R.IAVNVQQVESR.F
337	648.09	1294.16	1294.36	-0.20	0	12	36	8	K.AVTLCDDESKR.K + Carbamidomethyl (C)
360	666.47	1330.92	1331.45	-0.52	0	8	80	2	K.QNLQSSVDELAK.T